Optimisation of Biodiesel Production from *Croton Gratissimus* Oil

Submitted in fulfilment of the requirements for the degree of Master of Engineering: Chemical in the Faculty of Engineering and the Built Environment

Phiwe Charles Jiyane

June 2018

Supervisor: Prof P Musonge

Co supervisor: Dr K Tumba

Dedication

This dissertation is dedicated to my family. I extend my sincere gratitude to my lovely wife, Hlobisile, for her understanding and unwavering support of my work throughout this journey. Your words of encouragement kept me going and have been a constant reminder of the glorious goal that lies ahead. At times you had to assume the role of a father to our children due to many hours of my absence on account of this work. For that, I am grateful.

To my children, Sinalo, Lwandzile and Esasa. Their constant nagging and demand for my attention has taught me to be patient and to take time off and reflect on things. This has elevated my spirit and invoked within me the willingness to succeed. From the bottom of my heart, I thank you.

Declarations

I, **PHIWE CHARLES JIYANE** declare that:

(i) The research reported in this thesis, except where otherwise indicated, is my own original work.

(ii) This thesis has not been submitted for any degree or examination at any other University or academic institution.

(iii) This thesis does not contain other persons' data, pictures, graphs or other information, unless specifically acknowledged as being sourced from other persons.

(iv) This thesis does not contain other persons' writing, unless specifically acknowledged as being sourced from other researchers. Where other sources have been quoted, then:

(a) Their words have been re-written but general information attributed to them has been referenced;

(b) Where their exact words have been used, their writing has been placed inside quotation marks, and referenced.

(v) Where I reproduced a publication of which I am an author, co-author or editor, I have indicated in detail which part of the publication was actually written by myself alone and have fully referenced such publications.

(vi) This thesis does not contain text, graphics or tables copied and pasted from the internet, unless specifically acknowledged, and the source being detailed in the thesis and in the References section.

Sig 

NAME OF SUPERVISOR: …….....
PROF PAUL MUSONGE

NAME OF CO SUPERVISOR: .....
DR KANIKI TUMBA

Acknowledgements

I am grateful to my supervisor, Prof Musonge, for guiding me through this research study. His invaluable advices gave me strength and helped keep my focus when the work load seemed unbearable. Through his mentorship, I have reached milestones that I would never have dreamt of achieving in my career. For that, I will forever be grateful.

The work carried out in this research project would not have begun without the insight and support of Dr Kaniki. My deepest gratitude goes to him for initiating this work and also facilitating the delivery of *Croton gratissimus* grains from the Democratic Republic of Congo to our laboratories at MUT. He is a very resourceful and a patient man. His constant constructive criticism of my work has impacted positively on the results presented in this dissertation.

I would also like to thank Dr Isa, from the Department of Chemical Engineering at DUT, for allowing me to use his contacts at the Electron Microscope Unit of the UCT and NRF's iThemba LABS to get my synthesised catalyst analysed within a short space of time. I also give special thanks to Nomaxhosa Msimango from the Department of Chemistry at MUT, without whom I would not have been able to run samples on the GC-MS for my lipid and FAME profiling. Her time and patience is hereby acknowledged and much appreciated.

To my colleagues at MUT, Dr Bakare, Dr Qwabe, Dr Gumede, Mrs Makhathini and Mrs Baah. No words can ever be able to express my gratitude for your selfless and kind support. Thank you all.

Abstract

Consumption of liquid energy products, primarily fossil-based fuels, by the transportation industry, is high and has caused an escalation of the energy crisis facing global communities. This protracted use of fossil fuels has inadvertently resulted in an increased concentration of CO_2 and other greenhouse gases (GHG) in the atmosphere, leading to environmental degradation. An environmentally friendly alternative fuel source, in the form of biofuels, has been found. These biofuels are biodegradable, boasting reduced levels of particulate matter (PM), carbon monoxide (CO), obnoxious sulphur (SO_x) and nitrogen compounds (NO_x) in their combustion products.

In African countries, particularly the Republic of South Africa (RSA), the urgency for the establishment of a viable biodiesel industry is driven by the vulnerability of crude oil prices, high unemployment, climate change concerns and the need for the continent's growing economies to use their resources in a sustainable manner. In order to address these concerns, this investigation focused on the extraction of non-edible oil from the seeds of the indigenous *Croton gratissimus* plant, the catalytic synthesis of biodiesel and the optimisation of the developed biodiesel production process.

In this optimisation study, biodiesel was produced from oil extracted from *Croton gratissimus* seeds using synthesised monoclinic sulphated zirconia (SO_4^{2-}/ZrO_2) and KOH as catalysts. Low oil extraction yields (29.35%) obtained for this crop were attributed to its low unsaturated fatty acid content of 25.4%. From the model developed for the esterification of *Croton gratissimus* oil, the concentration of SO_4^{2-}/ZrO_2 catalyst had the most significant effect in the reduction of the Acid Value of oil. This was substantiated by flat response surfaces observed on the RSM surface plots when all other design factors were varied whilst keeping catalyst concentration constant. The operating conditions for the esterification process that could give an optimum Acid Value of 2.693 mg KOH/g of oil were therefore found to be; 10.96 mass % SO_4^{2-}/ZrO_2 catalyst concentration, 27.60 methanol-to-oil ratio and 64 ^{0}C reaction temperature.

In the optimisation of the transesterification process, the model showed that catalyst concentration, methanol-to-oil ratio, reaction temperature, and their interactions were all significant model terms. But catalyst concentration and methanol-to-oil ratio, were the terms found to have the most influence on the percentage fatty acid methyl ester (FAME) yield and

percentage FAME purity. It was established from the combined model that optimum responses of 84.51% FAME yield and 90.66% FAME purity could be achieved when operating the transesterification process at 1.439 mass % KOH catalyst concentration, 7.472 methanol-to-oil ratio and at a temperature of 63.50 ^{0}C.

The two-step biodiesel process used in this work, produced biodiesel with a high FAME purity and a relatively high FAME yield. Improvement of the oil extraction process may be possible with polar co-solvent such as ethyl acetate, which may increase the FAME yield in the *Croton gratissimus* biodiesel production process.

Table of Contents

List of Abbreviations and Acronyms

2FI	Two-factor interaction model
ANN	Artificial Neural Networks
ANOVA	Analysis of Variances
AV	Acid value
BBD	Box-Behnken Design
BET	Brunauer-Emmett-Teller
BIS	Biofuels Industrial Strategy
BP	British Petroleum
BTT	Biofuels Task Team
C.V.	Coefficient of Variances
CCD	Central Composite Design
CCRD	Central Composite Rotatable Design
CR	Chemical Reaction
CSE	Chemical Solvent Extraction
DD	Doehlert Design
DME	Department of Mineral and Energy
DMSO	Dimethyl sulphoxide
DRC	Democratic Republic of Congo
DST	Department of Science and Technology
DUT	Durban University of Technology
EDS	Energy Dispersive Spectroscopy
EIA	Energy Information Administration
FAME	Fatty Acid Methyl Esters
FFA	Free Fatty Acid
GC-MS	Gas chromatography Mass spectroscopy
GDP	Gross Domestic Product
GHG	Greenhouse gases
IEO	Internal Energy Outlook
LCT	Long-chain triglycerides
MCT	Medium-chain triglycerides
MeOH	Methanol
MUT	Mangosuthu University of Technology

NSI	National Systems of Innovation
OFAT	One-Factor-At-a-Time
PM	Particulate matter
R&D	Research and Development
rpm	Revolutions per minute
RSA	Republic of South Africa
RSM	Response Surface Methodology
SEM	Scanning Electron Microscopy
SETAs	Sector Education and Training Authorities
SFE	Supercritical Fluid Extraction
STDs	Sexually Transmitted Diseases
TEM	Transmission Electron Microscopy
THF	Tetrahydrofuran
UAE	Ultrasonic-assisted Extraction
UCT	University of Cape Town
UKZN	University of KwaZulu Natal
XRD	X-ray diffraction

List of Figures

List of Tables

Chapter 1. Introduction

1.1 Background and Motivation

Industrialised nations of the modern times are facing the biggest challenge ever. Over the years there has been a dramatic increase in the demand for coal, liquid fuels and natural gas, causing a sharp decline and depletion of fossil fuel resources, worldwide. Petroleum-based fuels, derived from crude oil and mainly used by the transportation industry, have for many centuries been the biggest contributors to global warming as the net atmospheric levels of CO_2 continue to increase. As fossil fuels continue to be the primary provider of energy to our civilization, accounting for 78% of the total world energy consumption (U.S. Energy Information Administration, 2016), their contribution to environmental degradation can no longer be overlooked. The Internal Energy Outlook 2016 (IEO2016) projections from 2012 to 2040, show a steady growth in the consumption of petroleum-based fuels, with a 1.1% growth per year in the transportation sector and a 1.0% growth per year expected in the industrial sector. These protracted petroleum fuel consumption growths will see the world carbon dioxide related emissions (greenhouse gases, GHG) increasing by 34% between 2012 and 2040, from 32.3 to 43.2 billion metric tons, respectively (U.S. Energy Information Administration, 2016).

According to the Energy Information Administration (EIA) 2012 estimates, South Africa contributed 40% towards carbon dioxide emissions in the African continent and was the 13th largest carbon dioxide producer in the world, during the reporting period. All of this was as a result of South Africa's heavy dependence on coal as its primary source of energy. To further substantiate this co-dependence of the Republic of South Africa's (RSA) economy in fossil derived energy, in 2013 the British Petroleum's (BP) Statistical Review of World Energy 2014 reported that 72% of South Africa's total primary energy consumption came from coal,

followed by 22% from oil, 3% from natural gas, 3% from nuclear, and less than 1% coming from renewables (primarily hydropower). So without an extensive exploitation of the available alternative fuel sources, the problems of atmospheric pollution in the Republic of South Africa will escalate to unmanageable levels.

Globally, liquid fuels (oil in particular) were the most consumed energy source in 2015, accounting for 32.9% of the world's energy consumption (BP, 2016). Likewise, in South Africa liquid fuels make up about 30% of the country's energy usage. Yet, they constitute approximately 70% of the total energy expenditure, 65% of which is being sourced from crude oil imports (Department of Mineral and Energy, 2006). This massive expenditure on crude oils and their harmful effects on the environment are the major motivations to finding a substitute, preferably renewable fuel source. Currently, biofuels (of which biodiesel is part) have been identified as the only significant substitute to crude oil-derived transportation fuels.

In its attempts to address the energy crisis and socio-economic challenges facing the country, in December 2007 the South African Cabinet approved the Biofuels Industrial Strategy (BIS) document after an intensive public consultative process conducted by an inter-departmental Biofuels Task Team (BTT). For the production of biofuels in South Africa, the BIS proposed that sugar cane and sugar beet be used as crops for bio-ethanol production, and that for the production of biodiesel, sunflower, canola and soya beans crops be used as feedstock. The selection of these crops was based on locally available crops mainly grown on currently underutilised land in the country (Department of Mineral and Energy, 2007). In contrast, elsewhere in the world other crops (second and third generation crops) are being explored; crops that would not impact negatively on food security and water resources and crops that would require less or no tillage of soil for productive cultivation.

The BIS document, as presented, sought to develop partnerships along the value chain and across all affected sectors. And with the proposed 2% penetration level of biofuels in the national liquid fuel supply, amounting to 400 million litres per annum, BIS intends ensuring that the sales of bio-ethanol and biodiesel as blending components are capped at a price that covers the costs associated with running a biofuels plant, including agricultural feedstock production. Further to this protection mechanism, additional incentives to biofuels manufacturers included a 100% exemption in Fuel Levy, access to government's agricultural support programmes for small-scale and emerging farmers, and the training and capacity building of emerging entrepreneurs by the Sector Education and Training Authorities (SETAs) (Department of Mineral and Energy, 2007). Government's agricultural support programmes available to these emerging farmers will include crop selection, hedging, agricultural methods, logistics, infrastructure management, research and development and contract negotiations (Department of Mineral and Energy, 2007).

With the envisaged increased demand for biofuels in South Africa, the Department of Science and Technology (DST) and other relevant stakeholders within the National Systems of Innovation (NSI) have pledged to create an R&D platform. The focus of research undertaken in this platform will be the investigation of alternative feedstock, the development of energy crops that are drought tolerant, offer high yield per hectare and are energy efficient; and also the improvement of known technologies whilst further developing, supporting and piloting the second generation technologies (Department of Mineral and Energy, 2007).

In the developed countries, biodiesel produced from oil extracted from vegetable crops (first generation feedstock) and animal fats and non-edible oils (second generation feedstock) has shown great potential as replacement fuel candidates in driving diesel engines. But excitement over biodiesel produced using edible crops has been marred with criticism from various

organisations citing pending threats to food security. Biodiesel derived from animal fat, on the other hand, faces additional quality challenges of high cloud and pour points because of high levels of unsaturation in their fatty acid source. The development of processes that use renewable non-edible energy resources to produce biodiesel in these countries, has therefore been made a priority.

In RSA, non-edible oil extracted from *Croton gratissimus* grains has proven to have a potential of producing high quality biodiesel (Bahadur *et al*., 2014). In only a few experiments, Bahadur *et al.* (2014) reported an oil extraction yield and FAME yield of 23.5% and 72.26%, respectively. But so far no attempt has been made to find the optimum operating conditions of both these processes when using this feedstock, hence the purpose of this optimisation study.

In this study, oil from *Croton gratissimus* seeds was extracted using *n*-hexane and the suitability of using a heterogeneous acid catalyst, sulphated zirconia (SO_4^{2-}/ZrO_2) in driving the esterification reactions is evaluated. Potassium hydroxide (KOH) was used as a catalyst to facilitate the final conversion of triglycerides to biodiesel in the transesterification step. Results obtained from experimental and modelling studies were to help in the determination of the optimum operating conditions necessary for the development of a biodiesel production process.

1.2 Problem Statement

What are the optimum operating conditions, of catalyst concentration, methanol-to-oil ratio and reaction temperature, under which biodiesel can be produced from *Croton gratissimus* oil to give the highest biodiesel yield and high FAME purity?

1.3 Research Aim and Objectives

The study was aimed at optimising the biodiesel production process from non-edible oil extracted from *Croton gratissimus* seeds when sulphated zirconia (SO_4^{2-}/ZrO_2) and potassium hydroxide (KOH) are used as catalysts. The models used to optimise the process will be developed using the Response Surface Methodology (RSM) based on Central Composite Design (CCD) technique. This broad aim will be achieved through the execution of the following objectives:

- To chemically extract and characterise non-edible virgin oil derived from *Croton gratissimus* seeds.

- To synthesise and characterise a heterogeneous acid catalyst, sulphated zirconia (SO_4^{2-}/ZrO_2), prepared from $ZrOCl_2 \cdot 8H_2O$ and H_2SO_4.

- To produce fatty acid methyl esters (FAME) derived from oil extracted from *Croton gratissimus* seeds. FAME produced will further be subjected to quality testing to determine its composition and purity.

- To optimise the esterification process that uses the synthesised SO_4^{2-}/ZrO_2 catalyst to find optimum operating conditions responsible for lowering the Acid Value of oil.

- Perform an optimisation study on the FAME production process to determine operating conditions that give the highest purity (methyl ester concentration in the biodiesel) and the highest yield (mass of methyl esters produced per mass of oil) of FAME. The study will use the RSM methodology based on the CCD and the analysis of variances (ANOVA) techniques.

1.4 Dissertation Structure

The dissertation is divided into 6 parts. The first part, Chapter 1, gives a brief background and motivation of the study. Chapter 2, the second part, seeks to explain how the aims and objectives of the study would be achieved. Through literature search, the research topic is dissected into sections that begin with a brief description of factors driving the need for the deployment of the biofuels industry in the African continent. A detailed description of the properties of the *Croton gratissimus* plant, whose grains could be an important source of a second generation feedstock (oil) in biodiesel production, is provided. This is followed by an in-depth analysis and a reflection of related work done by other researchers in the field of biofuels. Oil extraction techniques, biodiesel production technologies and catalyst synthesis techniques used to support the study are discussed. Different optimisation techniques and tools available to researchers are discussed with specific attention given to the RSM, selected as the optimisation tool in this work.

Chapter 3, the third part of the dissertation, contains a detailed description of the materials and methods used in all the experiments conducted. This chapter begins with a process flow chart that gives a summary of the experimental work carried out in the study. Laboratory-assembled equipment used in process operations (oil extraction, catalyst synthesis and biodiesel production) and instruments used in the analysis of experimental work are presented. Description of techniques and analytical methods used to synthesise and characterise *Croton gratissimus* oil, SO_4^{2-}/ZrO_2 catalyst and FAME are also provided.

The fourth part of the dissertation, Chapter 4 contains tables of experimental data, the results and findings. Response surface plots showing the effects of catalyst concentration, methanol-to-oil molar ratio and reaction temperature on the Acid Value of oil, the FAME yield and the

purity of FAME are presented. The 3 quadratic models developed for the biodiesel process are presented and their validity evaluated.

In Chapter 5, the research findings and final results are discussed with reference to related literature. Here, the broad aims and objectives of the research study are interrogated.

Finally, the sixth part of the dissertation, Chapter 6 provides conclusions. Drawing from the analyses made on the findings of the study in the previous chapter, Chapter 6 gives concluding remarks and charts the way forward for further work in oil extraction, SO_4^{2-}/ZrO_2 catalyst synthesis and the optimisation of biodiesel production processes, in general.

Chapter 2. Literature Review

2.1 Introduction

Biodiesel processes are fed from a wide range of feed sources; from vegetable crops to waste animal fats. Countries in Africa, rich in flora and fauna and with land in abundance, therefore stand to benefit. For these countries, biodiesel producing technologies promise to eradicate poverty by creating the most needed jobs and boosting regional economic growth. The adoption of these technologies by the African continent will therefore lead to the continent being lesser dependent on a few crude oil producing countries for their energy products.

Earlier work, that saw the birth of the biodiesel industry, focused mainly on the use of edible vegetable crops, animal fat and a selection of tropical plant species as biodiesel feedstock. But low cold flow properties associated with biodiesel derived from animal fats and the unresolved food security issues raised against the use of edible crops in biodiesel production, have shifted the attention of investigative work towards the high free fatty acid (FFA) non-edible vegetable crops. Unlike vegetable oils extracted from edible crops, the production of biodiesel from these high FFA crops requires a two-step process approach; that which first reduces the Acid Value of oil to below 4 mg KOH/g in the esterification reaction step over a homogeneous or heterogeneous acid catalyst before the main base-catalysed transesterification reaction step.

For the continued sustainability of the biodiesel industry, economic challenges facing the industry must be addressed. The success and future survival of the biodiesel industry, therefore, will depend entirely on its economic viability. An economically viable biodiesel production process must be capable of providing an ultimate gain in energy over all the energy sources used in the process. For this to happen, a biodiesel process must be energy efficient, allowing

sufficient throughput volumes to be achieved whilst keeping the energy demand to a bare minimum. It is for this reason that a wholesale of non-edible vegetable crops (*Croton gratissimus* being one of them) is being investigated as potential feedstock in biodiesel processes to produce high quality biodiesel whilst operating at moderate conditions, of temperature and pressure, and over shorter reaction times.

Croton gratissimus plant promises to be a future second generation crop for biodiesel production on the African continent. For productive cultivation, the plant does not require frequent soil tillage nor demand constant irrigation for growth. The plant grows naturally in uninhabitable places; as it is often found in stony terrains of the warmer and drier regions of the African continent (Mulholland *et al*., 2010).

2.2 Background

Uncertainties in the long-term supplies of fossil fuels, increasing energy prices, particularly that of oil and the increasing greenhouse gas (GHG) emissions have generated a keen interest amongst researchers in finding alternative fuel sources (Blanchard *et al*., 2011). To this end, biofuels have been identified as having a potential to displace petroleum-based fuels in the transportation industry and in some stationary applications. In the developing world (mainly the African continent), biofuels promise to provide local and regional benefits such as energy security, rural development and an improvement in the regional gross domestic product (GDP), in addition to the mitigation of local emissions of pollutant (van Eijck *et al*., 2014).

The following factors are therefore seen as the main drivers of the deployment of biofuels in the African continent.

- Global and local environmental impacts of fossil fuels

- Envisaged job creation opportunities
- Access to new research and technological advances
- Economic development and
- Ensuring that development in the African countries meets the Millennium Development Goals and is on a sustainable path by accessing globally available energy services (Amigun *et al*., 2011).

In addition, high and fluctuating crude oil prices (Fig. 2.1) could also be one of the major driving forces behind the urgent need to develop the biofuels industry in the Sub-Saharan Africa as many of the countries in this region are net energy importers. They import petroleum products at a cost that burdens them economically, significantly reducing their energy security thus threatening their economic independence.

Fig. 2.1: Crude Oil Prices: Daily Chart. Source: Macrotrends LLC (2010 – 2017)

Forty two countries in Africa are net energy importers and only 4 (Nigeria, Algeria, Egypt and Libya) are energy exporting countries. Of the world's proven oil reserves, Africa possesses 9.5% and contributes a mere 12% towards global oil production (Amigun *et al*., 2011). Liquid fuels in South Africa make up about 30% of the total energy usage, yet they constitute

approximately 70% of the total energy expenditure, 65% of which is being sourced from crude oil imports (Department of Minerals and Energy, 2006).

2.3 Global Biofuels Production

Global biofuels production is increasing. It is estimated that biofuels production will experience an average of 2.6% annual change, increasing production from 1.3 to 2.8 million barrels per day between 2010 and 2040 (U.S. Energy Information Administration, 2013). In another study, biofuels production is projected to reach 1160 million barrels by 2021, with bioethanol and biodiesel sharing between them 81% and 19% of the biofuels production volumes, respectively (Blanco *et al*., 2013). In 2015, the United States of America and Brazil were the top producers of biofuels in the world, both countries contributing 65% towards the total global biofuels production (USA, 41.4% and Brazil, 23.6%) (BP, 2016), Figure 2.2.

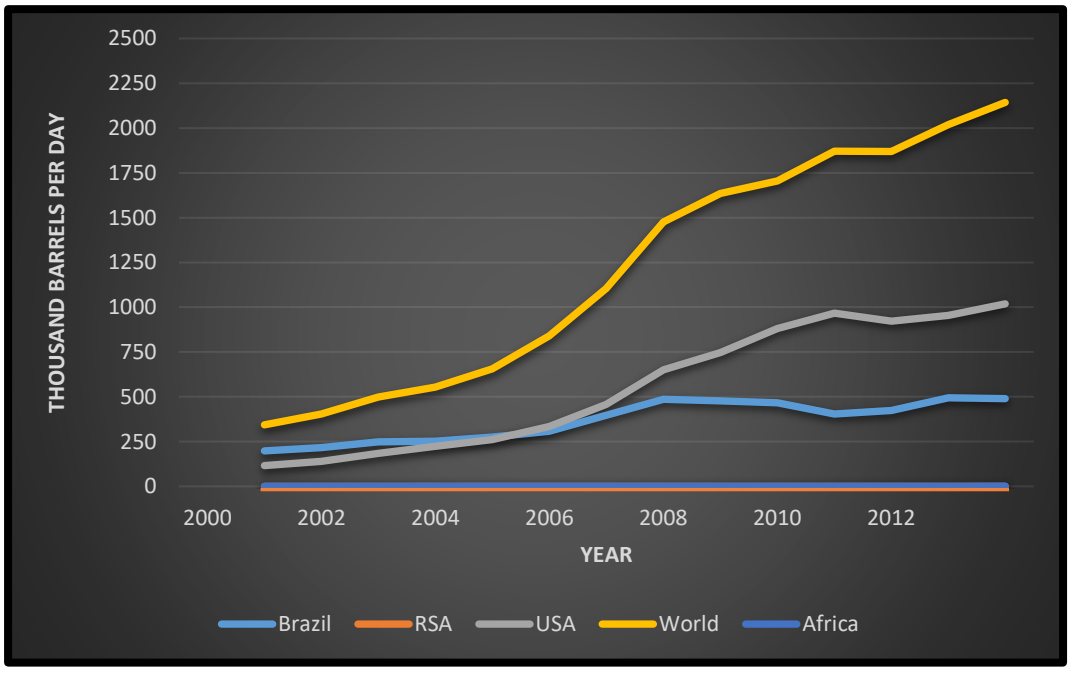

Fig. 2.2 Comparison of Global Biofuels Production: Data sourced from BP Statistical Review of World Energy 2016

Africa, on the other hand, still lags behind in biofuels production, with a contribution of only 0.1% in the same reporting period. Since year 2000, the global contribution of South Africa in

biofuels production averages at much less than 0.01% (Pradhan and Mbohwa, 2014). With an urgent need for alternative sources to cope with its energy security and emission issues and to save on heavy foreign exchange spent on imported oil, South Africa must thrive towards increasing its biofuels production targets.

Biodiesel and bioethanol, derived from waste feedstock and biomass, are the most common forms of biofuels. Bioethanol is an alcohol that contains about 70% of the energy found in fossil petrol. It is the product of the fermentation process that consumes sugar and starch components of crops using yeast. Biodiesel, on the other hand, contains between 91% and 94% of the energy obtained from fossil diesel. It is a fuel made up of mono-alkyl esters of long chain fatty acids produced by the reaction of triglycerides in vegetable oils or animal fats or waste oils with alcohol. These biofuels are usually blended with their fossil counterparts to improve vehicle emissions and increase octane number and cetane number in cases of bioethanol and biodiesel, respectively (Pradhan and Mbohwa, 2014).

In South Africa, biodiesel is produced from first generation feedstock (sunflower, canola, and soya beans) using first generation processing technologies. These technologies are notorious for relying heavily on the conversion of surplus food and edible feed crops to vegetable oil components needed for biodiesel processing (Blanchard *et al*., 2011). Moreover, biodiesel production from these feedstock may promote excessive land use which could lead to deforestation as large portions of land will be needed to cultivate these crops for biodiesel production. This has a potential of creating a serious ecological imbalance as forests will be cut down to give way for biodiesel crops (Ahmad *et al*., 2011). It is for this reason that in South Africa, the Biofuels Industrial Strategy document recommended a 2% biofuel penetration level which require about 1.4% of arable land from the 14% underutilised arable land in the country (Pradhan and Mbohwa, 2014). In addition, the country is investing in research and development

that promotes the use of second generation (non-edible) feedstock in biodiesel production, through more efficient second generation technologies.

2.4 *Croton gratissimus*: A Second Generation Feedstock

Croton gratissimus is a terrestrial plant of a semi-deciduous tree species belonging to the family of *Euphorbiaceae*. It is commonly found in rocky terrains, mostly in the warmer and drier regions, from north-eastwards regions of South Africa to the very top of Africa (Mulholland *et al*., 2010). Almost the entire plant (from roots to leaves) is used in traditional medicine to treat a wide variety of ailments. It offers a range of diverse bioactivities essential for human health management systems in most of under developed regions of Africa (Ndhlala *et al*., 2013). These include analgesia, febrifugal, aphrodisiac, purgative, emetic, soporific, antibiotic and antiviral (Mulholland *et al*., 2010); none of which could be attributed to its fruits, the three-lobed capsules. This capsule dries out in late autumn and explodes throwing the seeds at some distance away from the mother plant. Unlike other parts of the plant, the seeds are of no use in traditional medicine hence are only harvested for re-growing back into trees (Coates, 2002), until now.

The leaves of *Croton gratissimus* are aromatic (lavender *croton*) and often used as infusions to treat coughs. Liquor obtained from boiled roots has been used as an aphrodisiac (Mulholland *et al*., 2010) and also to treat chest pains, coughs, fever and sexually transmitted diseases (STDs) (van Vuuren and Viljoen, 2008). The bark is frequently used to treat abdominal disorders, bleeding gums, earaches, skin inflammation, as well as chest problems. Combinations of leaves and roots are good at treating respiratory conditions whereas combinations of roots and bark treat respiratory disorders. The combination of the bark of *Croton gratissimus* and the root of *Amaryllidaceae* have been found good in treating swelling

when rubbed into incisions. The powdered bark of *Croton gratissimus* together with a bark of *Ocotea bullata* is used to treat uterine disorders (van Vuuren and Viljoen, 2008). Recently, it has been reported that oil extracted from *Croton gratissimus* seeds could be a promising second generation feedstock in the large-scale production of biodiesel (Bahadur *et al*., 2014).

2.5 Oil Extraction

Generally, large-scale seed oil extraction is achieved either by mechanically pressing the seeds against a solid surface or by using chemical solvents (as in hot water extraction, Soxhlet extraction and ultrasonic techniques). Alternatives to these well-established industrial processes include supercritical fluid extraction (SFE), ultrasonic-assisted extraction (UAE) and enzymatic oil extraction which are currently under investigation by many researchers over the world (Atabani *et al*., 2013). The most common and efficient solid-liquid extraction method used in producing oil for biodiesel production is the solvent extraction method; where a solute fraction (oil) is transferred from a solid material (seed) to a liquid solvent (Amin *et al*., 2010). The use of *n*-hexane as an extraction solvent in the Soxhlet extraction technique results in the highest oil yield making it the most common technique (Atabani *et al*., 2013) surpassing the supercritical fluid extraction (SFE) and ultrasonic-assisted extraction (UAE) techniques. Solvents such as *n*-hexane, used in this method are relatively cheap and can be recycled (Li *et al*., 2004). The SFE and UAE techniques, despite their high oil recovery yields, have drawbacks of being highly energy intensive and difficult to scale-up for commercial biodiesel production (Kumar and Sharma, 2015). The mechanical extraction method, on the other hand, requires large quantities of seeds for very slow oil recovery rates. It is known to damage both the oil and the meal as pressing generates high temperatures during operation (Atabani *et al*., 2013). Moreover, mechanical presses used are seed-type specific; making the mechanical press

incapable of being used to extract oil from different type of seed. In the case of the enzymatic oil extraction method, long oil processing times are a major drawback (Atabani *et al*., 2013).

Sanchez-Arreola *et al*. (2015) performed a Soxhlet extraction of *Jatropha curcas* oil using *n*-hexane, ethyl acetate and ethyl ether as extraction solvents. Of the three solvents used, the best yield was obtained with ethyl acetate extraction (54.3%). Extractions using *n*-hexane and ethyl ether gave oil yields of 47.7% and 45.9%, respectively (Sanchez-Arreola *et al*., 2015). Bahadur *et al*. (2014) reported a 23.5% oil yield (based on dry seed weight) when *n*-hexane was used as an extraction solvent in *Croton gratissimus* seeds and from an un-optimised process, a biodiesel yield of 84.65% after transesterification was obtained. The thermophysical properties of biodiesel produced from these seeds were well within those reported elsewhere in the literature for samples similar to *Croton gratissimus*. Evidently, better extraction oil yields could be obtained from *Jatropha curcas* than *Croton gratissimus* seeds for the same solvent selection in extraction. These differences can be attributed to the differences in lipid profiles of the oils extracted from these two crop species. *Croton gratissimus* oil has 24.71% unsaturated fatty acids (Bahadur *et al*., 2014) compared to 75.46% found in *Jatropha curcas* (Sanchez-Arreola *et al*., 2015). High number of double bonds (unsaturation) in fatty acids leads to greater oil solubility (Kostic *et al*., 2013). This increased solubility of oil leads to increased mass transfer between the oil and the surface of the ground seed particles resulting in higher extraction yields.

2.6 Biodiesel Synthesis

Biodiesel is mainly produced in a transesterification reaction, a chemical reaction where alcohol from an ester is displaced by another alcohol in a process similar to hydrolysis, except that transesterification uses an alcohol instead of water. During this reaction, triglycerides from oils and fats react with an alcohol in the presence of a catalyst to produce fatty acid esters (biodiesel)

and by-product glycerol. It is important to note that with recent advances in research in this field, other methods have been developed that do not require the use of a catalyst, i.e., catalyst-free. In this regard supercritical methods that employ supercritical methanol have been successfully used in biodiesel processing (Madras *et al*., 2004) albeit being energy intensive and inherently unsafe. In a catalytic environment, a basic or acidic catalyst is used to convert the glycerol based esters (triglycerides), which make up fats or oils, to alcohol based esters (methyl esters) giving off free glycerol as a by-product, as shown in reaction mechanism CR1 (Fig. 2.4). Glycerol, after separation from the reaction mixture and purified, is usually used by the pharmaceutical, cosmetics, foods and plastics industries (Vicente *et al*., 1998).

Fat or Oil	+	*3 Methanol*	⟶	*3 Methyl Ester*	+	*Glycerol*
1000 kg		*110.50 kg*		*1004.64 kg*		*105.86 kg*

Fig. 2.3: Mass balance for *Croton gratissimus* biodiesel production

The mass balance in Figure 2.3 assumes complete conversion of the triglycerides to fatty acid methyl esters (biodiesel).

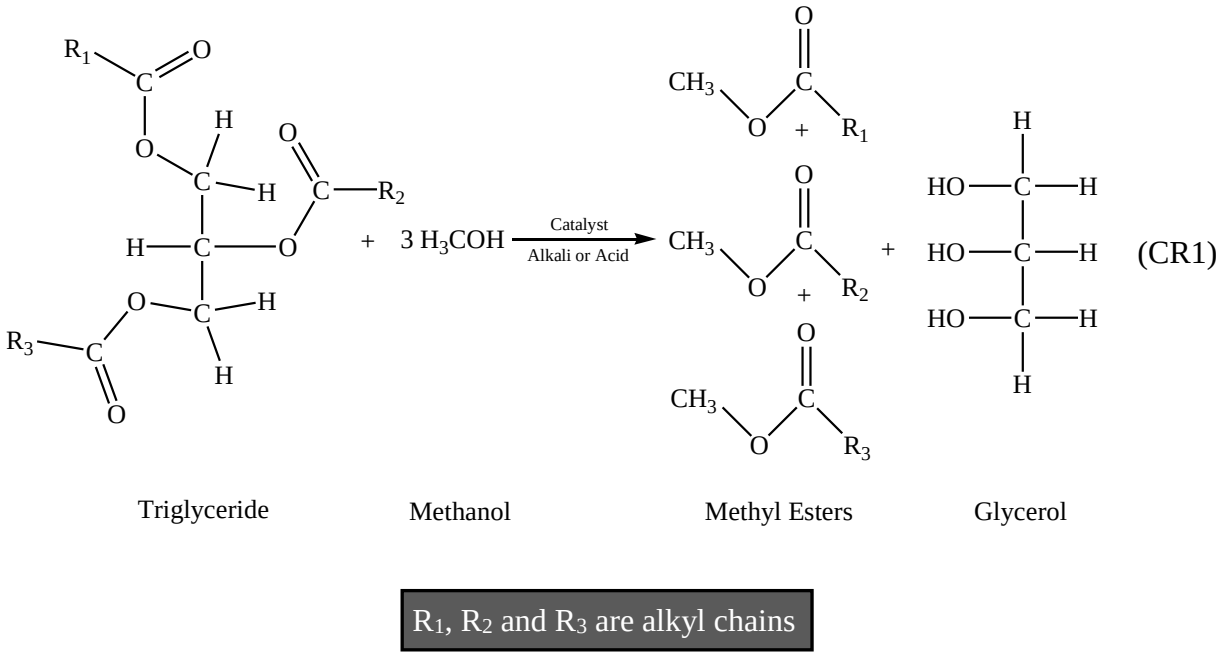

(CR1)

Fig. 2.4: Molecular representation of the transesterification reaction

The actual transesterification mechanism consists of three reversible reaction occurring in series, viz.; the conversion of a triglyceride to diglyceride followed by the conversion of the diglyceride to monoglyceride and finally the conversion of the monoglyceride to the fatty acid esters and a glycerol molecule (Chouhan and Sarma, 2011) as shown in reaction CR2 below.

$$\text{Triglyceride (TG)} + \text{R'OH} \rightleftharpoons \text{Diglyceride (DG)} + \text{R'COOR}_1$$
$$\text{Diglyceride (DG)} + \text{R'OH} \rightleftharpoons \text{Monoglyceride (MG)} + \text{R'COOR}_2 \quad \text{(CR2)}$$
$$\text{Monoglyceride (MG)} + \text{R'OH} \rightleftharpoons \text{Glycerol (GL)} + \text{R'COOR}_3$$

R′ represent an alkyl group of the alcohol used

The course of the transesterification reaction is influenced mainly by the type of catalyst (base, acid or enzyme), alcohol-to-oil molar ratio, the reaction temperature, purity of reactants, and the free fatty acid (FFA) of the oil used (Demirbas, 2008). Other variables like the type of alcohol used, residence time and agitation intensity have also been widely reported by researchers in various platforms to have an impact on the conversion of triglycerides to fatty acid esters.

In the catalytic transesterification of vegetable oils with an excess of methanol, conversions of between 90 and 97% have been recorded (Graboski and McCormick, 1998). Jeong *et al*. (2009), when working on animal fat esters, obtained impressively high triglyceride conversion rates (98.6%) where molar ratios of alcohol to oil were in the order of 7.5:1. All of these results were obtained when a single alkali catalyst was used in the transesterification of oils (vegetable oils and animal fat) to biodiesel.

When using CaO-MgO mixed oxide catalyst in biodiesel synthesis from *Jatropha curcas* plant oil, the optimisation study carried out by Lee *et al*. (2011) revealed that biodiesel yield of 93.55% could be obtained under optimum conditions of 38.67:1 methanol-to-oil ratio,

3.70wt.% catalyst, 115.87 ^{0}C reaction temperature and time of 3.44 hours. They observed that even after using CaO-MgO catalyst for 4 times, it still showed good activity giving FAME yields greater than 80%, confirming the high commercial value associated with heterogeneous catalysts.

The mechanism of an alkali catalysed transesterification (Fig. 2.6) begins with the reaction of the alcohol with the base resulting in the formation of an alkoxide and the protonated catalyst. This is followed by the nucleophilic attack of the alkoxide at the carbonyl group of the triglyceride. A tetrahedral intermediate formed then generates the alkyl ester and the corresponding anion of the diglyceride. The diglyceride produced further deprotonates the catalyst, regenerating the active species that reacts with another alcohol molecule. This catalytic cyclic activity continues until triglycerides, diglycerides and monoglycerides have all been converted to alkyl esters and the glycerol formed in the finishing of the process (Demirbas, 2008; Samios *et al*., 2009).

Sometimes, it is often necessary to carry out esterification reactions in a pre-treatment step, to reduce the Acid Value of the oil (measured as mg KOH required to neutralise 1 g of fatty acids) to below 4 mg KOH/g when dealing with high free fatty acid (FFA) oils as feedstock in biodiesel production (Zanuttini *et al*., 2014).

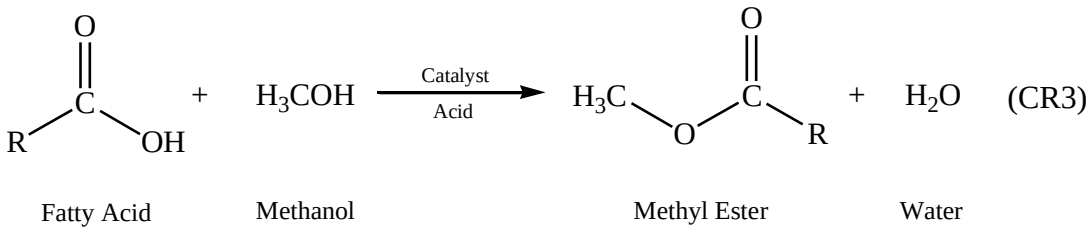

Fig. 2.5: Molecular representation of the esterification reaction

This pre-treatment step (reaction CR3) involves the use of an acid catalyst in an esterification reaction (Fig. 2.5) prior to employing either an acid or alkali catalyst in the transesterification

reaction. This prevents the formation of soaps (saponification reaction) that results when alkali catalysts are exclusively used in the process. Acid catalysts used to catalyse esterification reactions involving high FFA oils can either be homogenous or heterogeneous in nature.

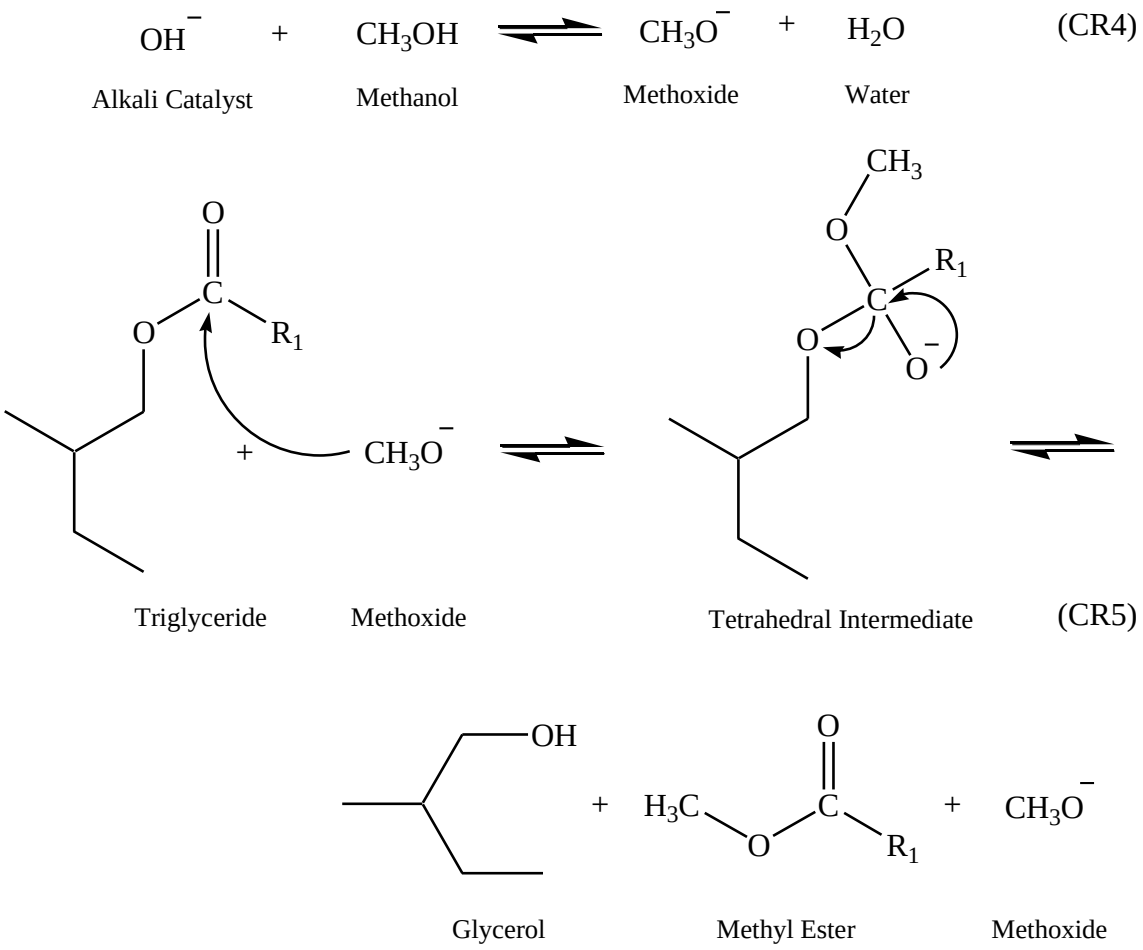

Fig. 2.6: Mechanism of alkali-catalysed transesterification of esters to produce alkyl esters

FAME yields of 99.8% from non-edible oil extracted from Jatropha seeds have been reported by Shuit *et al.* (2010). In their attempt to reduce production cost, they combined both the oil extraction process step and the transesterification step to produce biodiesel with an impressive FAME yield in one single processing step (Shuit *et al*., 2010).

High concentrations of acid catalysts have also been used to drive both the esterification and transesterification reactions to completion in a single step. This route was taken by Bahadur *et*

al. (2014) to produce biodiesel from high FFA *Croton gratissimus* oil using a superacid, sulphated zirconia (SO_4^{2-}/ZrO_2) as a catalyst. This catalyst was preferred because of its added advantage over other heterogeneous catalysts. Its ability to simultaneously catalyse esterification and transesterification reactions makes it stand out as a catalyst with high acid strength and stability. It has been reported that it also possesses a combination of acid sites (Brønsted and Lewis) that are significant factors in the enhancement of selectivity and activity (Rattanaphra *et al*., 2012).

Acid catalysed transesterification mechanism (Fig. 2.7) starts with the protonation (electrophilic H^+ attack on the oxygen) of the carbonyl group of the triglyceride. This leads to carbocation where a nucleophilic OH^- attack of the alcohol on carbon produces a tetrahedral intermediate. The intermediate dissociates via the transition state and eliminates the glycerol to form a new ester and to regenerate the catalysts (Demirbas, 2008).

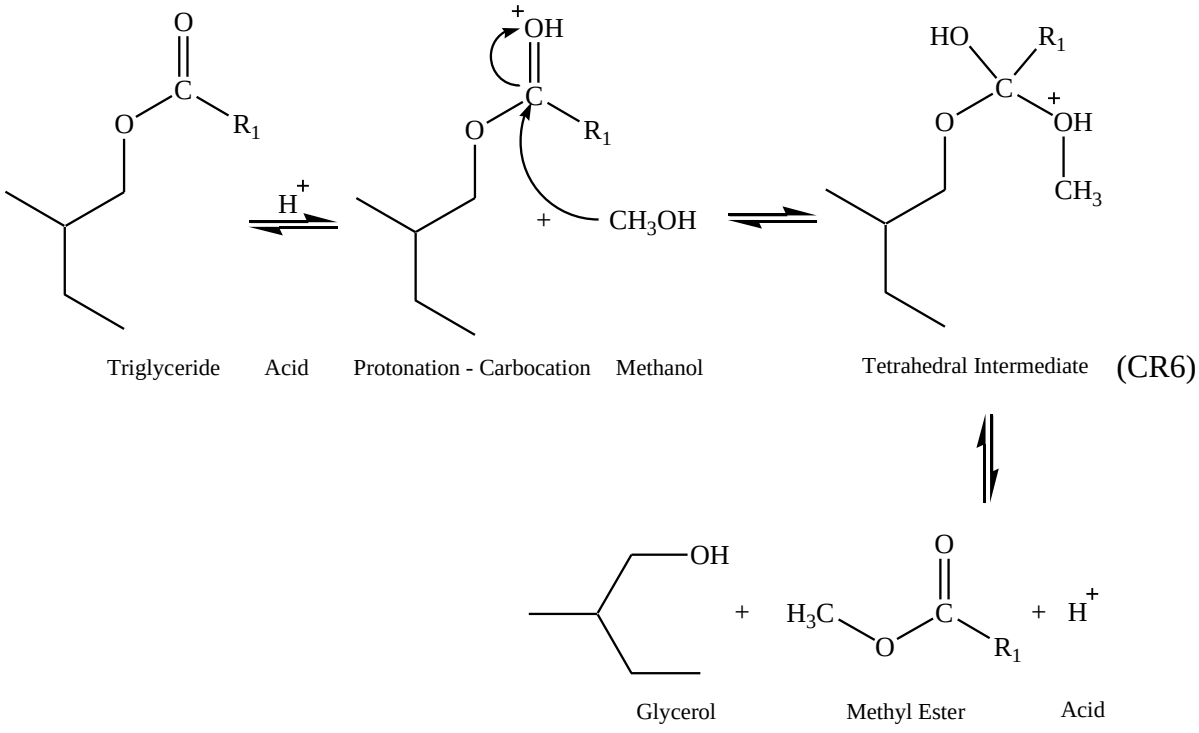

Fig. 2.7: Mechanism of acid-catalysed transesterification of esters to produce alkyl esters

2.7 Catalysts in Biodiesel Synthesis

Esterification and transesterification reactions, which usually occur at low temperatures and pressures, need catalysts to drive them forward otherwise the conversion of free fatty acids and triglycerides to fatty acid esters may not be realised. Catalysts in these reactions enhance the solubility of alcohols in oils and fats thus increasing the rate of reaction (Atabani *et al*, 2012). When catalysts are not used, the reaction can only proceed under supercritical conditions; the conditions that are unfavourable as they increases the energy requirements for biodiesel processes. It is for this reason that catalytic methods are most preferred in the esterification and transesterification mechanisms (Endalew *et al*, 2011).

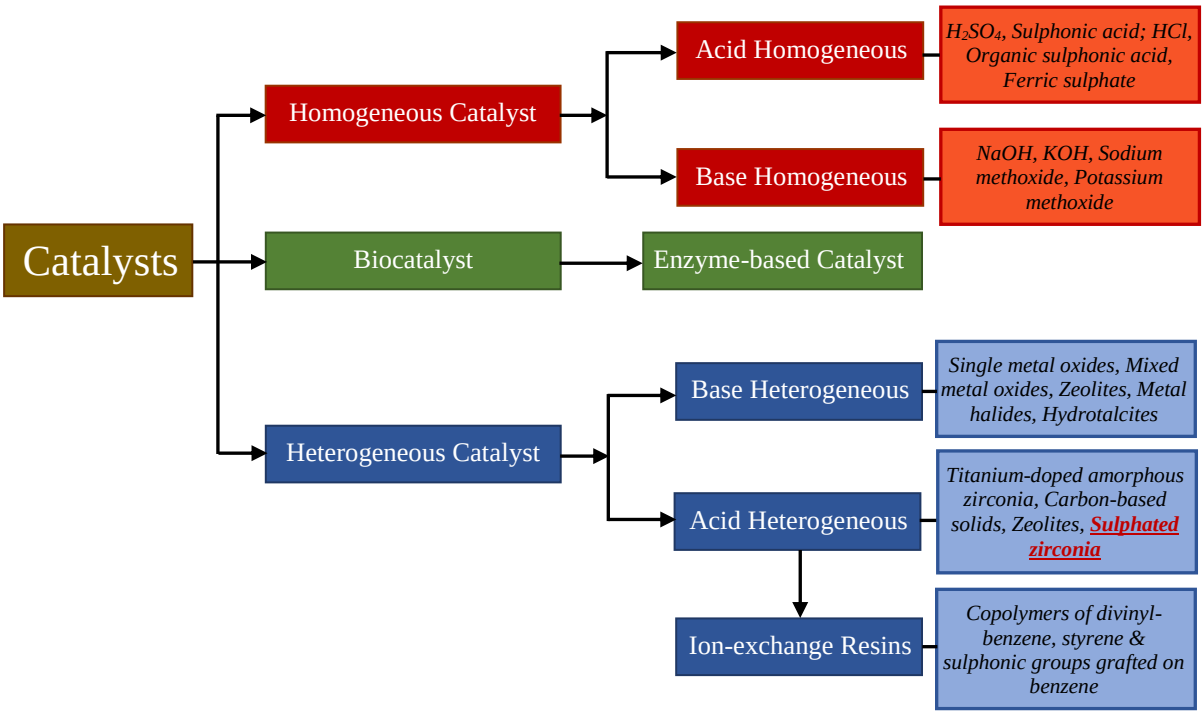

Fig. 2.8: Classification of Catalysts used in Biodiesel

Biodiesel production is characterised by the use of three categories of catalysts, viz., alkalis (bases), acids and enzymes (Fig. 2.8). Enzyme catalysts are deemed not commercially viable because of their high costs and longer reaction times (Leung *et al*, 2010). Alkalis and acids, the most commonly used catalyst types in biodiesel synthesis, are further classified into

homogeneous and heterogeneous catalysts (Talha and Sulaiman, 2016). During transesterification, homogeneous catalysts remain in the same (liquid) phase as the reactants whereas heterogeneous catalysts remain as a different phase (i.e., solid, immiscible liquid or gaseous) to that of the reactants (Helwani *et al*, 2009; Zabeti *et al*, 2009).

2.7.1 Homogeneous Catalysts

Homogeneous alkali catalysts commonly used in the transesterification of triglycerides are the metal hydroxides, viz., sodium hydroxide and potassium hydroxide and their alkoxide derivatives, viz., sodium methoxide, and potassium methoxide. The alkaline metal alkoxides ($NaOCH_3$ and $KOCH_3$) have shown superior qualities of giving high biodiesel yields (greater than 98%) in short residence times (30 min) at low molar catalyst concentrations (0.5 mol %) and low reaction temperatures and atmospheric pressure. For the same percentage conversion of vegetable oils to biodiesel, the catalyst concentration of the less active alkaline metal hydroxides (NaOH and KOH) must be increased to between 1 and 2 mol % (Helwani *et al*, 2009). A known drawback of using homogeneous alkali catalysts is their hygroscopic nature that enables them to absorb water during storage (Leung *et al*, 2010). The presence of water (produced when wet catalyst dissolves in alcohol) and high free fatty acids (FFAs) promote the formation of soaps and more water. This leads to product separation and purification challenges which could require expensive and sophisticated equipment to solve.

Homogeneous acid catalysts are insensitive to high FFA feedstock (non-edible oils) and are thus able to simultaneously catalyse both the esterification and the transesterification reactions. In this category, catalysts commonly used in biodiesel processing are sulphuric acid, sulphonic acid, hydrochloric acid, organic sulphonic acid and ferric sulphate (Atadashi *et al*, 2013). A major drawback with these catalysts, when compared to their alkali counterparts, is their slow

activity that results in longer reaction times. To counteract this and get good product yields within reasonable reaction times, high alcohol-to-oil molar ratios and high catalyst concentrations are often employed (Helwani *et al*, 2009). Even with these measures taken to improve the acid-catalysed transesterification reactions, they remain many folds slower than the alkali-catalysed reactions. It is for this reason and the fact that they are highly corrosive strong liquid acids, posing serious threat to the environment, that they are not favoured in the biodiesel industry (Lotero *et al*, 2006).

However, homogeneous acid catalysts have been used with success in the esterification of high free fatty acid oils. This pre-treatment step reduces the Acid Value of oil in preparation for the base-catalysed transesterification process. Betiku *et al*. (2014) used H_2SO_4 as a homogeneous acid catalyst in the esterification of non-edible *Azadirachta indica* seed oil and obtained an 88% Acid Value reduction from 10.18 mg KOH/g to 1.23 mg KOH/g. The optimum conditions given by their developed RSM model were; 0.55 ($^v/_v$) methanol-to-oil ratio, 0.45% ($^v/_v$) catalyst concentration, 36 min reaction time and 60 ^{0}C reaction temperature.

2.7.2 Heterogeneous Catalysts

Sani *et al*. (2014) best describes heterogeneous solid catalysts as either “non-equilibrium” or “dynamic” in nature as the prevailing synthesis reaction conditions have a heavy influence on their final catalytic structures. When small changes in the reaction medium occur, large or complete morphological changes on the catalyst surface structure occur as a result of the adsorbate-induced surface-reconstruction relationship that exists in these catalysts. Hence, for a solid acid heterogeneous catalyst, its active state is only predominant during the catalytic process (Sani *et al*, 2014).

Although these solid catalysts show greater potential when compared to homogeneous catalysts, their use is faced with diffusion limitations leading to reduced rates of reaction. This mass transfer difficulty originates from the catalyst during reaction, forming a three-phase mixture with immiscible combination of oil and alcohol. To assist with the miscibility problem between the oil and alcohol, a co-solvent such as *n*-hexane, ethanol, tetrahydrofuran (THF) or dimethyl sulphoxide (DMSO) is usually added into the reaction mixture to increase the rate of reaction (Semwal *et al,* 2011).

According to the Hattori's classification, examples of heterogeneous base catalysts in common use in biodiesel production, from the one with the lowest to the highest catalytic activity, are the single metal oxides (e.g., CaO, ZnO and MgO), mixed metal oxides (Al_2O_3-SnO_2, Al_2O_3-ZnO and MgO-La_2O_3), zeolites, supported metal halides and hydrotalcites (e.g., Mg-Al hydrotalcites) (Hattori, 2004). This progressive improvement in the search for novel heterogeneous base catalysts was prompted by earlier catalysts developed in this category (the metal oxides) that were frequently subjected to leaching rendering them less active than their homogeneous counterparts. These metal oxide catalysts are known to require high temperatures and pressures and high alcohol-to-oil ratios to achieve respectably high ester conversions. They are susceptible to temporary active site poisoning due to the reaction between the basic sites on the surface and the alcohol. This results in the di and mono-glyceroxide anions failing to dissolve in the oil phase and staying near the positive counter ion on the surface of the catalyst (Santacesaria *et al,* 2012).

Heterogeneous solid acid catalysts, on the other hand, have the ability to simultaneously catalyse both the esterification and transesterification reactions within reasonable short reaction times. Other advantages of catalysts found in this class include:

- Insensitivity to free fatty acid (FFA) oils thus allowing the use of low grade non-edible feedstock,
- Complete elimination of the biodiesel washing step,
- Much purer products obtained as a result of ease of separating catalyst from the reaction mixture,
- Regeneration and recycling of the solid catalyst is possible which reduce biodiesel processing costs,
- Corrosion problems are greatly minimised even when reaction species used are acidic,
- Ease of incorporation into continuous processes,
- Deactivation of the catalyst is minimised by sterically hindering solvation of the catalytic active sites from water contamination (Chouhan and Sarma, 2011; Sani *et al*, 2014).

These catalysts are suitable for both low and high temperature operations (Aransiola *et al*, 2014). They have drawn much of the attention from industry and academia because of their high activity at low temperature that makes operation where thermodynamic equilibrium compositions contain a fraction of the desired products possible (Srinivasan *et al*, 1995). They possess multiple sites with varying strengths of Brønsted and Lewis acidity. Brønsted acid catalysts promote simultaneous esterification and transesterification reactions. Compared to Brønsted acid sites, Lewis sites are more active but are susceptible to water poisoning (Talha and Sulaiman, 2016). A heterogeneous solid acid catalyst that possesses both Brønsted and Lewis acid sites is therefore the most sort out catalyst in biodiesel synthesis; and one such catalyst is claimed to be the sulphated zirconia (SO_4^{2-}/ZrO_2).

2.8 Optimisation of Biodiesel Processes

In the manufacturing industry where responses like product yields, product quality and equipment efficiencies are all influenced by an array of process variables, it is often necessary to conduct optimisation studies aimed at obtaining economically feasible processes. Such processes are characterised by their low operating costs which can be attributed to low utility costs, optimal materials usage and reduced energy consumption. To achieve this economical goal and obtain the optimum operating conditions, a number of optimisation tools are available for use; and one such tool is the Response Surface Methodology (RSM).

The RSM is a collection of mathematical and statistical techniques that are used for modelling and analysis in applications where a response of interest is influenced by a number of variables and the objective is to optimise (minimise or maximise) this response. Its main objective is "to determine the optimum operating conditions for the system or to determine a region of the factor space in which operating specifications are satisfied" (Montgomery and Runger, 2003). This method uses multiple regression and correlation analyses as tools to assess the effects of the chosen independent factors on the dependent variables. It is known to generate sufficient data for statistically acceptable results from a few experimental runs (Jeong *et al*, 2009). The RSM uses the Central Composite Design (CCD) or the Box-Behnken Design (BBD) to fit a model by the least squares technique and verify the adequacy of the model using a diagnostic tool, the Analysis of Variance (ANOVA) (Ahmadi *et al*, 2005).

CCDs are based on 2-level factorial designs, augmented with centre points, n_c and axial points, α to fit quadratic models. These designs usually have 5 levels $(-\alpha, -1, 0, +1, +\alpha)$ for each factor, k and can be made to be rotatable by proper selection of the axial spacing to give axial points. The axial points are encoded as $+\alpha$ and $-\alpha$ with a value of α being $2^{k/4}$ where k

is the number of factors (independent variables). When this has been achieved, the standard deviation of the predicted response is constant at all points equidistant from the centre, resulting in the rotatability of the design (Montgomery and Runger, 2003). The Central Composite Rotatable Design (CCRD) has therefore a total of $2^k + 2k + n_c$ points that equates to the number of experimental runs necessary for the RSM optimisation. Replicates of test at the centre point represented by n_c provide an independent estimate of the experimental error. The complete quadratic model for k factors has, therefore, $(k+1)(k+2)/2$ terms (Ferreira *et al*, 2007a), which include regression coefficients, individual factors and interaction factors, and is given by;

$$Y = \beta_0 + \sum_{i=1}^{k} \beta_i X_i + \sum_{i=1}^{k} \beta_{ii} X_i^2 + \sum_{i<j} \sum \beta_{ij} X_i X_j + \varepsilon \qquad (1)$$

where *Y* is the predicted response, β_0 is the intercept coefficient, β_i is the linear coefficient, β_{ij} is the interaction coefficient, β_{ii} is the quadratic coefficient, X_i and X_j are the uncoded values of the independent variables and ε is the random error (Tan *et al*, 2008).

The BBD, an alternative to CCD, are a class of second-order rotatable or almost rotatable designs that are based on 3-level partial factorial designs (Ferreira *et al*, 2007a). These designs do not have runs at the extreme combinations (higher or lower levels) of all the factors, but compensate by possessing better prediction precision in the centre of the factor space. Compared to the CCD, the BBD always gives fewer experimental runs. For the development of the Box-Behnken Design, a total of $2k(k-1) + n_c$ experimental runs is required, where k is the number of factors and n_c is the number of replicate runs taken at the centre point (Ferreira *et al*, 2007b).

With these two design techniques (Central Composite and Box-Behnken Designs) available, one has to select the specific one to use in a particular situation. The most important factors to consider are the number of experimental runs and the effects of interactions. Either way, these techniques are both used with the ANOVA, a statistical tool that is able to give a rigorous analysis of the developed model.

Doehlert Design (DD) is yet another optimisation tool that has been extensively exploited by many researchers in a variety of fields. Unlike the CCD and the BBD, these designs are characterised by being asymmetrical, affording the researcher the freedom to study different factors at different numbers of levels (Doehlert, 1970). DDs are incapable of rotation, despite being spherical but have the ability to fill the entire design space hence the claim that they are "uniform space fillers". These designs make it possible to cover an experimental range with a uniform grid of points, even when the range being studied is irregular (Ferreira *et al*, 2007a; Doehlert, 1970).

An optimisation study carried out using RSM involves three stages. First, the determination of independent variables and their levels followed by the selection of the experimental design prediction and verification of the model equation and finally the graphical presentation of the model equation and the determination of the optimum operating conditions (Bas and Boyaci, 2007). The determination of independent variables and their levels is a critical stage as choosing wrong levels may result in an unsuccessful optimisation. The classical one-factor-at-a-time (OFAT) optimisation approach is usually used at this stage to develop screening experiments to help identify important independent parameters that are most likely to affect the chosen responses. This gives the experimenter direction in which the improvements lie and hence facilitate the identification of the levels of parameters (Bas and Boyaci, 2007).

Vicente *et al*. (2007) successfully developed a model for FAME synthesis from sunflower oil over a potassium hydroxide (KOH) catalyst. They applied a full CCD for 3 independent variables at 2 levels. Independent variables investigated for the responses of biodiesel yield and purity were initial catalyst concentration, methanol-to-oil molar ratio and temperature. The second-order models they developed to predict these responses were significant. Their results revealed that the operating conditions of a temperature of 25 ^{0}C, a catalyst concentration of 1.3% wt and a 6:1 methanol-to-oil molar ratio could give maximum purity and yield of 100% and 98.4%, respectively.

Dwivedi and Sharma (2015) conducted an optimisation study to maximise the biodiesel yield from Pongamia oil. They used a Box-Behnken design with 4 factors, viz., methanol-to-oil ratio, reaction time, reaction temperature and amount of KOH catalyst, to study the response pattern and to determine the optimum combination of these factors. The model developed was significant, validating its reliability in establishing a correlation between the process variables and the Pongamia biodiesel yield. They found that a biodiesel yield of 98.4% was achievable with a methanol-to-oil ratio of 11.06 using 1.43% w/w KOH catalyst in 81.4 minutes at a temperature of 56.6 ^{0}C.

Two optimisation tools were used by Betiku *et al*. (2014) in their work on biodiesel produced from non-edible Neem (*Azadirachta indica*) seed oil. They used the response surface methodology (RSM) to optimise the esterification process followed by the transesterification process where artificial neural networks (ANN) was used. The esterification reaction was catalysed by H_2SO_4 which reduced the Acid Value of Neem oil from 10.18 mg KOH/g oil to less than 2 mg KOH/g oil. A potassium hydroxide (KOH) catalyst was then used in the transesterification reaction giving a biodiesel yield of 98.7% at a catalyst concentration of 1.01%, temperature of 48.15 ^{0}C, methanol-to-oil ratio of 0.200 in a time interval of 42.9 min.

The model developed by Mendonca *et al*. (2011) using the Doehlert matrix had a good predictive performance for both the chosen responses of biodiesel purity and yield. They first applied the 2-level full factorial design to establish the factors with greater influence on the beef tallow biodiesel purity and yield. Thereafter a full optimisation study was carried out using the Doehlert matrix method. To find the critical point of the second-order equation developed, they use the Lagrange criterion. From the factorial design they found the methanol-to-oil ratio and KOH catalyst to have had greater influence on tallow biodiesel purity and yield and selected these factors for the Doehlert optimisation. Reaction time and temperature were less significant in factorial design optimisation hence were fixed at their minimum, 20 min and 50 ^{0}C, respectively, in the Doehlert matrix. The Lagrange criterion revealed that according to the quadratic model obtained, the point of highest purity was at a methanol-to-oil ratio of 9.30 and KOH catalyst concentration of 3.49 wt%. The optimised models developed from the Doehlert matrix showed that 99.4% purity and 88.4% yield could be obtained when the reaction conditions are: Methanol-to-oil ratio = 7.5, KOH catalyst concentration = 1.5 wt%, reaction time = 20 min and temperature = 50 ^{0}C.

Chapter 3. Materials and Methods

All experiments were conducted in the Chemical Engineering laboratories at Mangosuthu University of Technology (MUT). The bulk of the funds for this work was obtained from the Research Directorate of the Durban University of Technology (DUT) and was used mainly to purchase glassware and chemicals. Analytical equipment used in the characterisation of extracted *Croton gratissimus* oil and finished biodiesel (FAME) were from the MUT Research laboratory. The sulphated zirconia catalyst, SO_4^{2-}/ZrO_2 was synthesised in our Chemical Engineering laboratories and calcined in the Chemistry Department of the University of KwaZulu Natal (UKZN) Westville Campus. Catalyst characterisation was done in the University of Cape Town (UCT) and the NRF's iThemba Laboratories in the Western Cape.

3.1 Materials and Equipment

Croton gratissimus grains were obtained from selected trees in the city of Lubumbashi, Upper Katanga province, South-Eastern region of the Democratic Republic of Congo (DRC). Zirconyl chloride octahydrate ($ZrOCl_2 \cdot 8H_2O$), 25% NH_4OH, $AgNO_3$ AR and ≥ 85% KOH pellets were purchased from Sigma-Aldrich South Africa. Methanol AR of 99% purity, 99.9% ($^v/_v$) Ethanol AR, 99% *n*-Hexane (ChromAR® HPLC), 98% H_2SO_4 AR, 99% Diethyl ether AR and Phenolphthalein were all purchased from Merck Laboratories in South Africa.

A kitchen blender and a mortar-and-pestle were used for the fine grinding of seeds. Drying of ground seeds and intermediate catalyst products was carried out by a Labcon Drier equipped with a timer (Fig. 3.1). An Orion Star A215 pH/Conductivity Meter was used during precipitation in the catalyst synthesis. An analytical balance, RADWAG® AS 220/C/2, was used for accurate weight measurement of catalyst samples used in FAME production. A

HERMLE Centrifuge (Fig. 3.2) was used for final separation of the esterification and

Fig. 3.1: Drier with Built-in Timer

Fig. 3.2: Variable Speed Centrifuge

transesterification products. Laboratory-assembled equipment, shown in Figures 3.6, 3.10 and 3.13, were used in oil extraction, solvent recovery and biodiesel production experiments, respectively. A PerkinElmer Clarus® 580 Gas Chromatograph equipped with a Clarus® SQ 8S Mass Spectrometer (GC-MS), Fig. 3.3, was used for the characterisation of the extracted oil and finished biodiesel product.

Fig. 3.3: PerkinElmer GC-MS

3.2 Experimental Methods

Figure 3.4 below, gives a step-by-step overview of all the experimental work done for the purpose of conducting a full optimisation study of the biodiesel production process.

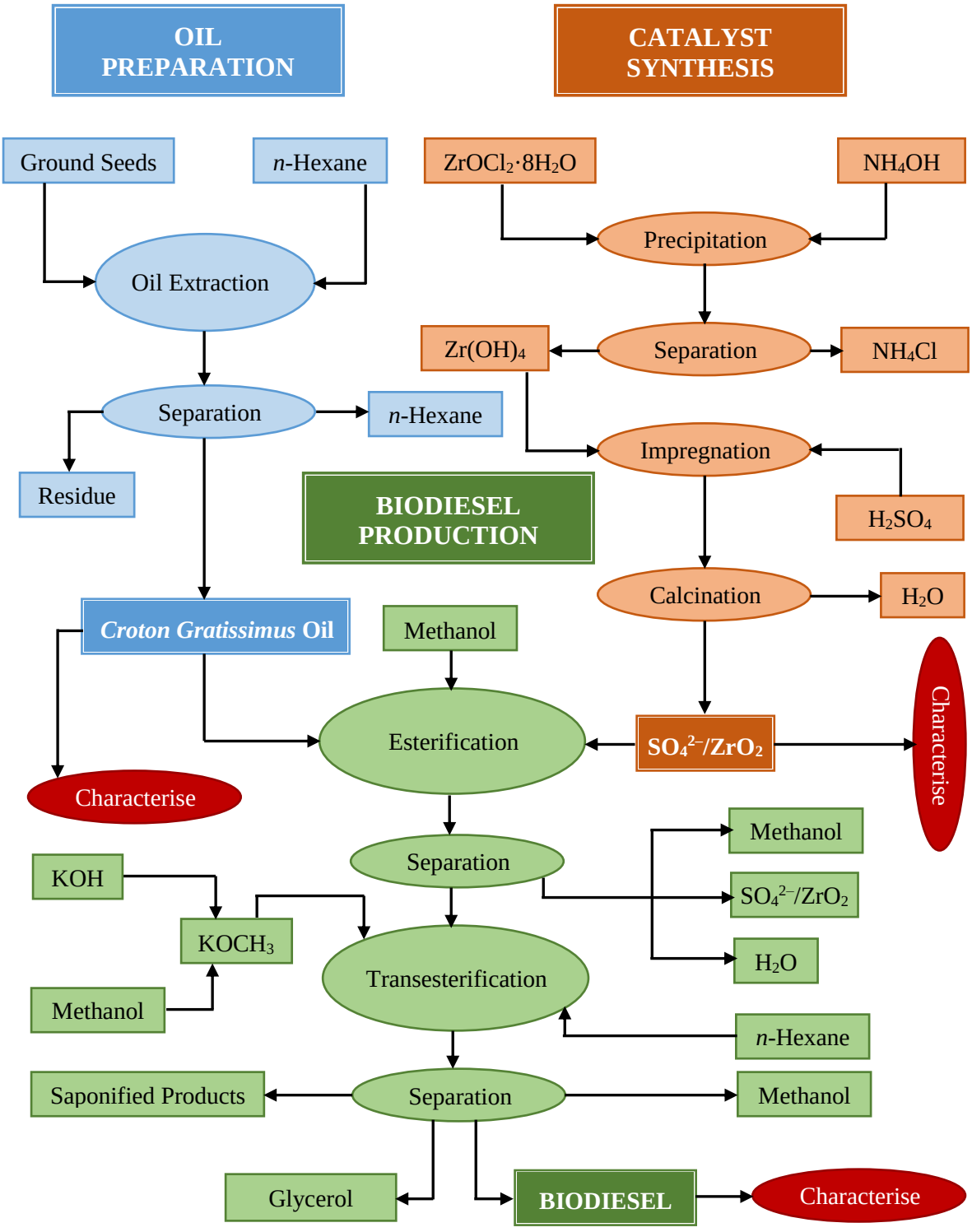

Fig. 3.4: Experimentation Process Flow Chart

3.2.1 Oil Extraction Process

The oil extraction process was carried out in 3 stages (feed preparation, solvent extraction and product separation) using the Chemical Solvent Extraction (CSE) technique. The solvent extraction stage began with solvent selection to determine which solvent between *n*-hexane and ethyl acetate should be used in the extraction of oil from *Croton gratissimus* grains. From the results obtained, *n*-hexane oil extraction process seemed to possess superior qualities when compared to ethyl acetate solvent (see Published Work in Appendix G). It is for this reason that in this work, *n*-hexane was selected as the extraction solvent as it gave the highest oil yields under moderate conditions of extraction temperature and residence times.

3.2.1.1 Feed Preparation:

On arrival in our laboratories, the *Croton gratissimus* grains were dried in open air under direct sunlight for 2 days. Thereafter they were de-shelled with a hammer to remove the 3-lobed fruit capsules and to expose the seeds (Fig. 3.5). A high speed kitchen blender was used

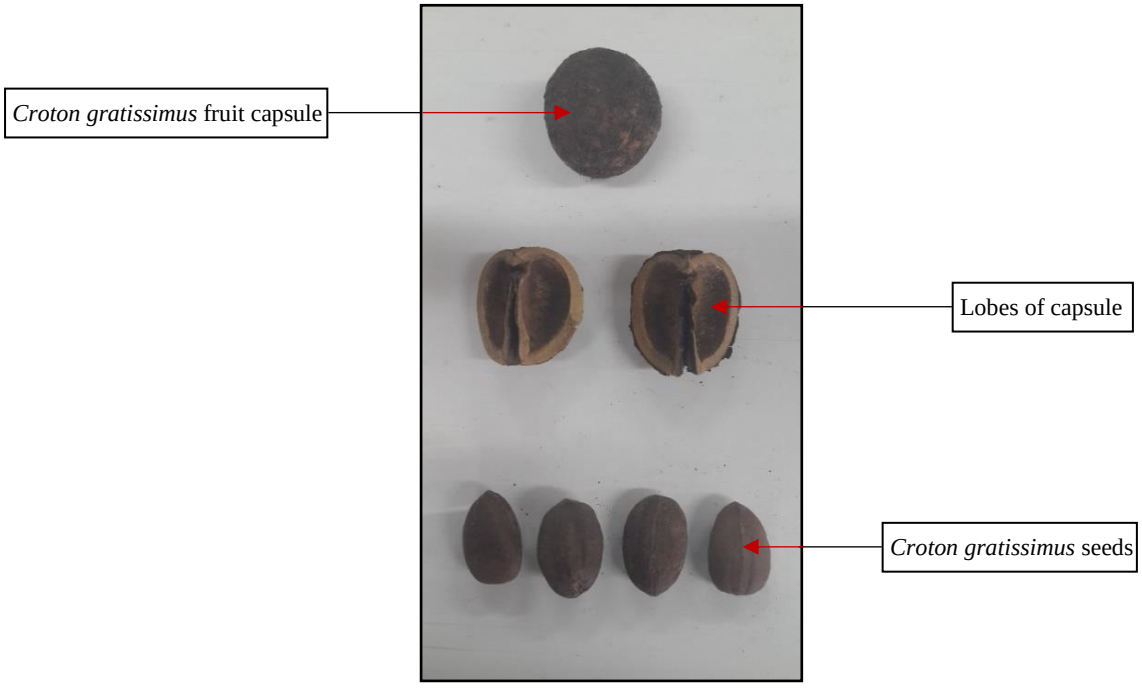

Fig. 3.5: *Croton gratissimus* seeds

to crush the seeds to small particles. Final grinding of seeds to the desired particle size was done using a laboratory mortar and pestle. Classification of ground seeds was done using a set of stainless steel laboratory sieves. Seeds collected for extraction were the ones that passed through a 1000 μm (18 mesh) sieve tray but still got retained by a 500 μm (35 mesh) sieve tray. The average moisture content of the seeds was found to be 3.70 ± 0.5% on dry basis. Hence collected seeds were oven-dried in a Labcon Drier at 105 ^{0}C for 6½ hours to remove moisture before extraction.

3.2.1.2 Solvent Extraction:

Solvent extraction was carried out in a 2-litre four-necked round-bottomed flask fitted with a Grahams reflux condenser. Continuous stirring was facilitated by a propeller-type impeller

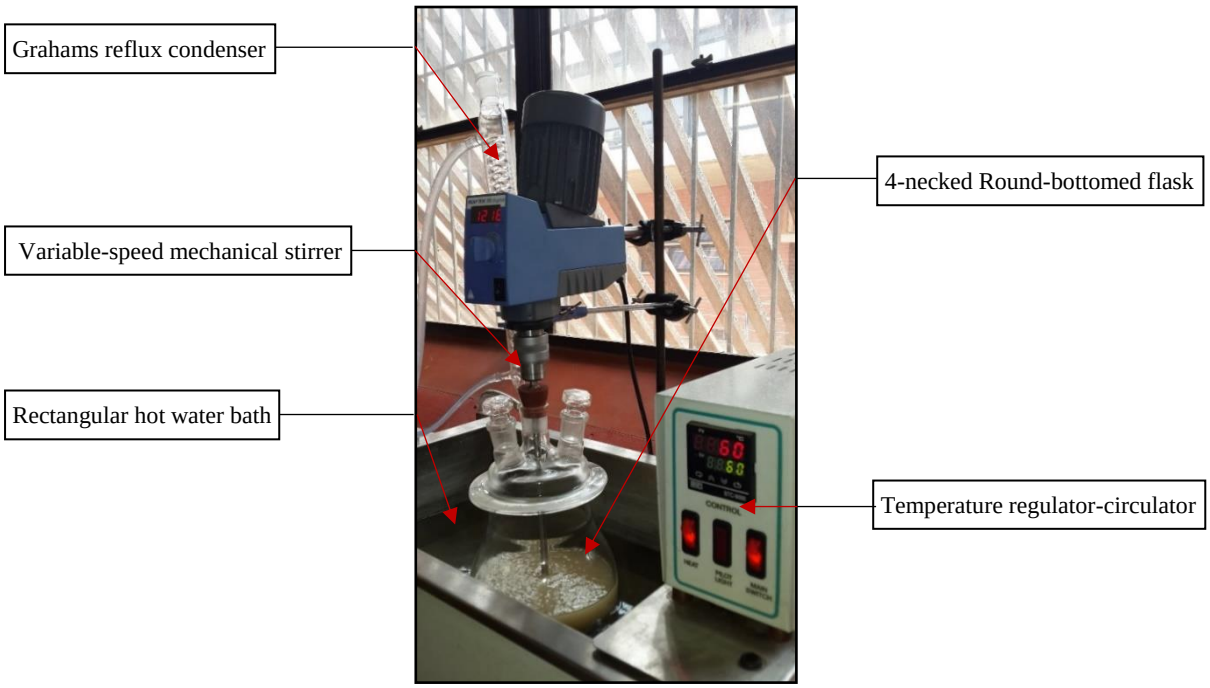

Fig. 3.6: Oil extraction set-up

connected onto a variable speed electric motor. A rectangular hot water bath with an immersion temperature regulator-circulator was used to offer consistent heating at predetermined temperatures (Fig. 3.6). Oil extraction process was carried out in 4 batches, of ± 290 g of ground

seeds each, at a constant temperature of 60 ^{0}C, solvent-to-feed ratio of 2.5 ml/g and allowed to mix for 4 hours. A known mass of dried seeds was placed in a round-bottomed flask and a proportional amount of *n*-hexane was added. A propeller-type impeller set at 1550 rpm (revolutions per minute) was used for agitation.

3.2.1.3 Product Separation:

After the 4 hours of mixing had elapsed, the miscella was filtered using a laboratory filtration equipment set-up, i. e., a Buchner flask fitted with a funnel and connected to a vacuum supply

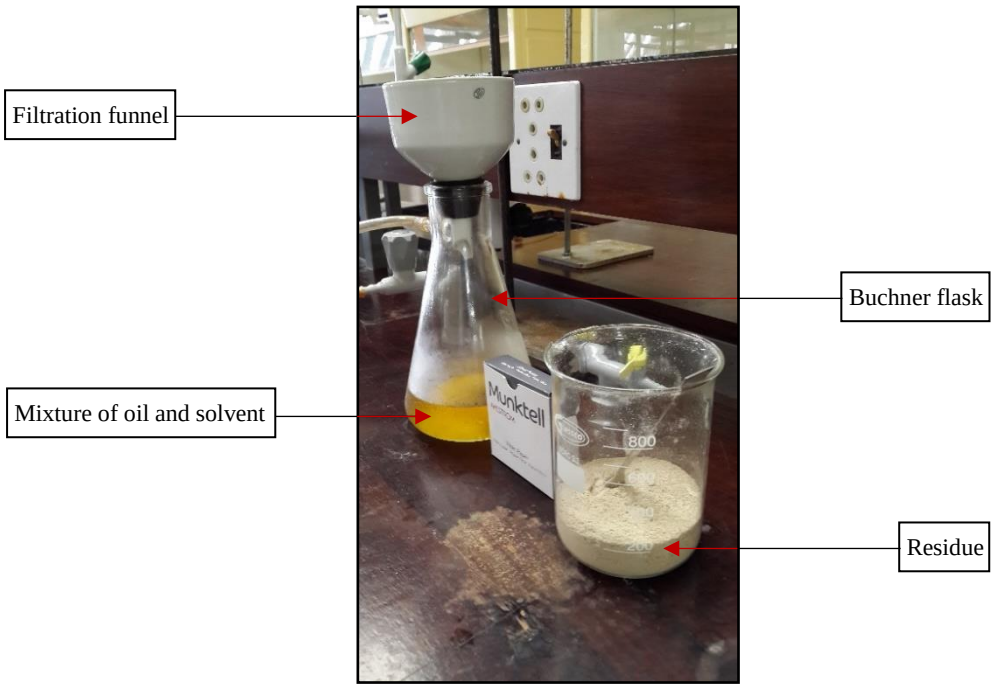

Fig. 3.7: Filtration equipment

line (Fig. 3.7). A mixture of oil and *n*-hexane was collected in the flask and the residue was discarded. The mixture was then fed to a flash distillation equipment set-up to separate the *n*-hexane from oil. This flash distillation equipment set-up consisted of a 1-litre round-bottomed flask, a reflux condenser, heating jacket and a collection flask attached to the end of the condenser (Fig. 3.8). Heating was effected by the Electro-Thermal constant-temperature

heating jacket set at 70 ^{0}C, a temperature slightly greater than the boiling point temperature of *n*-hexane (68 ^{0}C).

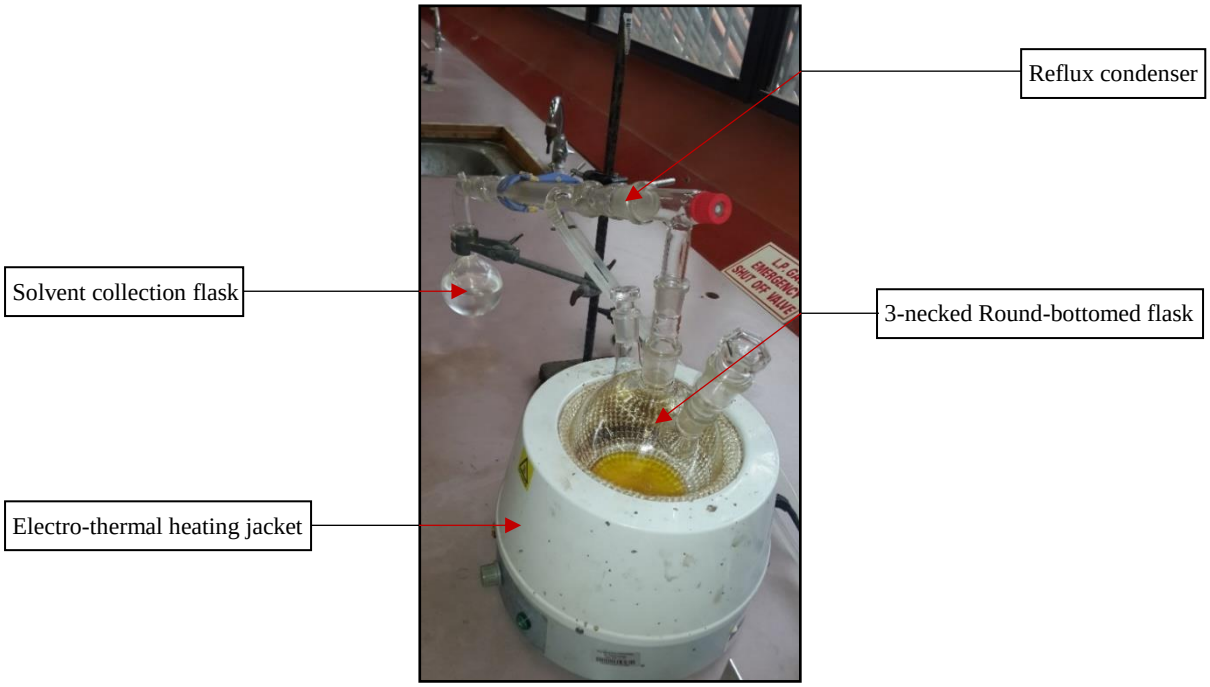

Fig. 3.8: Solvent recovery unit

The extraction yield was calculated as the ratio of the mass of the extracted oil to that of the *Croton gratissimus* seeds fed into the extraction flask. The solvent recovery rate was found as the ratio of the mass of the solvent in the collection flask after all the *n*-hexane has been evaporated and condensed to that which was fed into the extraction flask.

3.2.1.4 Oil Characterisation:

Acid Value (AV) of Oil: Standard solutions of the solvent diethyl ether in ethanol and 0.5 N potassium hydroxide (KOH) were prepared. A known mass (± 2.50 g) of oil was placed in an Erlenmeyer flask, dissolved with 150 ml of the solvent and few drops of phenolphthalein indicator added. With constant stirring, this was titrated against the KOH solution in a burette. The Acid Value of *Croton gratissimus* oil was given by the following equation:

$$\text{Acid Value}\left(\text{AV}\right)=\frac{56.1\times \text{N}\times \text{V}}{\text{m}} \tag{2}$$

where the constant 56.1 is the molar mass of KOH, N is the exact normality of the standardised KOH solution, V is the volume (ml) of the KOH solution and m is the mass (g), of the oil.

Saponification Value (SV) of Oil: Standard solutions of ethanolic potassium hydroxide, i.e., 0.5 N KOH in ethanol and 0.5 N aqueous hydrochloric acid were prepared. About ± 2 g of oil was placed in a 250 ml Erlenmeyer flask and 25 ml of ethanolic KOH solution added via a pipette. Onto the mouth of the flask, a reflux condenser was fitted and the unit placed on a hot magnetic plate. With constant low-speed stirring and heating, the mixture was boiled gently. After 1 hour of heating, ± 0.70 ml (few drops) of phenolphthalein was added to the hot solution and titrated with the standard HCl solution until the colour of the indicator changed. A blank test (titration) was carried out in the same way. The saponification value of *Croton gratissimus* oil was given by the following equation:

$$\text{Saponification Value}\left(\text{SV}\right)=\frac{56.1\times \text{N}\times \left(\text{V}_{\text{b}}-\text{V}\right)}{\text{m}} \tag{3}$$

where, N is the exact normality of the standardised HCl solution, V_b is the volume (ml) of the standardised HCl solution used for the blank test, V is the volume (ml) of the standardised HCl solution used for the oil and m is the mass (g) of the oil.

3.2.2 ZrO_2SO_4 Catalyst Synthesis

Sulphated zirconia catalyst was synthesised following the method proposed by Chen *et al* (1993) and modified by Reddy *et al* (2005).

3.2.2.1 Precipitation of Zirconia:

A 0.60 M standard solution was prepared in a 100 ml volumetric flask by dissolving a known mass (19.3878 g) of Zirconyl chloride octahydrate, $ZrOCl_2 \cdot 8H_2O$ (GR grade) in distilled water. The clear solution obtained was placed in a 300 ml beaker and agitation effected by a magnetic stirrer. With constant stirring, in the hydrolysis step, 25% dilute aqueous ammonia (NH_4OH) from a 50 ml flask, was cautiously added into the beaker to form a $Zr(OH)_4$ precipitate (Fig. 3.9). Dropwise addition of NH_4OH solution was stopped when the pH of the mixture in the beaker reached 10. The precipitate formed was filter-washed with de-ionised water till the chloride ions could no longer be detected by a 5% solution of $AgNO_3$.

$$ZrOCl_2 \cdot 8H_2O + 2NH_4OH \xrightarrow{Precipitation} Zr(OH)_4\downarrow + 2NH_4Cl + 7H_2O \quad (CR7)$$

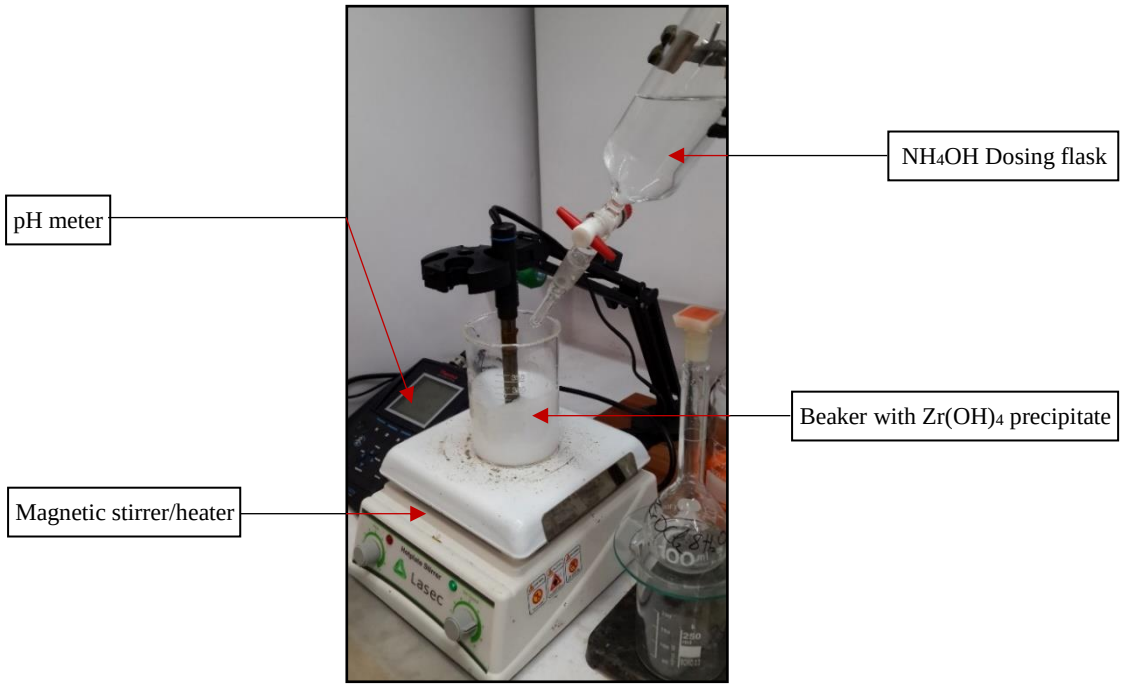

Fig. 3.9: $Zr(OH)_4$ Precipitation and Impregnation Set-up

3.2.2.2 Impregnation of Zirconium Hydroxide:

The filtered precipitate was oven-dried at 120 ^{0}C for 20 hours and thereafter ground to fine powder using a mortar and pestle. A standard solution of 0.50 M H_2SO_4 was prepared by dissolving a known volume (13.40 ml) of 98% H_2SO_4 in a 250 ml volumetric flask and filled to the mark with de-ionised water. This standard solution was then added to the fine powder at a rate of 15 ml per gram of powder to form $Zr(OH)_2SO_4$ in an impregnation (doping) step and the mixture was stirred vigorously for 3 hours.

$$Zr(OH)_4\downarrow + H_2SO_4 \xrightarrow{Impregnation} Zr(OH)_2SO_4\downarrow + 2H_2O \qquad \text{(CR8)}$$

3.2.2.3 Drying and Calcination:

When the 3-hour time had elapsed, water from impregnated zirconia was removed by filtration and the wet solid was oven dried at 120 ^{0}C for a further 20 hours. The dried product was allowed to cool at room temperature in preparation for the calcination step. The catalyst was then heated in the kiln set at 620 ^{0}C at a heating rate of 4 ^{0}C per min for 4 hours in an air atmosphere to remove the last traces of water and form crystals.

$$2Zr(OH)_2SO_4\downarrow + O_2 \xrightarrow{Drying\ \&\ Calcination} 2ZrO_2SO_4\downarrow + 2H_2O\uparrow \qquad \text{(CR9)}$$

The calcined ZrO_2SO_4 catalyst, existing as SO_4^{2-}/ZrO_2 in a crystal lattice, was stored in a vacuum desiccator until needed.

3.2.2.4 Catalyst Characterisation:

The calcined catalyst was characterised using the X-ray diffraction (XRD) analyses to establish the phases and measure the crystalline sizes; the Scanning Electron Microscopy (SEM) to evaluate the catalyst's surface topography and composition and the Transmission Electron

Microscopy (TEM) that provided morphological, compositional and crystallographic information on the catalyst.

3.2.3 *Croton gratissimus* Biodiesel Synthesis

High FFA content of the *Croton gratissimus* oil necessitated the use of a two-step catalytic process to synthesise biodiesel and produce FAME. In the esterification step (Step1), sulphated zirconia was used as a catalyst to lower the Acid Value of oil from ± 21.46 to ± 2.93 mg KOH/g. FAME was produced in the transesterification step (Step2), where potassium hydroxide (KOH) was used as the catalyst.

3.2.3.1 Esterification of oil:

A weighed sample (± 10 g) of oil was placed in a 50 ml jacketed beaker (reactor) fitted with a Grahams condenser. Hot water was allowed to flow through the jacket to keep the oil inside the beaker at a reaction temperature. A proportional amount of catalyst (SO_4^{2-}/ZrO_2) and methanol (MeOH) was added to the heated oil and the reaction mixture was stirred at 650

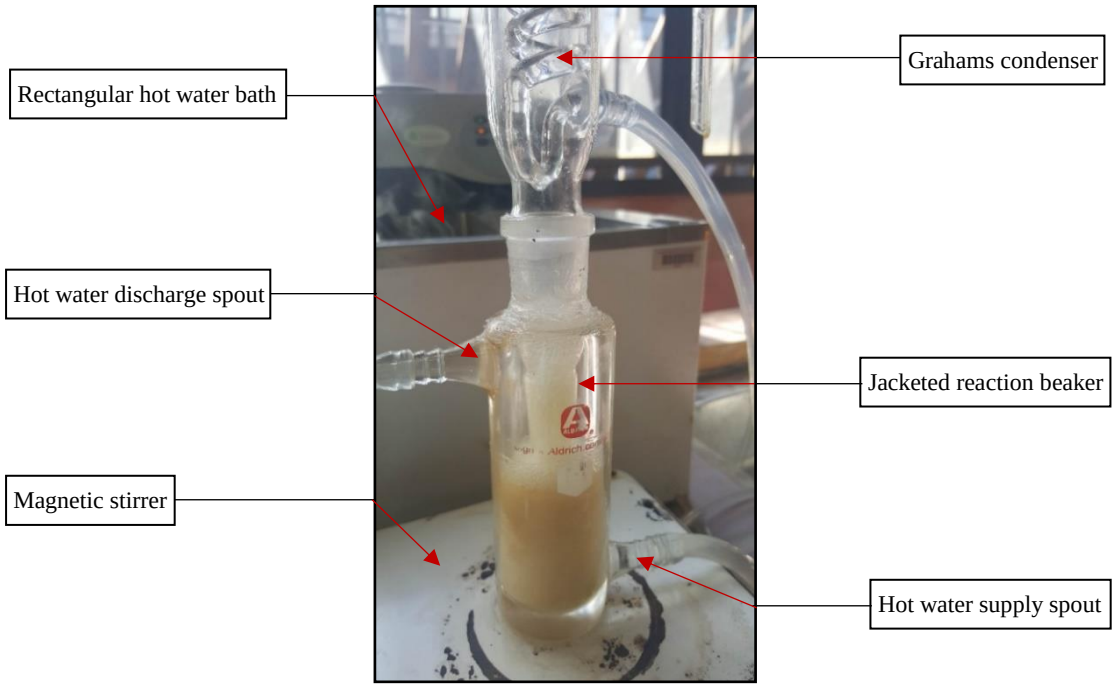

Fig. 3.10: Esterification of Oil

revolutions per minute (rpm). Reaction temperature was maintained at a predetermined level by water circulating from a rectangular hot water bath equipped with an immersion temperature regulator-circulator as shown in Figure 3.10. After the 1½-hour of reaction time, the mixture

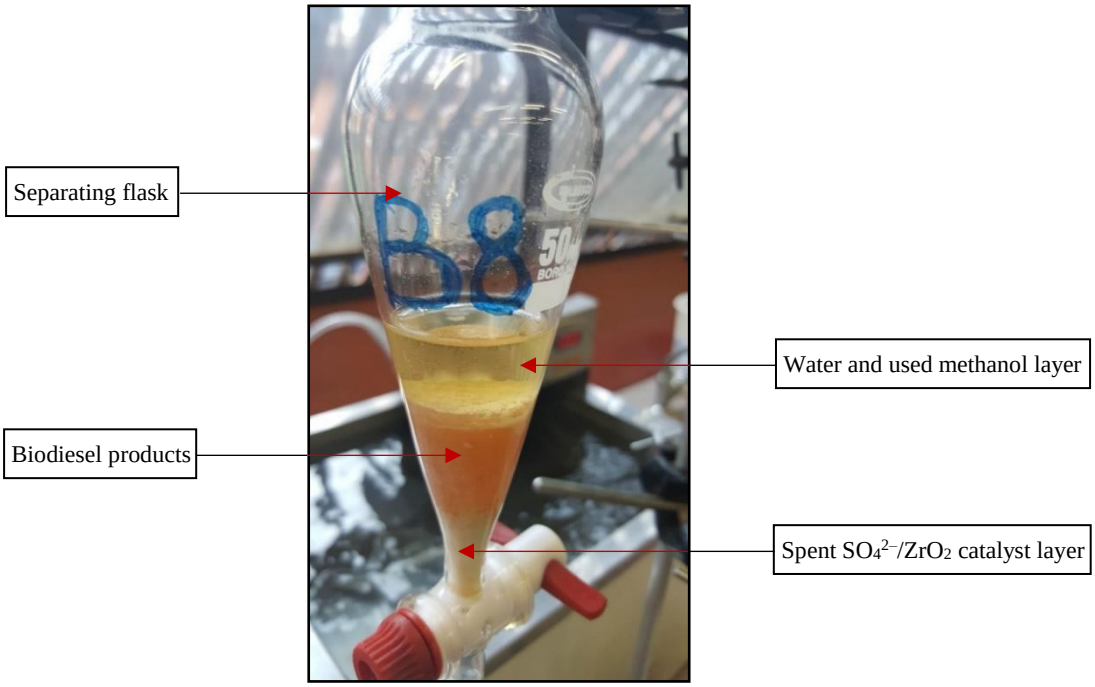

Fig. 3.11: Esterification Product Separation

was poured into a separating flask and allowed to settle. Three distinct layers were observed, i.e., the bottom layer consisting mainly of the used catalyst, next the product layer in the middle and the top layer consisting mainly of water and the unused methanol remaining from the reaction as shown in Figure 3.11. The bottom two layers were taken for further separation in a centrifuge (Fig. 3.2). The centrifuge was set at 4000 rpm for 5 min with an acceleration /deceleration speed set at 5 cycles per second.

The SO_4^{2-}/ZrO_2 catalyst was recovered and the intermediate product of esterification (Fig. 3.12) was stored for further processing. The same procedure was followed in all 20 experimental runs conducted.

Fig. 3.12: Product Samples from the Esterification Reaction

3.2.3.2 Transesterification of oil:

A known mass of esterified oil was placed in a 50 ml jacketed beaker and brought to the reaction temperature by circulating water from a hot water bath fitted with an immersion temperature regulator-circulator. About 5 ml of *n*-hexane was added into the oil to improve the miscibility of MeOH in oil. Potassium methoxide ($KOCH_3$) solution was then prepared in a 50 ml beaker by dissolving weighed mass of KOH catalyst in a known volume of MeOH. The $KOCH_3$ solution was poured into the beaker and agitated, using a magnetic stirrer. A Grahams condenser, connected to the jacketed beaker, was used to capture MeOH escaping from the reaction vessel (Fig. 3.13).

After 1½ hours of reaction time, the mixture was poured into a 50 ml beaker to remove the bottom dark brown glycerol layer (Fig. 3.14). The top biodiesel layer was transferred into a 50ml separating flask. Water (±25 ml) was added and the mixture was vigorously shaken for 6 mins, taking 30 seconds breaks after every 2 minutes of continuous shaking. The mixture was then left to settle in the separating flask for a few hours. Figure 3.15 shows 2 distinct layers of the transesterification products (without glycerol) after water-wash. The bottom whitish layer

consists mainly of soap and the top clear yellow layer is the biodiesel layer with a high concentration of fatty acid methyl esters (FAME). After 5 washes, the final washed product

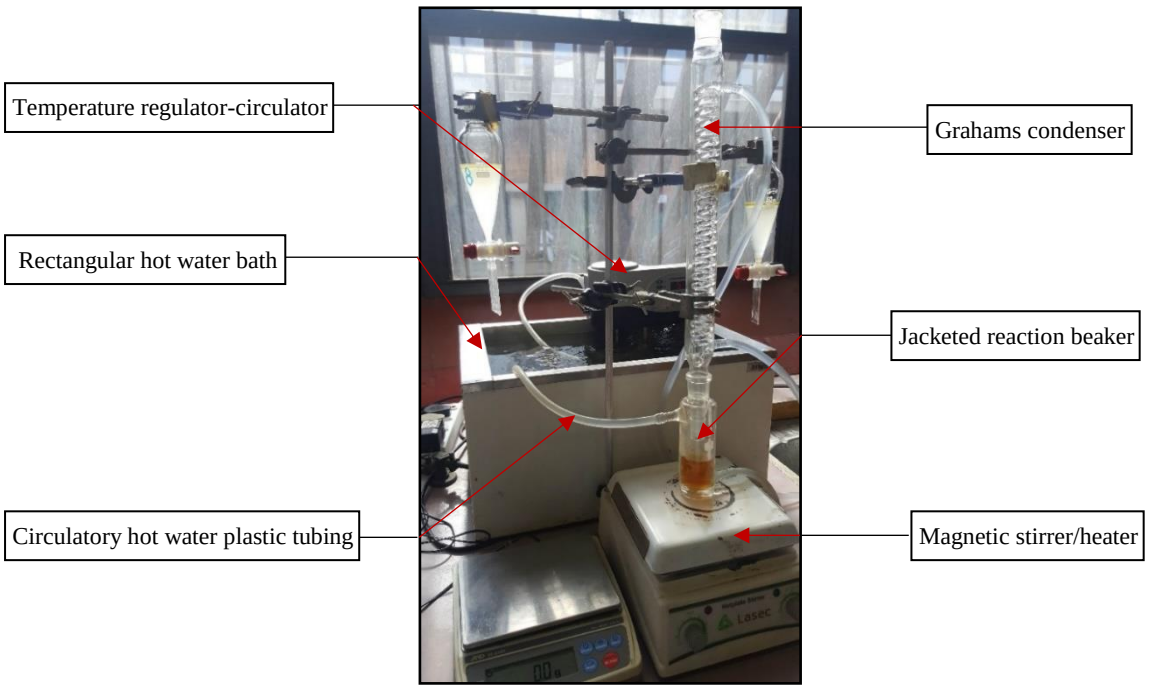

Fig. 3.13: Transesterification Equipment Set-up

was separated in a HERMLE centrifuge running at 4000 rpm for 5 minutes. *n*-Hexane solvent

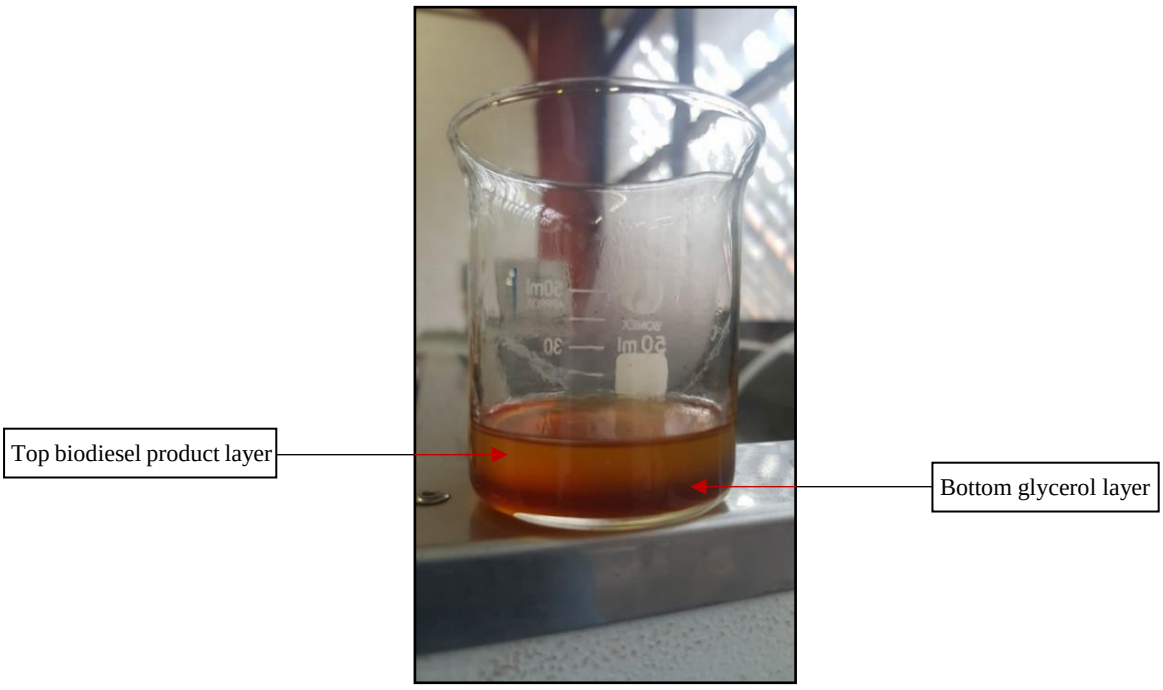

Fig. 3.14: Reaction Mixture with Glycerol & FAME

used to enhance miscibility of reactants and excess MeOH remaining after reaction were removed by flash evaporation.

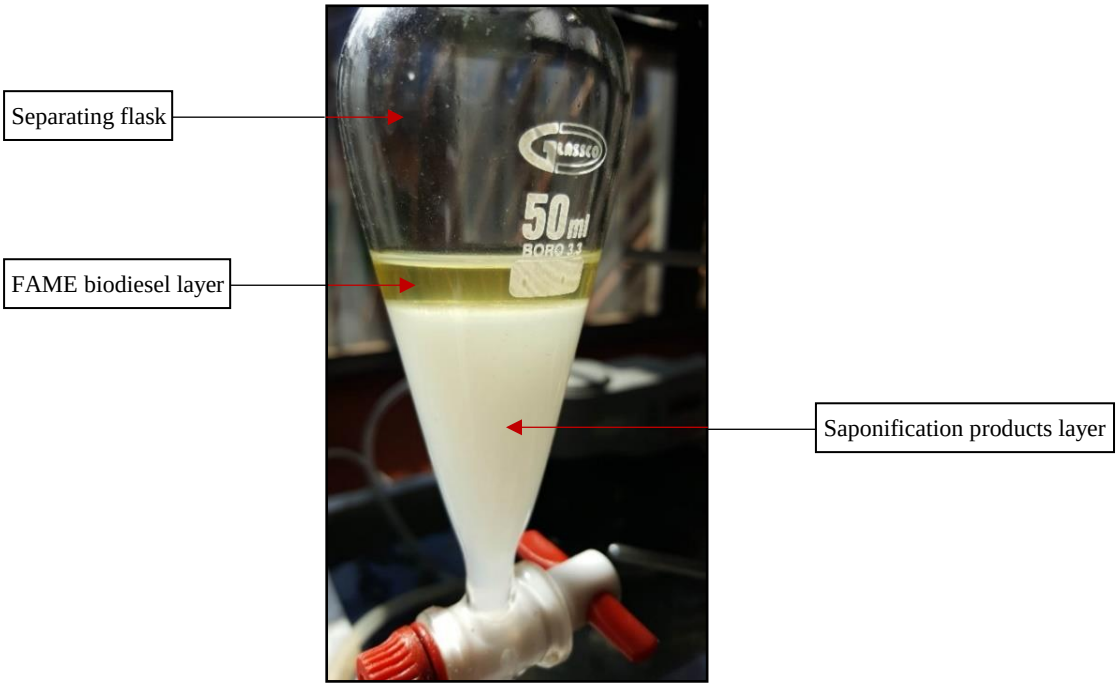

Fig.3.15: Transesterification Products after 1st Wash

The final biodiesel product was transferred into sampling bottles and weighed. The biodiesel yield was calculated as the ratio of mass of biodiesel (m) produced to the mass of *Croton gratissimus* oil, (M) used in the transesterification reaction.

$$Y = \text{Percentage Biodiesel Yield (\%)} = \frac{m}{M} \times 100 \qquad (4)$$

A total of 20 experimental runs were conducted, the results of which were to be used in the optimisation study. Biodiesel (FAME) samples characterised using the Gas chromatography Mass spectroscopy (GC-MS).

Fig. 3.16: Product Biodiesel Samples

3.2.3.3 Biodiesel (FAME) Characterisation:

A PerkinElmer Clarus® 580 Gas Chromatograph equipped with a Clarus® SQ 8S Mass Spectrometer (GC-MS) was used to measure the percentage purity (% P) of FAME samples. The gas chromatograph (GC) used has a 30 m length PerkinElmer Elite-5MS II capillary column of 0.5 µm film thickness and 0.25 mm inner diameter. The stationary phase in the column selected is a low polarity 5% diphenyl / 95% dimethyl polysiloxane and the mobile phase is pure helium (He), flowing at 1 ml/min, used as carrier gas.

FAME sample of 100 µl was dissolved in 10 ml of ethanol and a 1 µl volume of the diluted sample was injected into the GC. Methyl heptadecanoate was used as an internal FAME standard. The oven temperature was initially kept at 140 ^{0}C for 5 minutes and ramped up at 4^{0}C/min to a maximum of 240 ^{0}C for a total run time of 31 minutes. The sampling rate was maintained at 1.5625 pts/s enabling the detector to capture enough data points across very narrow peaks. The purity of FAME was then determined from the chromatographic peak areas using the following formula (Jeong *et al*., 2009):

$$\text{P = Percentage FAME Purity (\%)} = \frac{\left(\sum A_{FS}\right) - A_{IS}}{A_{IS}} \times \frac{C_{IS} \times V_{IS}}{m_{FS}} \times 100 \quad (5)$$

where, $\sum A_{FS}$ is the sum of all the methyl ester (FAME) peak areas, A_{IS} is the peak area of the internal FAME standard (methyl heptadecanoate), C_{IS} is the concentration in mg/ml of the solution of the internal standard, V_{IS} is the volume in ml of the internal standard solution and m_{FS} is the mass in mg of the FAME sample.

The FAME analysis method described above, that employs equation (5), was adopted in this study as it is the most preferred when the quantity (purity) rather than the quality (composition) of FAME is being investigated in biodiesel synthesis. But, when the composition of FAME in the biodiesel test sample is of an essence, FAME standards of known concentration are used to plot calibration curves which are then used in the determination of individual methyl esters.

3.3 Optimisation Process

At the end of the experiments, the data collected was subjected to an optimisation study to find the optimum operating conditions for both the esterification and the transesterification processes. Henceforth the optimisation studies of these processes will be referred to as OPTIMA1 and OPTIMA2, respectively. An optimisation study, further carried out to find a set of optimum independent variables that could simultaneously satisfy both optimum values of FAME yield and FAME purity obtained in OPTIMA2, will be referred to as OPTIMA3. Thereafter the response surface methodology (RSM), that employs the central composite design (CCD) and analysis of variance (ANOVA) techniques, was employed in these studies.

The CCD was applied with three design factors, viz., catalyst concentration (X_1), methanol-to-oil ratio (X_2) and the reaction temperature (X_3). These factors were selected to optimise

the chosen responses of acid value (Y_A) in OPTIMA1, and FAME yield (Y_Y) and FAME purity (Y_P) in OPTIMA2. The selection of levels (uncoded variables) for each factor was based on the literature related to the optimisation of similar biodiesel processes. Processes of interest were those that draw their feedstock from high FFA non-edible vegetable crops and use the two-step production process approach, i.e., esterification and transesterification reactions.

For both processes (OPTIMA1 and OPTIMA2), 2^3 full-factorial rotatable CCD designs for three independent variables at five levels were employed and the total number of experiments conducted was 2×20, including axial and replicate experimental runs. Experiments were performed in a randomized order to balance out the effect of any nuisance variable that may influence the observed response (Montgomery and Runger, 2003). The Design-Expert® version 10 software was used to design the experiments and for regression and graphical analyses of the data obtained. Acid Values obtained in OPTIMA1 and the FAME yield and purity obtained in OPTIMA2 and OPTIMA3 were all taken as responses of the designed experiments.

Statistical analysis of the model was performed to evaluate the analysis of variance (ANOVA). The Fisher's *F*-test was performed to test the significance of adding quadratic terms to the two-factor interaction (2FI) model. Ideally a small *p*-value (Prob>*F* less than 0.05), is desirable as it indicates that the addition of these (quadratic) terms has contributed to an improvement in the model. The goodness of fit of the model was evaluated by the determination coefficient (R^2), adjusted determination coefficient (Adj. R^2) and the coefficient of variance (C.V.).

The coefficient of variation (C.V.) or most commonly known as the relative standard deviation is the standard deviation expressed as a percentage of the mean and is crucial in measuring the reproducibility of the model. Predicted R^2 is a measure of how well the model predicts a response value and adjusted R^2, on the other hand, measures the amount of variation around the mean that is explained by the model. For the model to fit the collected data, the predicted R^2

(Pred. R^2) value must be in reasonable agreement with the adjusted R^2 (Adj. R^2) value by not more than 0.2 point difference. The Adequate Precision (Adeq. Precision) measures the signal-to-noise ratio and should ideally be greater than 4. A value greater than 4 is desirable as it indicates that the developed model has a high degree of precision and can thus be used to navigate the entire design space.

From the developed quadratic regression model, a combination of independent variables (X_1, X_2 and X_3), forming an optimal set, that fell within the region of 95% confidence interval (95% CI) of the chosen response (Y_A, Y_Y or Y_P) was taken as the optimum set of variables that is most likely to produce that optimum response. To narrow down the search for the best compromise within the optimum region, comprising of a multitude of independent variables matching multiple responses, optimum Acid Value in OPTIMA1 and FAME yield and FAME purity in OPTIMA2 were targeted and one independent variable set as a constraint.

In OPTIMA1, an Acid Value of 2.963 and a reaction temperature of 64 ^{0}C were used as constraints to reduce the number of plausible optimum set. FAME yield of 84.51% and FAME purity of 90.66% obtained in OPTIMA2 and reaction temperature of 63.5 ^{0}C were selected as constraints for use in OPTIMA3. The choice of the final optimum set of independent variables was based on process economics, i.e., reduced temperatures and low levels of catalyst usage.

Overlay plots were drawn, in graphical optimisation, to display the areas of feasible response values within the factor space, and with a “flag insert” to show the optimum solution set. In the overlay plots shown in Figures 4.10 and 4.19, the region coloured in green represent a region where graphical optimisation solutions that meet the specific criteria can be found. The grey region represent the graph area with solutions outside of model prediction. The region coloured in red represent the graph area outside the interval bound for at least one response.

Chapter 4. Experimental Results

4.1 Oil Extraction

Prior to undertaking this work on the optimisation of the *croton gratissimus* biodiesel production process, an in-depth study aimed at finding a suitable extraction solvent for the extraction process of *croton gratissimus* oil was conducted. The results of this study have been published in the Journal of Oleo Science and a full paper can be found in Appendix G of this dissertation.

The two solvents investigated were *n*-hexane, a non-polar solvent mostly favoured by the industry and ethyl acetate, a polar solvent deemed to be an environmentally friendly alternative (Park *et al*., 2017; Wu *et al*., 2017). The RSM models developed using the CCD and analysed by the ANOVA revealed that in both *n*-hexane and ethyl acetate extraction processes, the extraction oil yield was almost entirely dependent on the amount of solvent used than on the extraction temperature and residence time. However, the latter two independent variables were used as constraints in finding the optimum set that gave the targeted optimum response.

From the results obtained, *n*-hexane oil extraction process showed low levels of material and energy utilisation when compared to the ethyl acetate process. *n*-Hexane oil extraction could be performed at much lower temperatures and reduced residence times than ethyl acetate extraction. For these reasons, it was then selected as the solvent of choice in the current study.

In this work, 4 batches of chemical solvent extractions were carried out, producing a total of 343.90 g of *Croton gratissimus* oil (as seen in Table 4.1). The product mixture was observed to have a light yellowish colour that turned dark yellow as the solvent was removed. The

average extraction oil yield and solvent recovery rate obtained from these batches were 29.35% and 32.80%, respectively.

Table 4.1: *Croton gratissimus* Oil Extraction Yield and Solvent Recovery

Batch Number	Mass of Dried Seeds (g)	Mass of Oil Extracted (g)	Vol. of Solvent used (ml)	Vol. of Solvent Recovered (ml)	% Oil Yield	% Solvent Recovered
1	313.90	87.10	785	250	27.75	31.85
2	305.90	98.20	765	248	32.10	32.42
3	281.80	79.90	705	226	28.35	32.06
4	269.40	78.70	674	235	29.21	34.87
TOTAL	**1171.00**	**343.90**	**AVERAGE**		**29.35**	**32.80**

The extracted oil was subjected to a series of tests to evaluate its physico-chemical properties (as seen in Table 4.2). High viscosity oils tend to require high agitation intensity and00 will eventually produce highly viscous biodiesel. The values of viscosity and specific gravity obtained for oils therefore are a good measure of the magnitude of these physical properties in the final biodiesel product. The Acid Value and Saponification Value of oil were also crucial parameters to evaluate, as they assist in establishing the need for either a one-step or a two-step process in the production of biodiesel. Depending on the catalyst selected, oils with high Acid Values (greater than 4 mg KOH/g of oil) require a pre-treatment esterification step performed before the main transesterification reaction.

Table 4.2: Properties of Non-edible Vegetable Oils
(*Kafuku and Mbarawa, 2010, # Singh and Padhi, 2009)

Property	*Croton gratissimus*	* *Croton megalocarpus*	#*Jatropha curcas L.*
Specific Gravity at 20^0C	0.924	0.918	0.918
Viscosity (mm^2/s) at 40^0C	58	64	35.4
Acid Value (mg KOH/g)	21.455	3.343	11.0
Free Fatty Acid (%FFA)	10.78	1.68	5.53
Saponification Value (mg KOH/g)	190.15	194.9	194

Croton gratissimus oil was further characterised in a GC-MS to determine its lipid profile and a comparison was made with non-edible vegetable oils from other biodiesel feed crops. Besides the *croton gratissimus* oil consisting predominantly of long-chain (C16 to C20) triglycerides (LCT), the presence of the medium-chain (C6 to C12) triglycerides (MCT) in the lipid profile was noted as shown in Table 4.3.

Table 4.3: Lipid Profile of Vegetable Oils (*****Zhang et al, 2015, [#] Sarin *et al*, 2007)

Fatty Acid			***Croton gratissimus***	**** Zanthoxylum bungeanum***	***[#]Jatropha curcas L.***
Structure	**Formula**	**Common Name**	**Mass %**		
C16:0	$C_{16}H_{32}O_2$	Palmitic	35.8	13.50	14.2
C16:1	$C_{16}H_{30}O_2$	Palmitoleic Acid	0.3	6.23	1.4
C18:0	$C_{18}H_{36}O_2$	Stearic Acid	31.2	1.32	6.9
C18:1	$C_{18}H_{34}O_2$	Oleic Acid	8.7	32.25	43.1
C18:2	$C_{18}H_{32}O_2$	Linoleic Acid	10.5	22.54	34.4
C18:3	$C_{18}H_{30}O_2$	Linolenic Acid	5.9	24.16	–
C20:0	$C_{20}H_{40}O_2$	Arachidic Acid	2.2	–	–
C20:1	$C_{20}H_{38}O_2$	Gadoleic Acid	–	–	–
Other (MCT)			5.4	–	–
Acid Value (mg KOH/g oil)			**21.46**	**56.9**	**12.5**
Extraction Oil Yield (%)			**29.35**	**24.70**	**75.22**
Unsaturated Fatty Acid (%)			**25.4**	**85.2**	**78.9**

4.2 SO_4^{2-}/ZrO_2 Catalyst Characterisation

Figure 4.1 below shows the X-ray diffraction profile obtained from the measurements carried on the SO_4^{2-}/ZrO_2 catalyst. The main phase was found to be ZrO_2 which matched the tetragonal

lattice pattern (red lines). The tetragonal phase was predominant at 2θ of 30.5^0 and Baddeleyite, a monoclinic ZrO_2 phase (powder blue lines), was mostly found at 2θ of 28.2^0. The presence of both phases (with a dominant monoclinic phase) in the crystal lattice indicated that the doped sulphate ions did not successfully influence the phase modification of zirconia from the thermodynamically more stable monoclinic phase to the metastable tetragonal phase. For this reason, the synthesised SO_4^{2-}/ZrO_2 catalyst was observed to be highly active in catalysing only the esterification reaction and not the transesterification reaction.

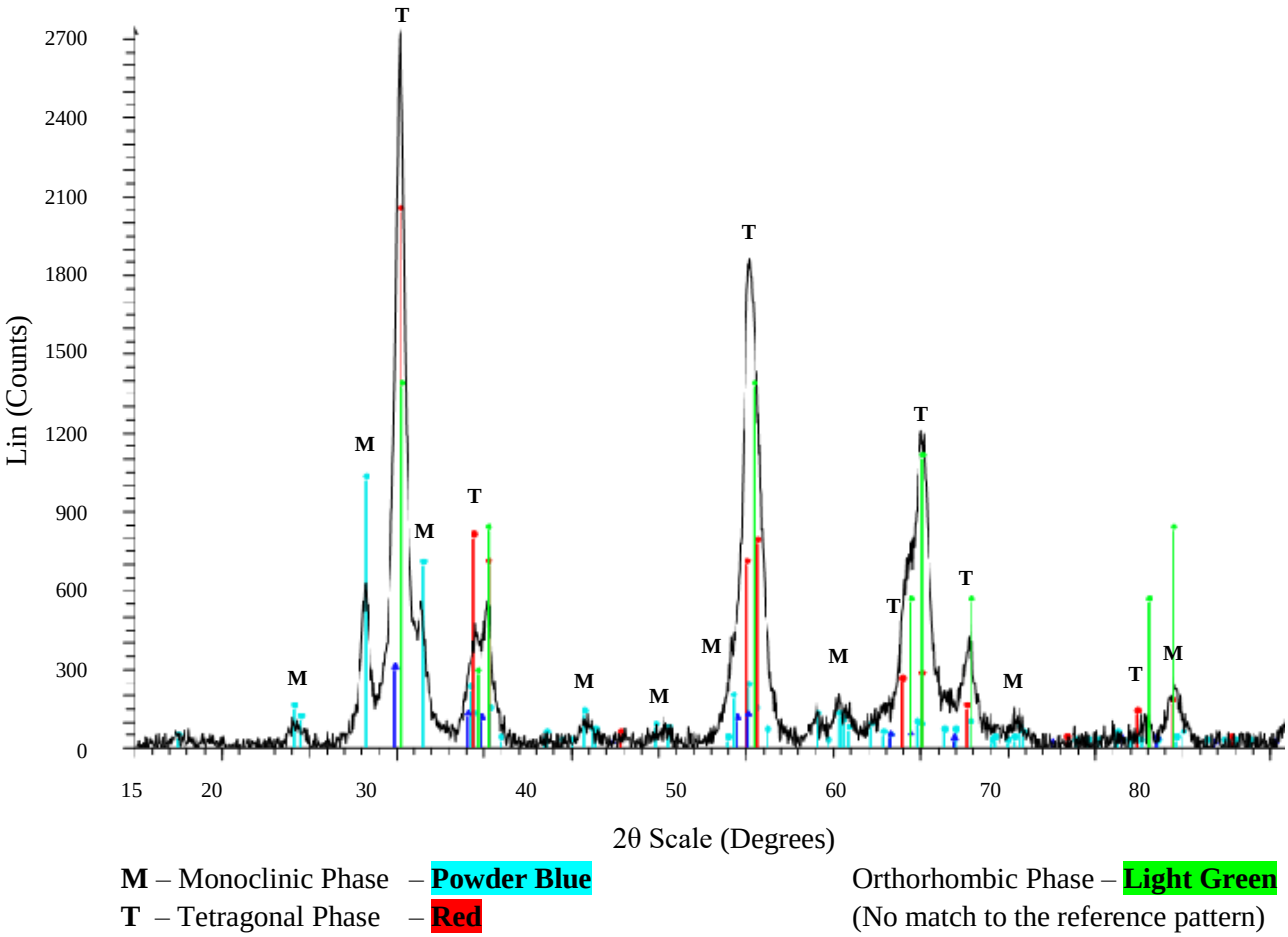

Fig. 4.1: X-ray diffraction profiles of the SO_4^{2-}/ZrO_2 catalyst calcined at 620 ^{0}C

Morphological studies on the catalyst were performed using the Transmission Electron Microscope (TEM) and its composition was analysed using the Scanning Electron Microscope (SEM). Figure 4.2 shows the morphology of SO_4^{2-}/ZrO_2 catalyst calcined at 620 ^{0}C for 4 hours. Highly packed crystal morphology with irregularly arranged ZrO_2 aggregation was observed.

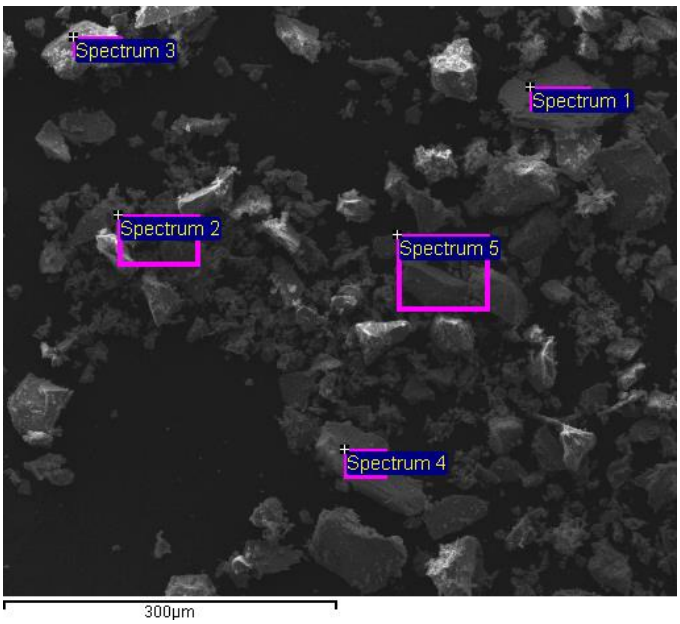

Fig. 4.2: SEM micrograph of SO_4^{2-}/ZrO_2 catalyst calcined at 620^{0}C

There was a high loading amount of Zr in the catalyst structure as proven by a 61.78 mass % Zr from the elemental analysis of the catalyst (Table 4.4).

Table 4.4: SEM – EDS Elemental Composition of the SO_4^{2-}/ZrO_2 Catalyst

Spectrum Number	Oxygen Mass% O	Sulphur Mass% S	Zirconium Mass% Zr
Spectrum 1	39.85	0.83	59.32
Spectrum 2	34.84	0	65.16
Spectrum 3	34.96	1.18	63.85
Spectrum 4	40.44	0.74	58.82
Spectrum 5	38.24	0	61.76
Mean	**37.67**	**0.55**	**61.78**
Standard Deviation	**2.65**	**0.53**	**2.76**

The presence of all the constituent atoms (Zr, O and S) that make sulphated zirconium catalyst was confirmed by spectrum 1 in Figure 4.3. The spectrum was developed from a randomly picked area on the face of the sample (Fig. 4.2). Because of its rather lower mass and abundance in the catalyst, the concentration of sulphur was low and in some spot spectra (spectra 2 and 5

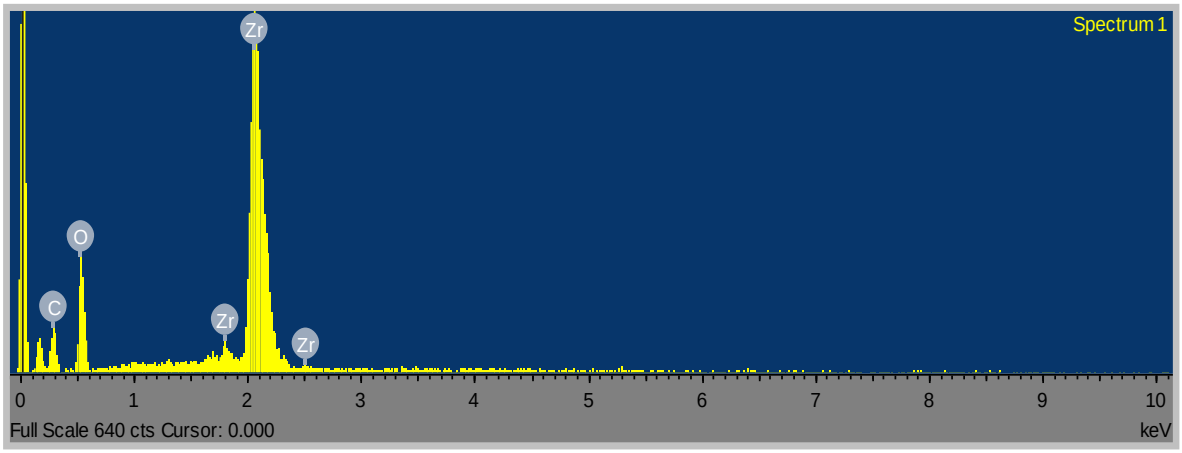

Fig. 4.3: SEM – EDS Spectra for the Elemental Composition of the SO_4^{2-}/ZrO_2 catalyst

on Table 4.4) of Figure 4.2 remain undetected. To determine the concentration of sulphates and hence the acidity and activity of sulphated zirconium catalyst, other methods are employed.

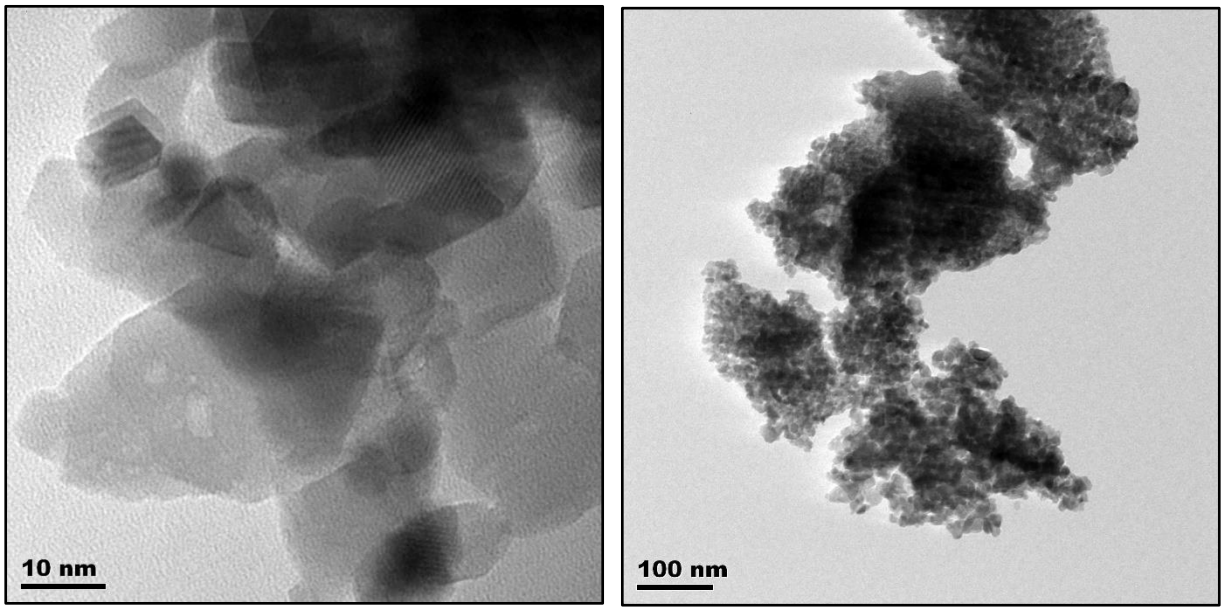

Fig. 4.4: TEM Micrographs of the Monoclinic SO_4^{2-}/ZrO_2 catalyst

The mean diameter of the monoclinic zirconia crystals is ± 30 nm while that of the tetragonal crystals is ± 200 nm (Miranda *et al*., 2015). In Figure 4.4 above, the TEM micrographs show the sizes of most of the crystals in the SO_4^{2-}/ZrO_2 sample to range between 10 and 100 nm, indicating an overwhelming presence of the monoclinic phase.

4.3 Biodiesel Characterisation

Figure 4.5 below, shows a representative GC-MS spectrum used for the analysis of FAME purity in a biodiesel sample. FAME composition was evaluated using the GC-MS library that identified the most prominent methyl ester on each peak. The presence of the following methyl esters and their peak areas (Table 4.5) were noted on each spectrum; oleate, palmitate, stearate, linoleate, palmitoleate, arachidate and linoleneate. Percentage FAME purity was then calculated using Equation 5 (Jeong *et al*., 2009).

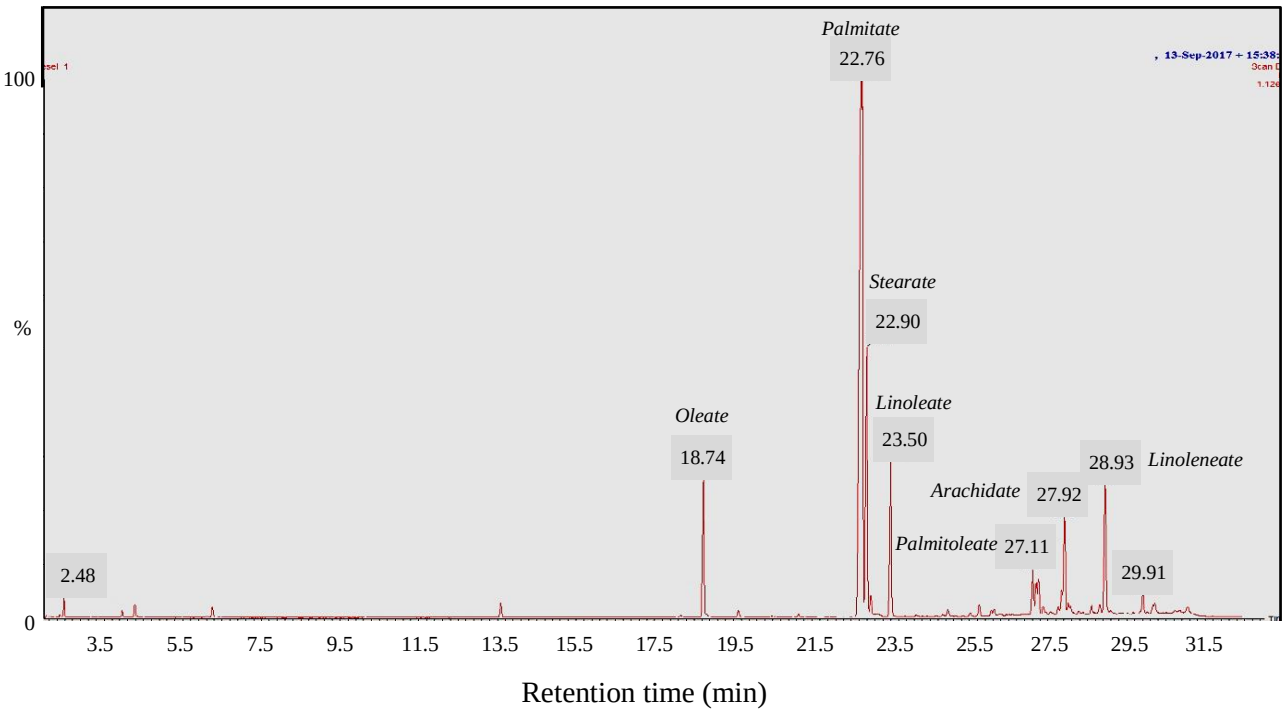

Fig. 4.5: GC-MS Spectrum for *Croton gratissimus* FAME

Table 4.5: GC-MS Spectrum Peak Areas for *Croton gratissimus* FAME

Spectrum Number	Area x10^5	Spectrum Number	Area x10^5	Spectrum Number	Area x10^5	Spectrum Number	Area x10^5	Spectrum Number	Area x10^5
1	30123	**5**	24916	**9**	29692	**13**	28049	**17**	27883
2	25239	**6**	30544	**10**	26316	**14**	29667	**18**	29724
3	25968	**7**	29462	**11**	24414	**15**	29507	**19**	26559
4	26195	**8**	30942	**12**	29178	**16**	25232	**20**	25069

4.4 Optimisation of the Esterification Process (OPTIMA1)

High Acid Value of *Croton gratissimus* oil (21.455 mg KOH/g) necessitated that an esterification reaction be conducted prior to the main transesterification reaction. This was done in order to reduce the acid value of the extracted oil to below 4 mg KOH/g of oil. The effects of catalyst concentration (X_1), methanol-to-oil ratio (X_2) and the reaction temperature (X_3) on the acid value were investigated. They were each varied in 5 levels as shown in Table 4.6. The values of the levels were established through the OFAT esterification experiments conducted over the synthesised monoclinic SO_4^{2-}/ZrO_2 catalyst.

Table 4.6: Independent Variables and Levels used for the CCRD in the Esterification Process

Variables	Symbols	Levels				
		$-\alpha$	-1	**0**	**+ 1**	$+\alpha$
Catalyst concentration (mass%)	X_1	6	7.65	10	12.45	14
Methanol-to-oil ratio	X_2	20	25	32.5	40	45
Reaction temperature (^{0}C)	X_3	60	64	70	76	80

Table 4.7 gives the results of Acid Value reduction for the 20 experimental runs carried out to find the optimum conditions for the esterification process.

To evaluate the accuracy of the model in predicting the response values that match the actual experimental values, a plot of Predicted Response vs. Actual Response values was developed. The developed model was able to predict most of the response values as the points on the plot lie in close proximity to the 45^0 diagonal line (Fig 4.6).

Table 4.7: Acid Value of *Croton gratissimus* Oil after Esterification

Experimental Run		Catalyst Concentration (Mass %)	MeOH-to-Oil Ratio	Reaction Temperature (^{0}C)	Acid Value (mg KOH/g)
Standard	**Random**				
13	**1**	10	32.5	60	2.805
10	**2**	14	32.5	70	2.006
9	**3**	6	32.5	70	4.091
15	**4**	10	32.5	70	2.727
7	**5**	7.65	40	76	3.659
6	**6**	12.45	25	76	2.227
14	**7**	10	32.5	80	2.991
3	**8**	7.65	40	64	3.659
16	**9**	10	32.5	70	2.727
12	**10**	10	45	70	2.876
5	**11**	7.65	25	76	3.659
8	**12**	12.45	40	76	2.306
11	**13**	10	20	70	2.978
18	**14**	10	32.5	70	2.727
17	**15**	10	32.5	70	2.727
19	**16**	10	32.5	70	2.978
20	**17**	10	32.5	70	2.727
1	**18**	7.65	25	64	3.737
2	**19**	12.45	25	64	2.566
4	**20**	12.45	40	64	2.366

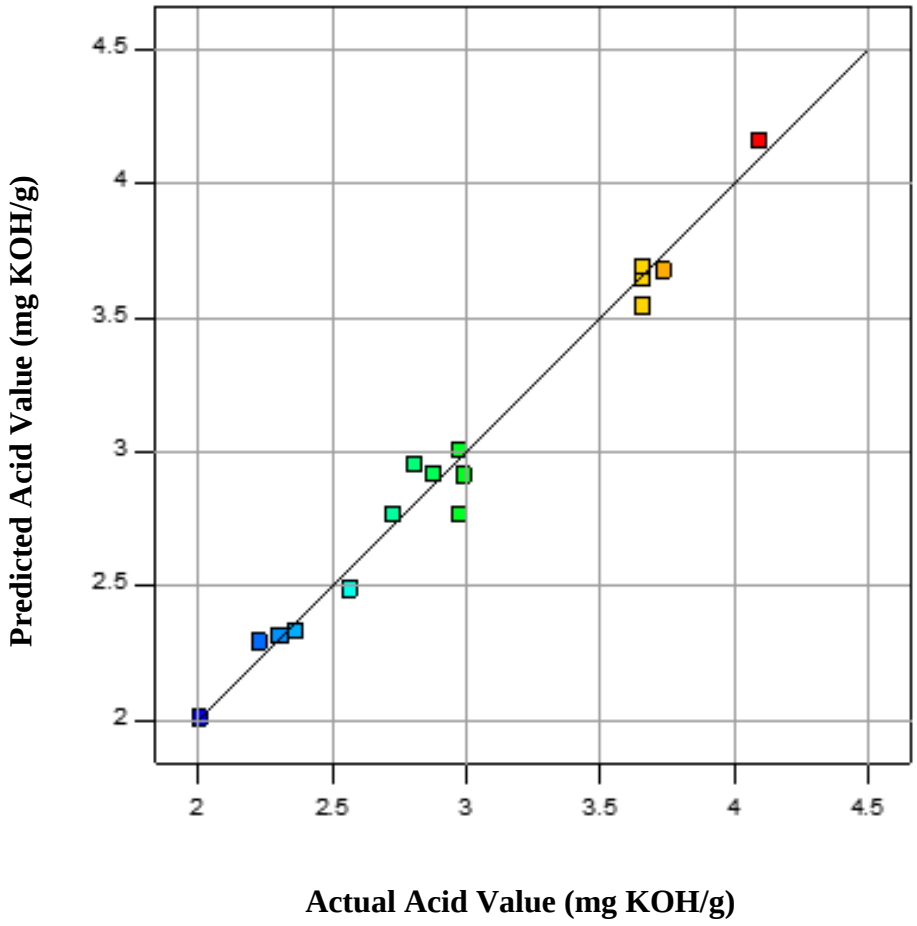

Fig. 4.6: Graphical Plot of experimental results versus predicted results of the Esterification Process

Table 4.8: ANOVA Results for the Quadratic Model of the Esterification Process

Source of Variation	Sum of Squares	Degree of Freedom	Mean Square	*F*-value	*p*-value Prob > *F*
Model	5.90	9	0.66	55.94	< 0.0001
Residual	0.118	10	0.012	–	–
– Lack of Fit	0.065	5	0.013	1.23	0.4126
– Pure Error	0.053	5	0.011	–	–
Total	6.02	19	–	–	–
C.V. = 3.70%	**R^2 = 0.9805**	**Pred. R^2 = 0.9045**	**Adj. R^2 = 0.9630**	**Adeq. Precision = 28.141**	

The experimental data obtained in the esterification process was analysed by the ANOVA and is best described by the following quadratic regression model:

$$Y_A = 17.362 - 0.456X_1 - 0.152X_2 - 0.239X_3 - 2.958\times10^{-4}X_1X_2 - 2.854\times10^{-3}X_1X_3 + 9.917\times10^{-4}X_2X_3 + 0.020X_1^2 + 1.254\times10^{-3}X_2^2 + 1.670\times10^{-3}X_3^2 \quad (6)$$

where Y_A is the acid value (mg KOH/g) of the esterified oil and X_1, X_2 and X_3 are uncoded values of the independent variables, viz., catalyst concentration (mass %), methanol-to-oil ratio and the reaction temperature (^{0}C), respectively.

An increase in either the catalyst concentration, methanol-to-oil ratio or the reaction temperature resulted in a reduction in the Acid Value of *croton gratissimus* oil. The negatively correlated linear terms in the developed quadratic regression model (Equation 6) are all evidence to this assertion. The quadratic model also revealed that the catalyst concentration was the most significant independent variable (*p*-value < 0.0001) exhibiting a larger negative value to its linear coefficient term when compared to other model factors terms.

The ANOVA results in Table 4.8 showed the significant nature of the developed quadratic regression model with a reasonably low probability value, Prob > F: (*p*-value) < 0.0001. The Fisher's *F*-test gave an *F* value for the model of 55.94 indicating a less than 0.01% chance that an *F* value this large could be due to noise. The Lack of fit with an *F*-value of 1.23 implied that the Lack of Fit was not significant and was proof that the model developed best represented the collected data. The value of the coefficient of determination (R^2) was found to be 0.9805, indicating that only 0.20% of the total variations was not explained by the developed regression model as shown in Figure 4.6. The predicted R^2 of 0.9045 was in reasonable agreement with the adjusted R^2 of 0.9630 with only an acceptable difference of less than 0.20. The developed

model had a high degree of precision as the Adequate Precision found was high enough at 28.141. The coefficient of variation (C.V.) of 3.70% indicated that the model was reproducible.

From the developed model, an Acid Value of 2.693 mg KOH/g could be obtained when operating the process under optimum conditions of 10.96 mass % catalyst concentration, 27.60 methanol-to-oil ratio of and a reaction temperature of 64 ^{0}C. The 88% reduction in the Acid Value of *Croton gratissimus* oil achieved in this esterification step, could positively influence the reaction extent in the next transesterification process step.

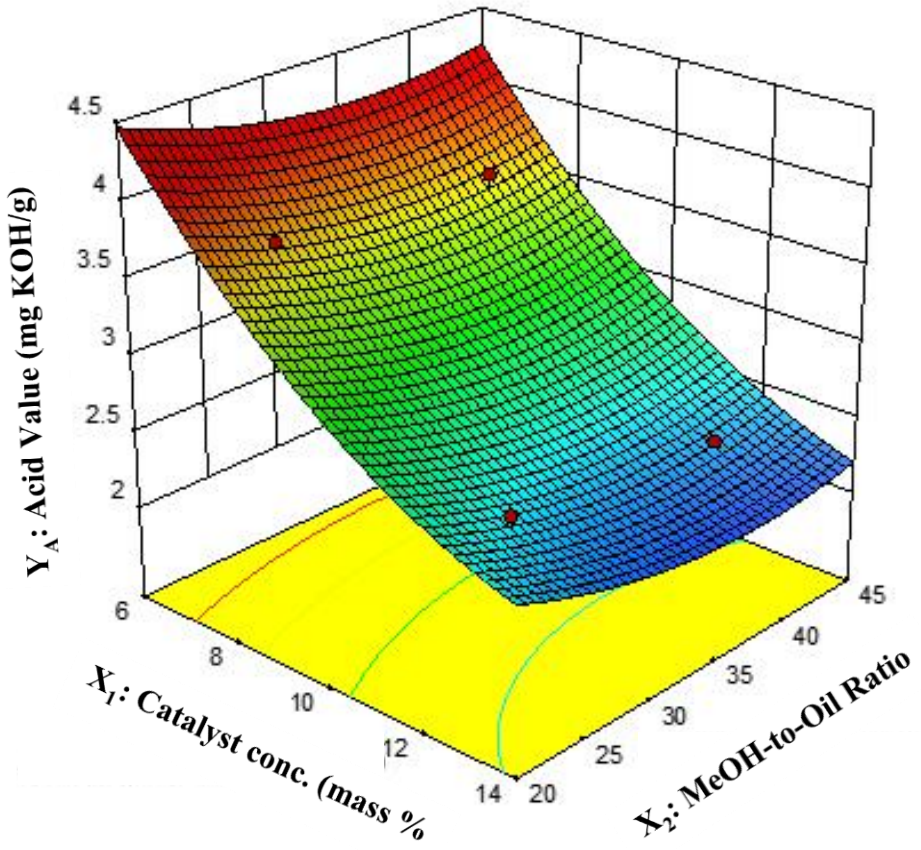

Fig. 4.7: Effect of Catalyst concentration and the Methanol-to-oil ratio on the Acid value at a Reaction temperature of 64 ^{0}C

Figures 4.7 – 4.9 show surface plots of the effects of catalyst concentration, methanol-to-oil ratio and the reaction temperature on the Acid Value of *Croton gratissimus* oil during the

esterification process. The amount of catalyst used had the most significant effect on the Acid Value of oil. This is shown by the almost flat-shaped response surfaces obtained for methanol-to-oil ratio and reaction temperature on the Acid Value when the catalyst concentration was kept constant at 10.96 mass % (Fig. 4.9).

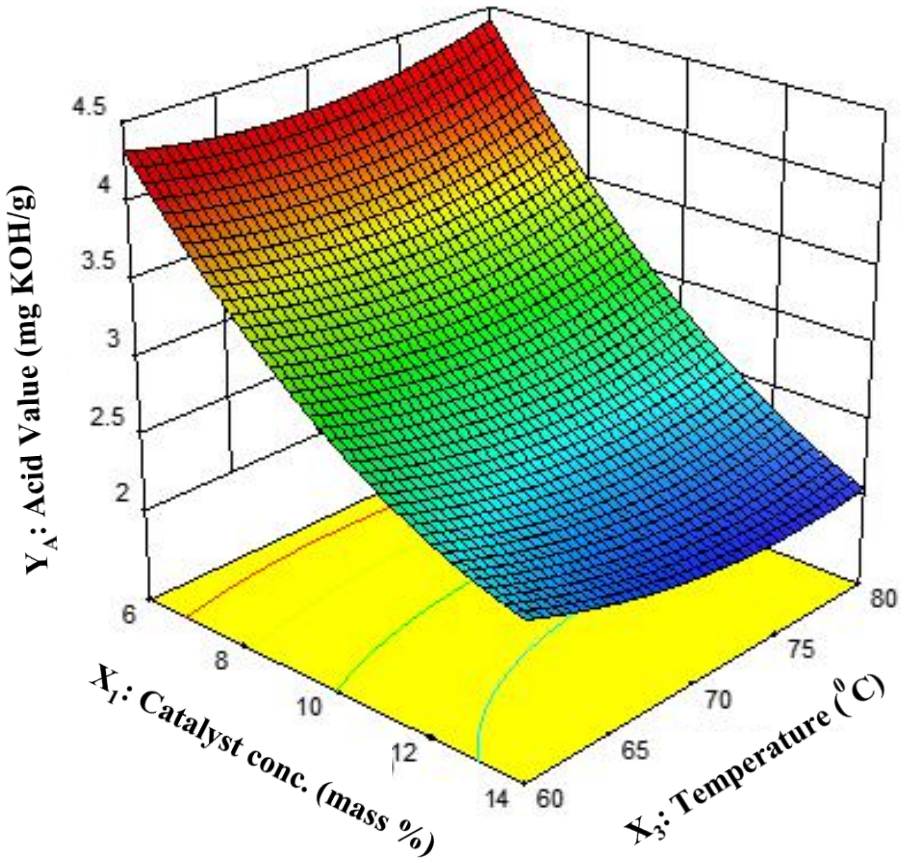

Fig. 4.8: Effect of Catalyst concentration and Reaction temperature on the Acid value at a Methanol-to-oil ratio of 27.60

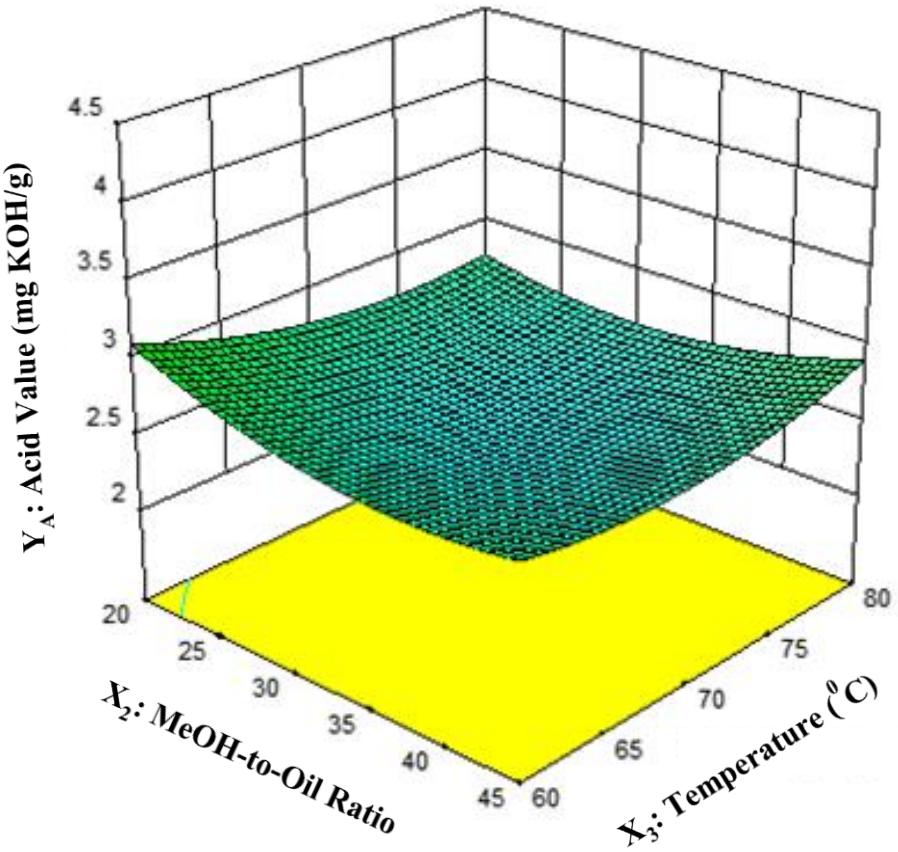

Fig. 4.9: Effect of Methanol-to-oil ratio and the Reaction temperature on the Acid value at a Catalyst concentration of 10.96 mass %

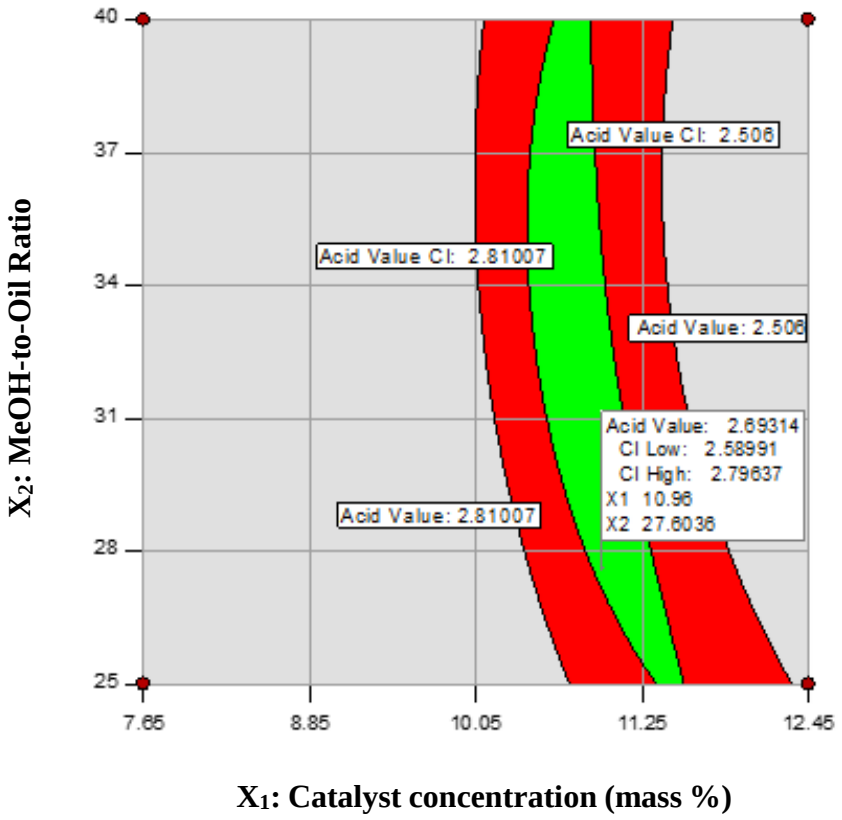

Fig. 4.10: Overlay Plot of Independent Variables satisfying targeted optimum response of Acid Value =2.693 mg KOH/g bound by 64 ^{0}C Reaction Temperature constraint

4.5 Optimisation of the Transesterification Process (OPTIMA2)

The esterified *Croton gratissimus* oil was further subjected to the transesterification process to produce fatty acid methyl esters (FAME). Independent variables selected for an investigation in an optimisation study were, catalyst concentration (X_1), methanol-to-oil ratio (X_2) and the reaction temperature (X_3). They were each varied in 5 levels, i.e., $-\alpha, -1, 0, +1, +\alpha$, as shown in Table 4.9, to establish their effects on the responses of FAME yield and FAME purity.

A Response Surface Methodology's 2^k full-factorial Central Composite Rotatable design (CCRD) was employed giving a total of 20 experiments, evaluated from $2^k + 2k + n_c$, where k = 3 and n_c = 6. Experiments were carried out in a randomised order to minimise the effects of uncontrolled factors. The final experimental results are presented in Table 4.10.

Table 4.9: Independent Variables and Levels used for the CCRD in the Transesterification Process

Variables	Symbols	Levels				
		$-\alpha$	-1	**0**	**+ 1**	$+\alpha$
Catalyst concentration (mass%)	X_1	0.65	0.90	1.30	1.70	2.00
Methanol-to-oil ratio	X_2	5.00	6.00	7.50	9.00	10.00
Reaction temperature (^{0}C)	X_3	45.00	52.00	62.50	73.00	80.00

To evaluate the analysis of variances (ANOVA), statistical analyses of the 2 developed quadratic models were carried out. Optimum operating conditions that gave the highest percentage FAME yield (Response 1) and FAME purity (Response 2) were evaluated.

Table 4.10: Central Composite Rotatable Design (CCRD) Arrangement and Responses for the Transesterification Process

Experimental Run		Coded Independent Variable Levels			Type of Factor	Responses	
Random	Standard	Catalyst Conc. (mass%)	MeOH-to-oil Ratio	Reaction Temp. (^{0}C)		% FAME Yield	% FAME Purity
20	**1**	−1	−1	−1	Factorial	67.09	75.34
5	**2**	+1	−1	−1	Factorial	69.14	74.86
16	**3**	−1	+1	−1	Factorial	74.63	75.85
10	**4**	+1	+1	−1	Factorial	81.52	79.24
4	**5**	−1	−1	+1	Factorial	78.98	78.86
1	**6**	+1	−1	+1	Factorial	81.18	91.15
19	**7**	−1	+1	+1	Factorial	81.48	80.00
8	**8**	+1	+1	+1	Factorial	93.33	93.71
11	**9**	−1.682	0	0	Axial	71.56	73.29
13	**10**	+1.682	0	0	Axial	85.35	84.66
3	**11**	0	−1.682	0	Axial	65.42	78.15
17	**12**	0	+1.682	0	Axial	84.71	84.14
2	**13**	0	0	−1.682	Axial	72.97	75.87
6	**14**	0	0	+1.682	Axial	93.65	92.40
7	**15**	0	0	0	Centre	82.93	89.09
14	**16**	0	0	0	Centre	82.58	89.72
9	**17**	0	0	0	Centre	84.21	89.80
12	**18**	0	0	0	Centre	84.71	88.19
18	**19**	0	0	0	Centre	81.99	89.90
15	**20**	0	0	0	Centre	82.05	89.22

4.5.1 Response 1: Percentage FAME Yield

The transesterification experiments conducted revealed that the highest FAME yield of 93.65% was achievable when the reactor was operated at 1.30 mass % catalyst concentration, 7.5 methanol-to-oil ratio and 80 ^{0}C reaction temperature. The lowest FAME yield was found to be 65.42% at 1.30 mass % catalyst concentration, 5 methanol-to-oil ratio and 62.50 ^{0}C reaction temperature. It is important to note that these values of % FAME yield were obtained from the experimental data collected before carrying out a full optimisation study.

Table 4.11: ANOVA of the % FAME Yield for the Quadratic Model of the Transesterification Process

Source of Variation	Sum of Squares	Degree of Freedom	Mean Square	*F*-value	*p*-value Prob > *F*
Model	1105.95	9	122.88	47.67	< 0.0001
Residual	25.78	10	2.58	–	–
– Lack of Fit	19.32	5	3.86	2.99	0.1270
– Pure Error	6.46	5	1.29	–	–
Total	1131.73	19	–	–	–
C.V. = 2.01%	**R^2 = 0.9772**	**Pred. R^2 = 0.8571**	**Adj. R^2 = 0.9567**	**Adeq. Precision = 24.790**	

The experimental data obtained for % FAME yield in the transesterification process was analysed by the ANOVA and can be described by the following quadratic regression model:

$$Y_Y = -53.369 + 3.983X_1 + 21.410X_2 + 0.598X_3 + 3.019X_1X_2 + 0.152X_1X_3 - 0.042X_2X_3 - 10.563X_1^2 - 1.296X_2^2 + 4.748\times10^{-4}X_3^2 \quad (7)$$

where Y_Y is the percentage FAME yield from the transesterification reaction and X_1, X_2 and X_3 are uncoded values of the independent variables, viz., catalyst concentration (mass %), methanol-to-oil ratio and the reaction temperature (^{0}C), respectively.

The model was observed to fit the experimental data as most of the predicted responses matched the observed responses of % FAME yield, as shown in Figure 4.11.

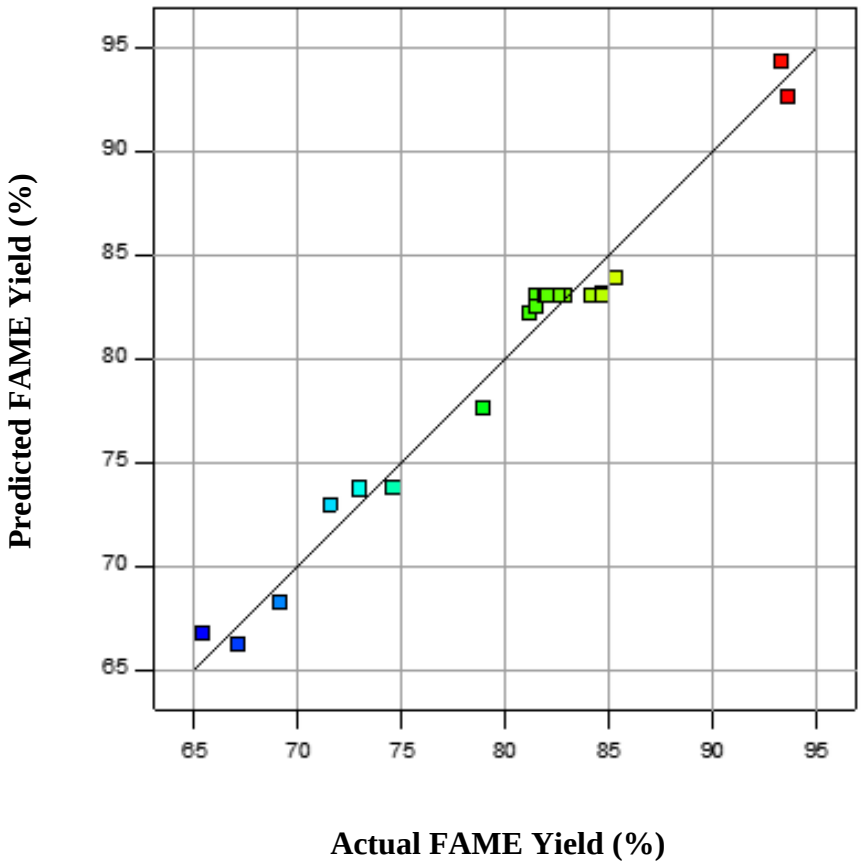

Fig. 4.11: Graphical Plot of percentage FAME yield's experimental results versus predicted results in the Transesterification Process

Equation 7 shows all 3 linear terms as positive, meaning that they all had a positive effect on the percentage FAME yield. An increase in the catalyst concentration, methanol-to-oil ratio or reaction temperature resulted in an increase in the percentage FAME yield. But larger magnitudes of the coefficient of methanol-to-oil ratio (p-value < 0.0001) when compared to the magnitudes of the coefficients of the other two independent variables indicated that the methanol-to-oil ratio was the most significant independent variable in controlling the transesterification process for an optimum FAME yield.

Table 4.11 shows the results of the ANOVA for the developed quadratic model. The ANOVA showed that the quadratic regression model (Equation 7) was significant. This was evident from the Fisher's *F*-test which gave an *F* value for the model of 47.67 with a very low probability value (*p*-value < 0.0001). The value of R^2 was found to be 0.9772, indicating that only 0.23% of the total variations was not explained by the developed regression model as shown in Figure 4.11. The predicted R^2 of 0.8571 was in reasonable agreement with the adjusted R^2 of 0.9567. The Lack of fit *F*-value of 2.99 implied that the Lack of Fit was not significant and that there was a 12.70% chance that a Lack of Fit that large could occur due to noise. The Adequate Precision was also evaluated and found to be high enough at 24.79. This meant that the developed model had a high degree of precision. The C.V. of 2.01% indicated that the model was reproducible.

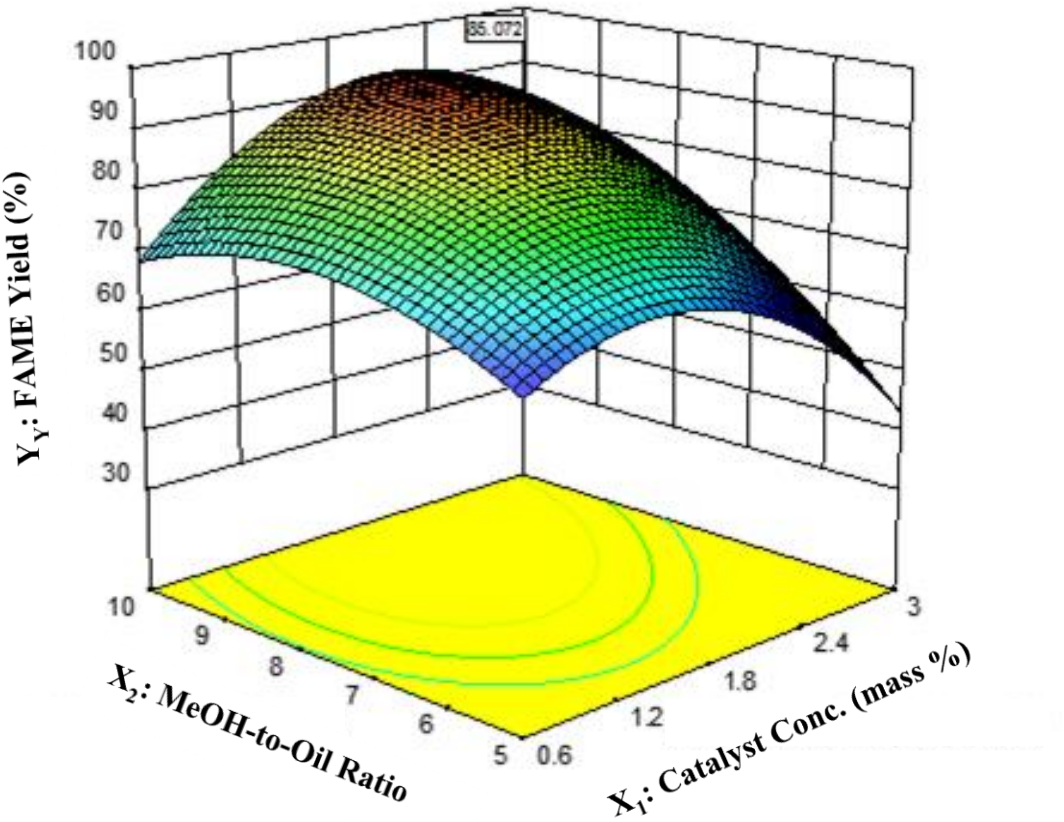

Fig. 4.12: Effect of Catalyst concentration and the Methanol-to-oil ratio on the percentage FAME yield at a Reaction temperature of 68 ^{0}C

It was found from the developed quadratic model (Equation 7) that an optimum % FAME yield of 84.51% could be obtained under the following operating conditions: 1.22 mass %, catalyst concentration, 7.3 methanol-to-oil ratio and 68 ^{0}C reaction temperature. Surface plots shown in Figures 4.12 – 4.14 are therefore meant to explain the behaviour of the developed process when the optimum values of the catalyst concentration, methanol-to-oil ratio and the reaction temperature are individualy fixed.

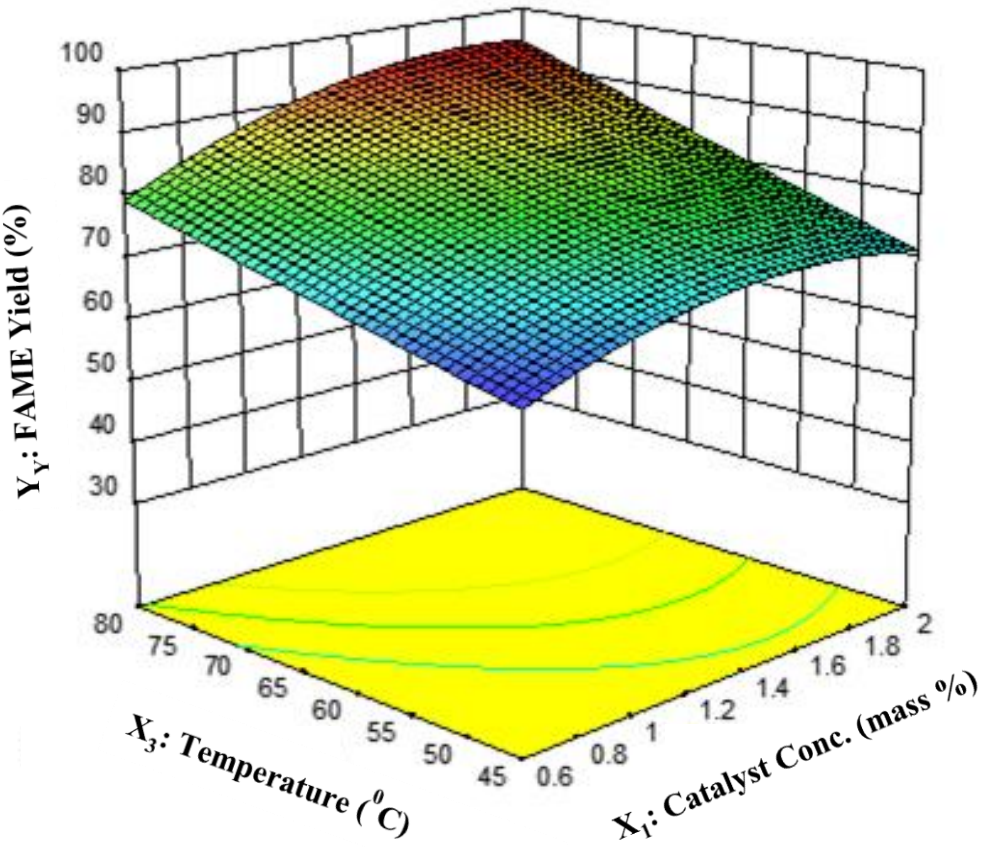

Fig. 4.13: Effect of Catalyst concentration and Reaction temperature on the percentage FAME yield at a Methanol-to-oil ratio of 7.30

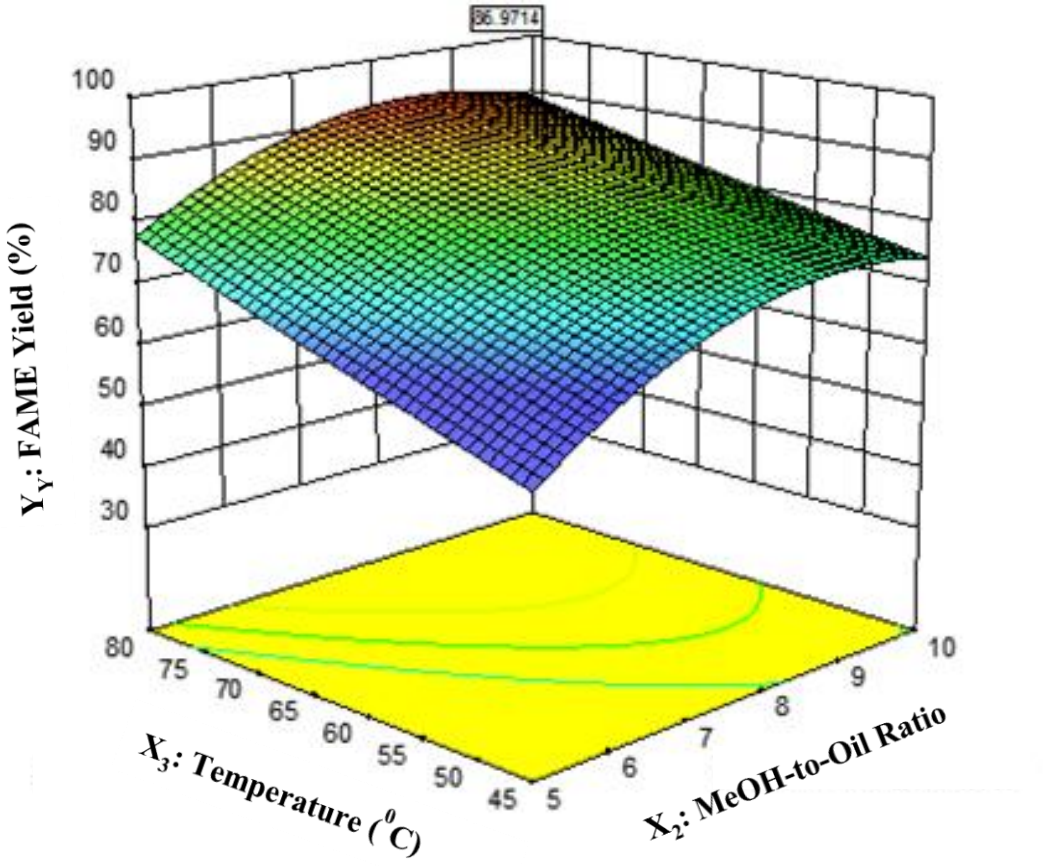

Fig. 4.14: Effect of Methanol-to-oil ratio and the Reaction temperature on the percentage FAME yield at a Catalyst concentration of 1.22 mass %

4.5.2 Response 2: Percentage FAME Purity

Experimental conditions that gave the highest and lowest percentage FAME purity were noted, before carrying out a full optimisation study. From the experiments carried out in the transesterification of *Croton gratissimus* oil, the highest FAME purity of 93.71% was obtained when the reactor was operated at 1.7 mass % catalyst concentration, 9 methanol-to-oil ratio and 73 ^{0}C reaction temperature. And the lowest FAME purity was found to be 73.29% when operating the reactor at 0.65 mass % catalyst concentration, 7.5 methanol-to-oil ratio and 62.50^{0}C reaction temperature.

Table 4.12: ANOVA of the % FAME Purity for the Quadratic Model of the Transesterification Process

Source of Variation	Sum of Squares	Degree of Freedom	Mean Square	*F*-value	*p*-value Prob > *F*
Model	886.01	9	98.45	193.22	< 0.0001
Residual	5.09	10	0.51	–	–
– **Lack of Fit**	3.02	5	0.60	1.46	0.3441
– **Pure Error**	2.07	5	0.41	–	–
Total	891.10	19	–	–	–
C.V. = 0.85%	**R^2 = 0.9943**	**Pred. R^2 = 0.9698**	**Adj. R^2 = 0.9891**	**Adeq. Precision = 40.903**	

The experimental data obtained for percentage FAME purity in the transesterification process was analysed by the ANOVA and can be described by the following quadratic regression model:

$$Y_P = -70.150 + 17.102X_1 + 19.212X_2 + 1.676X_3 + 1.102X_1X_2 + 0.687X_1X_3 - 9.444\times10^{-3}X_2X_3 - 22.719X_1^2 - 1.276X_2^2 - 0.016X_3^2 \quad (8)$$

where Y_P is the percentage FAME purity from the transesterification reaction and X_1, X_2 and X_3 are uncoded values of the independent variables, viz., catalyst concentration (mass %), methanol-to-oil ratio and the reaction temperature (^{0}C), respectively.

Equation 8 shows all 3 linear terms as positive, meaning that they all had a positive effect on the percentage FAME purity. An increase in the catalyst concentration, methanol-to-oil ratio or reaction temperature resulted in an increase in the percentage FAME purity. But larger magnitudes of the coefficient of catalyst concentration and methanol-to-oil ratio (both with *p*-value < 0.0001) when compared to the magnitudes of the coefficients of the reaction temperature indicated that they were the most significant independent variables in controlling the transesterification process for an optimum FAME purity.

The model was observed to fit the experimental data as most of the predicted responses matched the observed responses of % FAME purity, as shown in Figure 4.15.

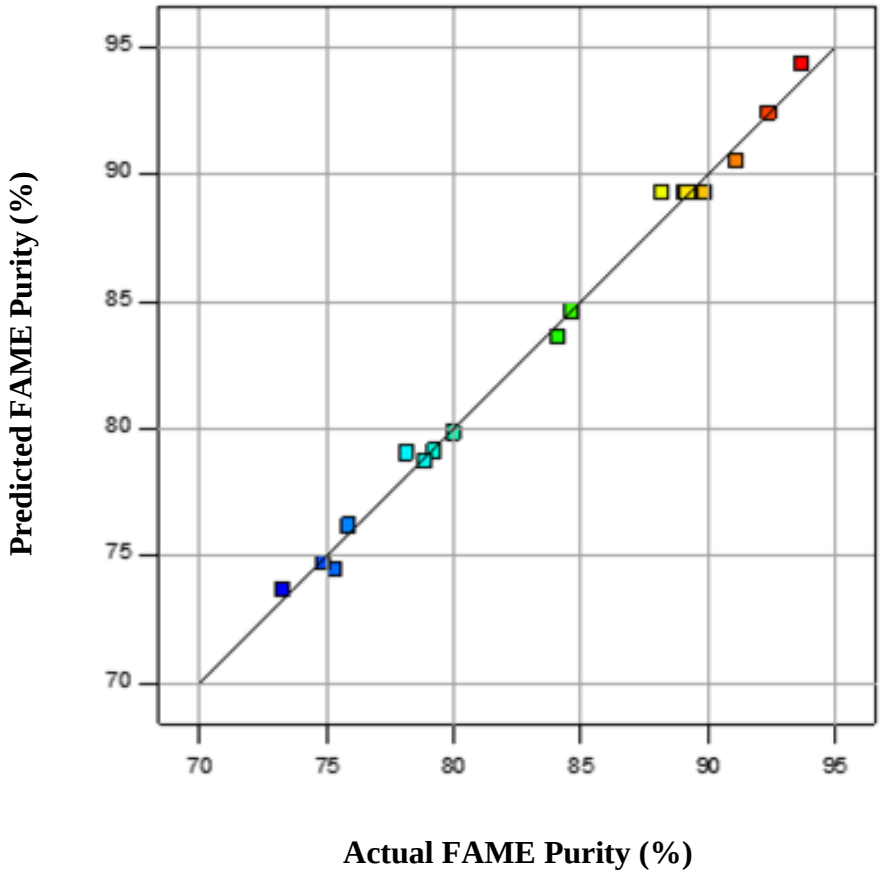

Fig. 4.15: Graphical Plot of percentage FAME purity's experimental results versus predicted results in the Transesterification Process

Table 4.12 shows the results of the ANOVA for the developed quadratic model. The ANOVA showed that the quadratic regression model (Equation 8) was significant. This was evident from the Fisher's *F*-test which gave an *F* value for the model of 193.22 with a very low probability value (*p*-value < 0.0001). The value of the coefficient of determination (R^2) was found to be 0.9943, indicating that only 0.06% of the total variations was not explained by the developed regression model as shown in Figure 4.15. The predicted R^2 of 0.9698 was in reasonable agreement with the adjusted R^2 of 0.9891. The Lack of fit *F*-value of 1.46 implied that the Lack of Fit was not significant and that there was a 34.41% chance that a Lack of Fit that large could occur due to noise. The Adequate Precision was also evaluated and found to be high enough at

40.90. This meant that the developed model had a high degree of precision. The coefficient of variation (C.V.) of 0.85% indicated that the model was reproducible.

From the developed quadratic model (Equation 8), it was found that an optimum % FAME purity of 90.66% could be obtained under the following operating conditions; 1.2 mass % catalyst concentration, 7.8 methanol-to-oil ratio and 66 ^{0}C reaction temperature. Surface plots shown in Figures 4.16 – 4.18 are therefore meant to explain the behaviour of the developed process when the optimum values of the catalyst concentration, methanol-to-oil ratio and the reaction temperature are individually fixed.

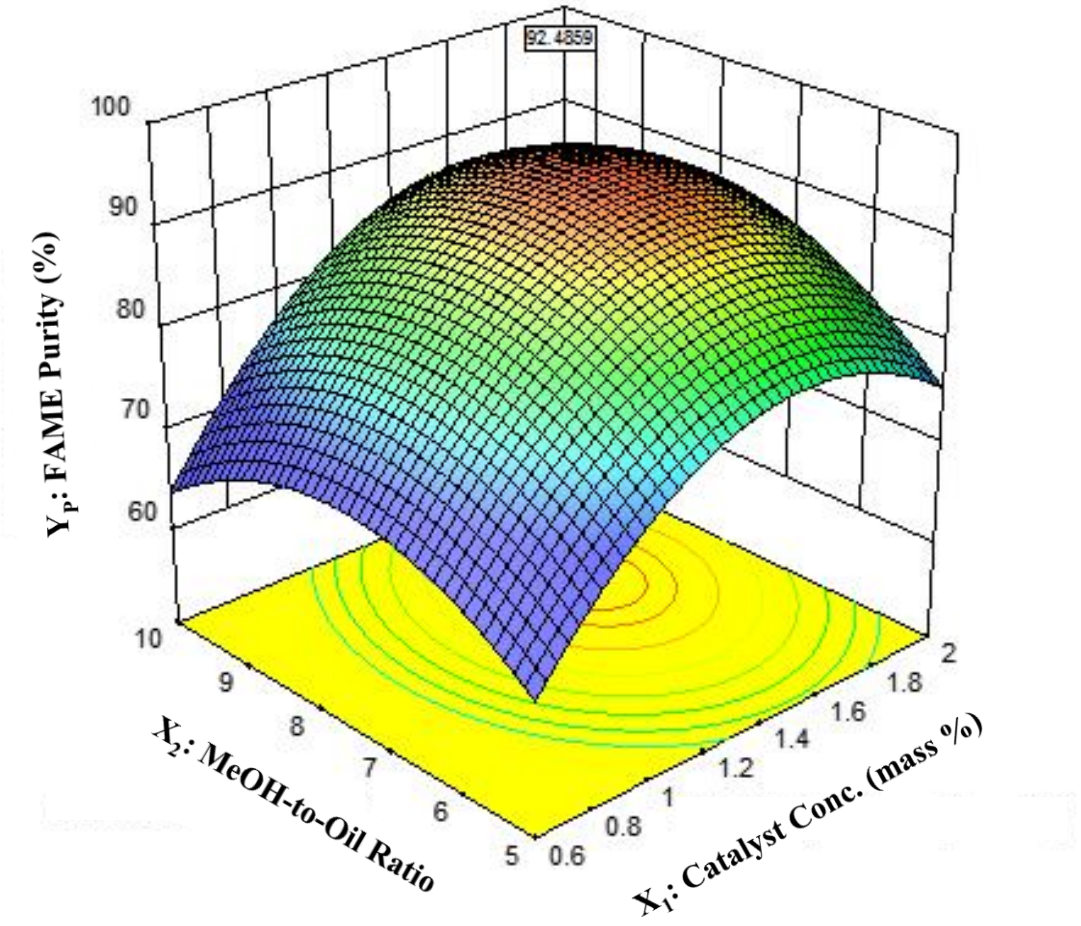

Fig. 4.16: Effect of Catalyst concentration and the Methanol-to-oil ratio on the percentage FAME purity at a Reaction temperature of 66 ^{0}C

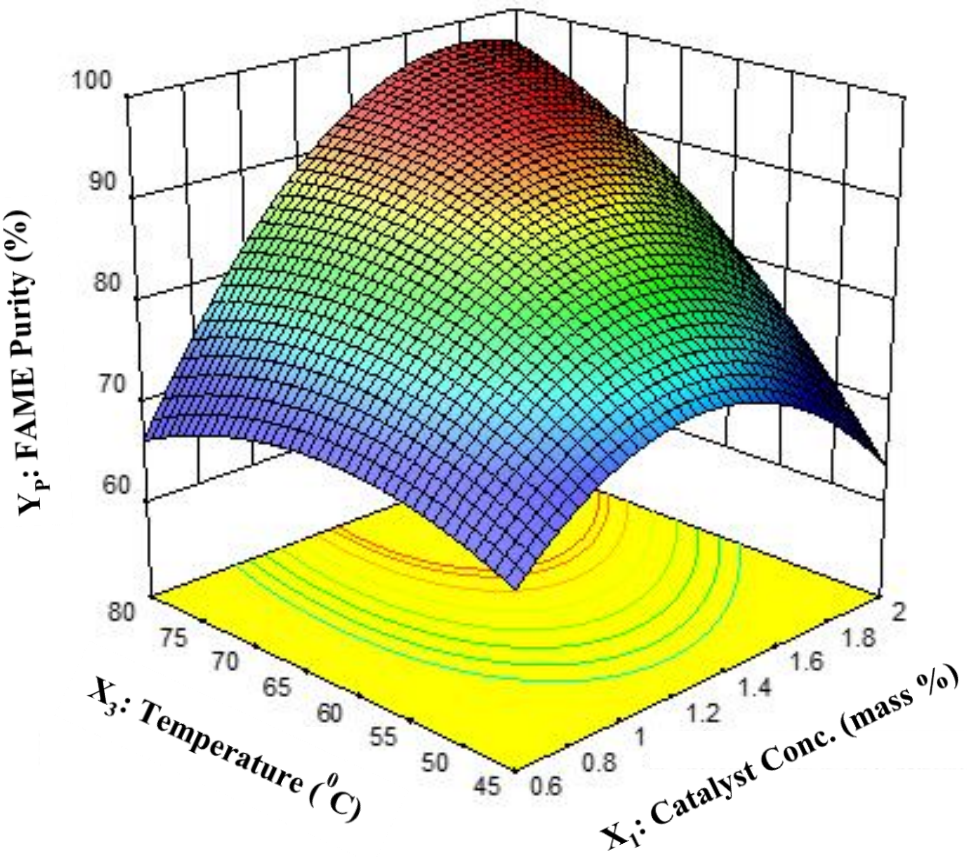

Fig. 4.17: Effect of Catalyst concentration and Reaction temperature on the percentage FAME purity at a Methanol-to-oil ratio of 7.80

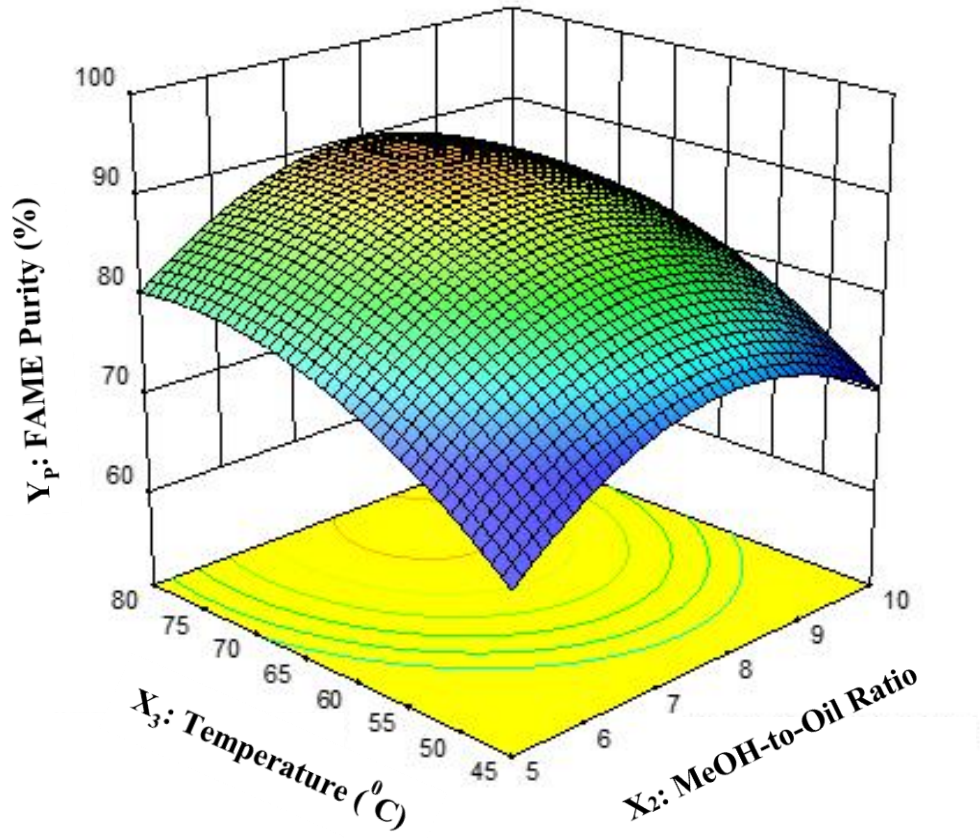

Fig. 4.18: Effect of Methanol-to-oil ratio and the Reaction temperature on the percentage FAME purity at a Catalyst concentration of 1.20 mass %

4.6 Combined Model Optimisation (OPTIMA3)

A combined model was developed for the optimum set of independent variables that gave responses of FAME yield and FAME purity within the region of 95% confidence interval (95% CI). This set of independent variables had to simultaneously satisfy the optimum responses obtained in OPTIMA2. Numerical optimisation techniques, that use the response targeting approach bound by constraints and the graphical optimisation technique, that utilises overlay plots to display regions of feasible responses that fit the optimisation criteria, were employed.

It was found that when the transesterification process is operated at 1.439 mass % catalyst concentration, 7.472 methanol-to-oil ratio and 63.50 ^{0}C reaction temperature, 84.51% FAME yield and 90.66% FAME purity could be achieved. These independent variables were therefore taken as the optimum set that satisfies optimum responses predicted by the developed models.

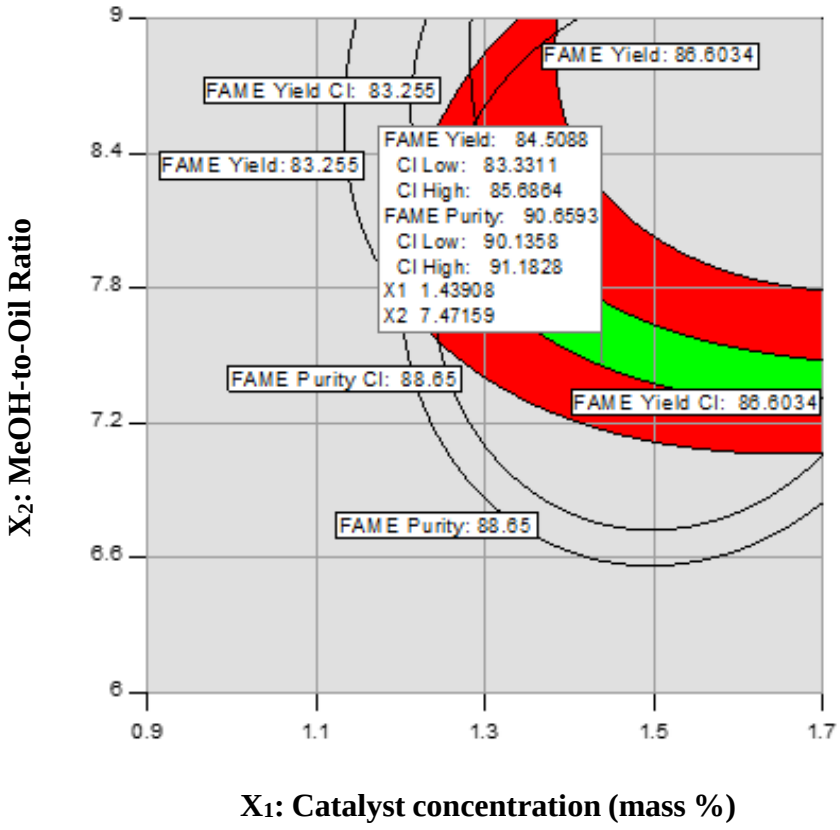

Fig. 4.19: Overlay Plot of Independent Variables satisfying targeted optimum responses of FAME Yield and FAME Purity bound by 63.50 ^{0}C Reaction Temperature constraint

Chapter 5. Discussion

The effect of particle size on the extraction oil yield has been extensively studied by a number of researchers. These studies have shown that a decrease in the particle size results in an increase in the extraction rate leading to high extraction oil yields (Mani *et al*., 2007; Liauw *et al*., 2008; Eikani *et al*., 2012). As seed particles get smaller, higher oil extraction yields are obtained and the opposite is observed when larger particle sized feeds are used in oil extraction. It is for this reason that no attempts were made in this study to investigate the effects of particle size on the extraction oil yield.

Roy *et al*. (2014) in their work on the transesterification kinetics in biodiesel production, established that the transesterification reaction is dependent, amongst other variables, on the mixing intensity of the reaction mixture. They developed a mathematical model that describes the effect of mixing intensity through stirring dynamics in the transesterification kinetics of *Jatropha curcas* oil and methanol when using an alkali catalyst. At a stirring speed of 600 rpm, they found that the transesterification reaction gave the highest yield of biodiesel. To substantiate their finding, they increased the reaction temperature, and discovered that the energy levels of the molecules were increased, leading to better diffusion into the continuous phase (Roy *et al*., 2014). It is for this reason that, in this study, the mixing intensity of both the esterification and transesterification reactions was kept constant at a conservative 650 rpm. Catalyst concentration, methanol-to-oil ratio and the reaction temperature were the only independent variables selected for the optimisation study.

The low extraction oil yield of 29.35% obtained for *Croton gratissimus* in this study was consistent with the findings from similar work performed by other researchers on non-edible vegetable oils (Amin *et al*., 2010; Liauw *et al*., 2008; Zhang *et al*., 2015). Amin *et al*. (2010)

performed the oil extraction procedures on *Jatropha curcas* seeds (from a non-edible tree species) following 3 different extraction techniques, viz., conventional *n*-hexane oil extraction, aqueous acidic hexane solution extraction and the mechanical pressing technique. The highest extraction oil yields obtained were from the conventional *n*-hexane extraction and the aqueous acidic hexane solution techniques giving oil yields of 23% and 24.216%, respectively. The mechanical pressing proved to be an inefficient technique with 6.595% extraction oil yield.

In this study, lipid profile of the extracted *Croton gratissimus* oil (Table 4.3) showed a low degree of unsaturation with only 25.4% unsaturated fatty acid content. Sarin *et al.* (2007), from an edible species of *Jatropha curcas* with 78.90% unsaturated fatty acid, obtained an extraction yield of 75.22% when using *n*-hexane as an extraction solvent. Evidently, *Jatropha curcas* gives better extraction oil yields than *Croton gratissimus* for the same solvent selection in extraction. These differences can be attributed to the differences in lipid profiles of the oils extracted from these two crop species. High number of double bonds (degree of unsaturation) in fatty acids leads to greater oil solubility (Kostic *et al*., 2013). This increased solubility of oil leads to increased mass transfer between the oil and the surface of the ground seed particles resulting in high oil extraction yields.

Depending on the method of preparation, heterogeneous SO_4^{2-}/ZrO_2 catalysts can either be used to catalyse the esterification reaction or simultaneously catalyse both the esterification and transesterification reaction. When used to simultaneously catalyse both reactions, monoclinic and tetragonal phases must be present with the tetragonal phase being the dominant phase. Naturally ZrO_2 crystals exist in a crystal lattice as the more thermodynamically stable monoclinic phase, with less catalytic activity in transesterification reactions. The doping of $Zr(OH)_4$ with the sulphates (SO_4^{2-}) transforms this stable phase to a less stable (metastable) but highly active tetragonal phase. The addition of sulphates also inhibits sintering by stabilising

the catalyst surface and help conserve part of the micropore volume (Vera *et al*., 2002). The subsequent calcination at temperatures in excess of 650 ^{0}C creates multiple active sites with varying strengths of Brønsted and Lewis acidity. In this study, the synthesised SO_4^{2-}/ZrO_2 catalyst was found to be predominantly monoclinic (Figures 4.1 and 4.4), making it suitable to catalyse only the esterification reaction.

Miranda *et al*. (2015) compared the catalytic activity of monoclinic and tetragonal SO_4^{2-}/ZrO_2 in catalysing the esterification of a mixture of glycerol and fatty acids. They found that the activity of monoclinic SO_4^{2-}/ZrO_2 was much higher than that of its tetragonal counterpart that achieved only 30% conversion of the glycerol-fatty acid mixture. They further established that monoclinic zirconium, surrounded by 7 oxygen atoms compared to 8 atoms in the tetragonal zirconium, is more susceptible to surface sulphate doping. In monoclinic zirconia, negative oxygen anions offer less electrostatic repulsion to the incoming sulphate anions (Miranda *et al*., 2015). This was indicative of the superior quality nature of the monoclinic-phased SO_4^{2-}/ZrO_2 in catalysing the esterification reactions that require strong acidic activity. With the synthesised SO_4^{2-}/ZrO_2 catalyst in the monoclinic form in this work, potassium hydroxide (KOH) was therefore employed in the transesterification step to facilitate the completion of the conversion of triglycerides to fatty acid methyl esters (FAME).

Sulphated zirconia, SO_4^{2-}/ZrO_2 in its current form, as a predominantly monoclinic phase, has never been used to catalyse the esterification reaction in biodiesel production. The focus of the esterification reaction was therefore squarely placed on the effectiveness of this catalyst in converting free fatty acids to di and mono-glycerides. For this reason, a much wider range of catalyst concentration, between 6 and 14 mass %, was selected for the study whilst feeding methanol in excess (more than the stoichiometric amount). Arora *et al*. (2015), in their work on the esterification of high free fatty acid Rice Bran oil, found out that there was no significant

increase in the FFA conversion when methanol-to-oil ratio was increased beyond 20. In the current work, methanol was fed in a range of between 20 and 40:1 to rule it out as the contributing factor should there be low or no conversion of FFA at the end of the reaction.

In the quadratic polynomial models developed (Equations 6, 7 and 8), a positive sign in front of the term indicated a synergistic effect on the intended response, whereas a negative sign indicates an antagonistic effect on that response (Lee *et al*., 2011). The amount of the SO_4^{2-}/ZrO_2 catalyst used in the esterification reaction was found to have the most significant effect in the reduction of the Acid Value of *Croton gratissimus* oil from 21.455 mg KOH/g to an average of 2.927 mg KOH/g oil. The lowest and highest Acid Values were obtained when the same operating conditions of temperature (70 ^{0}C) and methanol-to-oil ratio (32.50) whilst more than doubling the catalyst concentration from 6 to 14 mass % (Table 4.7 standard experimental run 9 and 10). This dependency of the esterification reaction on the catalyst concentration was consistent with the observations by Tiwari *et al*. (2007). Their optimised RSM model for biodiesel produced from high FFA *Jatropha curcas* oil showed that, catalyst concentration was the most significant factor (followed by methanol-to-oil ratio) in the conversion efficiency of free fatty acids (FFA) in oil.

Within the lower limit of the 95% confidence interval, the developed quadratic model predicted an optimum Acid Value of 2.693 mg KOH/g of oil when the esterification process was operated at 10.96 mass % catalyst concentration, 27.60 methanol-to-oil ratio and 64 ^{0}C reaction temperature. In a two-step biodiesel production process, Muthu *et al*. (2010) converted *Azadirachta indica A. Juss* oil to biodiesel using SO_4^{2-}/ZrO_2 and KOH as catalysts in the esterification and transesterification reactions, respectively. From an un-optimised process operating at methanol-to-oil ratio of 9:1, catalyst concentration of 1%, reaction time of 2 hours and reaction temperature of 65 ^{0}C, they obtained a 94% FFA conversion efficiency in the

esterification step with a predominantly tetragonal phased SO_4^{2-}/ZrO_2 catalyst. Their results were slightly better than the 88% FFA conversion efficiency obtained in this study from a SO_4^{2-}/ZrO_2 catalyst with a dominant monoclinic phase. High levels of methanol used in the esterification reaction in this study may have caused the leaching of the catalyst leading to the loss of the sulphur species thus deactivating the catalyst SO_4^{2-}/ZrO_2 (Lopez *et al*., 2008).

The significant factors in the transesterification reaction for the optimum FAME yield were, methanol-to-oil ratio and KOH catalyst concentration, the former having the most effect. At higher methanol-to-oil ratios (greater than stoichiometric values), reactions proceed faster, giving higher FAME yields. But excessive amounts of methanol in the reaction mixture result in the formation of water and soaps, inevitably leading to substantial loss of esters. In this work, this sudden decline in FAME yield was observed at a methanol-to-oil ratio of 8.47 that gave 86.97% FAME yield (Figure 4.14). Beyond this point, an increase in methanol-to-oil ratio caused a decrease in the FAME yield. The catalyst concentration also seemed to have a positive influence on the FAME yield, but up to a catalyst concentration of 1.74 mass % that gave 85.07% FAME yield. A decline in the FAME yield was observed beyond this point (Figure 4.12). These observations are in agreement with the work by Dwivedi and Sharma (2015). In their work on the optimisation of FAME yield from the KOH-catalysed synthesis of biodiesel from Pongamia oil, they discovered a strong relationship between catalyst concentration and the molar ratio of methanol-to-oil. Biodiesel yield increased with increasing amounts of catalyst and methanol in the reaction mixture. They noted a reverse in the trend when the amounts of these independent variables reached certain values. A conclusion was therefore made that when the amount of methanol used in transesterification is in excess of the optimum value, leaching of the catalyst in methanol become stronger and as a result a dramatic decrease of FAME yield could be expected (Dwivedi and Sharma, 2015). This phenomenon was also observed, in the present study, in the esterification of *Croton gratissimus* oil with exceedingly high amounts of

methanol. Leaching caused a decrease in the activity of SO_4^{2-}/ZrO_2, negatively affecting the conversion rate of fatty acids to methyl esters.

In the transesterification of the pre-treated *Croton gratissimus* oil, the purity of FAME depended mostly on the catalyst concentration and the amount of methanol fed into the reaction mixture. An increase in both these independent variables resulted in an increase in the purity of FAME produced. But at an optimum FAME purity of 92.49% the catalyst concentration and methanol-to-oil ratio reached their peak values of 1.57 mass % and 7.96, respectively. Beyond these maximum values, a sharp decline in the percentage FAME purity was observed (Figure 4.16). Vicente *et al* (2007) made the same observations in their work on the optimisation of biodiesel production from sunflower oil using KOH as a transesterification catalyst. Their statistical analysis identified the initial catalyst concentration and methanol-to-oil ratio as the most important factors in FAME purity response. According to their results, FAME purity reached its maximum value (virtual 100%) at the maximum catalyst concentration of 1.5 mass%, thereafter reaching a stability region (Vicente *et al*., 2007).

The two quadratic models developed for the transesterification process predicted two sets of factor values for catalyst concentration, methanol-to-oil ratio and reaction temperature corresponding to the optimum values of the 2 responses, FAME yield and FAME purity. Because the transesterification process is but one process, it must be described by one set of variable values for the attainment of these optimum responses. A set of common variable values of these operating conditions that satisfied the optimum responses for FAME yield and FAME purity within the 95% confidence interval, had to be found. This was achieved by overlaying critical response contours on a contour plot (overlay plot) after targeting optimum responses from OPTIMA2 and using constraints to narrow down the search for the optimum set. Reaction temperature range between 63.50 and 64 ^{0}C (below 64.50 ^{0}C, the boiling point temperature of

methanol) and low catalyst concentration between 10.50 and 10.98 mass % for OPTIMA1 and 1.40 and 1.60 mass % for OPTIMA3, were used as constraints. The choice of these constraints was based on process economics.

The results of the transesterification experiments performed, with the exception of standard experimental runs 8 and 14 (Table 4.10), gave an average FAME yield of 78.47% evaluated over a range of set factor limits. This is lower than the theoretically attainable maximum FAME yield of 90.47%; a value derived from the mass balance of *Croton gratissimus* biodiesel process shown in Figure 2.3. Certainly, there still is a potential of improving FAME yield beyond what was achieved in this optimisation study. And since KOH catalyst and methanol, both fed in excess, had significant effects in controlling the transesterification reaction, a reduction in the amounts of these two reactants could eliminate the problems associated with their excessive usage. In this work, the amount of KOH catalyst added into the reaction mixture, in the transesterification reaction, had a significant influence on both the extent of reaction and the ease of separation of the final products. It was established, therefore, that the addition of high quantities of KOH catalyst in an effort to compensate for possible low reaction rates resulted in the formation of emulsions that inadvertently increased the viscosity of the reaction mixture (Crabbe *et al*., 2001). Moreover, high concentrations of KOH catalyst in the reaction mixture promoted the formation of water as the hydroxides combine with methanol. This led to the hydrolysis of the methyl esters already formed, resulting in soap formation in an undesired saponification reaction (Hameed *et al*., 2009). The presence of soap in the final products therefore reduced the FAME yield to below the theoretical maximum and made the separation of glycerol from biodiesel difficult.

Chapter 6. Conclusions and Recommendations

The monoclinic sulphated zirconia, SO_4^{2-}/ZrO_2 catalyst has high acid strength and exhibits high catalytic activity; both qualities found in the tetragonal-phased type catalyst. But the monoclinic type, with low levels of anion repulsion, is more susceptible to sulphate doping than its counterpart. This makes the monoclinic-phased catalyst the most preferred form to catalyse the esterification reaction that require high acid activity. In the esterification of *Croton gratissimus* oil, the monoclinic SO_4^{2-}/ZrO_2 catalyst synthesised in this work, offered an 88% reduction in the Acid Value of oil, contributing immensely to the high yield and purity of FAME produced in the transesterification process. The RSM model developed for the esterification process showed that the Acid Value of *Croton gratissimus* oil could be reduced from 21.455 mg KOH/g to an optimum 2.693 mg KOH/g when the process is operated at 10.96 mass % catalyst concentration, 27.60 methanol-to-oil ratio and 64 ^{0}C reaction temperature.

The developed models for the transesterification processes were both significant, with the Fisher's *F*-test giving very low probability values (*p*-value < 0.0001) for both models. The coefficient of determinants, R^2 for both optimised processes were 0.9805 and 0.9772, respectively, indicating that only about 0.20% of the total variations could not be explained by the regression models. Regardless of these insignificant variations, both models showed a high degree of precision and were reproducible. For this process, an optimum FAME yield of 84.51% could be obtained from the process operating at 1.22 mass % catalyst concentration, 7.30 methanol-to-oil ratio and 68 ^{0}C reaction temperature. When the same process is operated at 1.20 mass % catalyst concentration, 7.8 methanol-to-oil ratio and 66 ^{0}C reaction temperature, an optimum purity of FAME of 90.66% could be achieved.

The optimisation models developed for the transesterification process in this study have therefore demonstrated sufficient degree of accuracy in predicting the *Croton gratissimus* biodiesel yield and the purity of its FAME. These two regression models were combined to give one set of optimum operating conditions for the attainment of the two responses. Operating conditions selected were from a wide range of process parameters found within the experimental domain in the optimum region. The selection was based on process constraints of energy consumption and resource utilisation, considered as important factors in the economic viability of biodiesel processes. For this reason, the final process chosen for development was the one that gave the desired optimum responses from minimal use of catalyst and methanol whilst operating at moderate conditions of temperature and pressure. The combined model predicted therefore that when this transesterification process is operated at 1.439 mass % catalyst concentration, 7.472 methanol-to-oil ratio and at a reaction temperature of 63.50 ^{0}C, an optimum FAME yield of 84.51% and a FAME purity of 90.66% is achievable.

The two-step biodiesel synthesis approach followed in this study had a significant impact in producing biodiesel of moderately high FAME yield and high FAME purity. The results of this study are in reasonable agreement with results of previous work by Bahadur *et al*., 2014. In their work on an un-optimised one-step *Croton gratissimus* biodiesel production process they obtained 84.65% FAME yield and 72.26% FAME purity from an unspecified phase of sulphated zirconia, SO_4^{2-}/ZrO_2 catalyst.

On the basis of the data collected and the results obtained in this work, *Croton gratissimus* crop has proven to be a good feedstock for biodiesel production processes in the Republic of South Africa and beyond. But lower extraction oil yields obtained from *Croton gratissimus* crop remain a cause for concern as competing crops with better oil extraction yields will always receive preference over this crop. Improvements to its oil extraction yield could be made

possible by undertaking further studies that involve the use of 2 extraction solvents of different polarity. The nonpolar solvent will release fatty acids from the least polar long-chain triglycerides (LCT) and the polar solvent (co-solvent) will release fatty acids from the highly polar medium-chain triglycerides (MCT) present in this crop. Park *et al*. (2017) successfully applied this technique in the *in situ* transesterification process of microalgae biodiesel production. Its application to *Croton gratissimus* oil extraction does not only has the potential of increasing the oil extraction yield but could subsequently improve the FAME yield in the transesterification step resulting in higher biodiesel throughput rates.

Bibliography

Ahmad, A.L., Yasin, M.N.H., Derek, C.J.C., Lim, J.K., **2011**. Microalgae as a sustainable energy source for biodiesel production: A review. Renewable and Sustainable Energy Reviews 15, 584-593.

Ahmadi, M., Vahabzadeh, F., Bonakdarpour, B., Mofarrah, E., Mehranian, M., **2005**. Application of the central composite design and response surface methodology to the advanced treatment of olive oil processing wastewater using Fenton's peroxidation. Journal of Hazardous Materials B123, 187-195.

Amigun, B., Musango, J.K., Stafford, W., **2011**. Biofuels and sustainability in Africa. Renewable and Sustainable Energy Reviews 15, 1360-1372.

Amin, S. K., Hawash, S., El Diwani, G., El Rafei, S., **2010**. Kinetics and Thermodynamics of Oil Extraction from *Jatropa Curcas* in Aqueous Acidic Hexane Solutions. Journal of American Science 6 (11), 293-300.

Aransiola, E.F., Ojumu, T.V., Oyekola, O.O., Madzimbamuto, T.F., Ikhu-Omoregbe, D.I.O., **2014**. A review of current technology for biodiesel production: State of the art. Biomass and Bioenergy 61, 276-297.

Arora, R., Toor, A.P., Wanchoo, R.K., **2015**. Esterification of High Free Fatty Acid Rice Bran Oil: Parametric and Kinetic Study. Chemical and Biochemical Engineering Quarterly 29 (4), 617-623.

Atabani, A.E., Silitonga, A.S., Badruddin, I.A., Mahlia, T.M.I., Masjuki, H.H., Mekhilef, S., **2012**. A comprehensive review on biodiesel as an alternative energy resourse and its characteristics. Renewable and Sustainable Energy Reviews 16, 2070-2093.

Atabani, A.E., Silitonga, A.S., Ong, H.C., Mahlia, T.M.I., Masjuki, H.H., Badruddin, I.A., Fayaz, H., **2013**. Non-edible vegetable oils: A critical evaluation of oil extraction, fatty acid compositions, biodiesel production, characteristics, engine performance and emissions production. Renewable and Sustainable Energy Reviews 18, 211-245.

Atadashi, I.M., Aroua, M.K., Abdul Aziz, A.R., Sulaiman, N.M.N., **2013**. The effects of catalysts in biodiesel production: A review. Journal of Industrial and Engineering Chemistry 19, 14-26.

Bahadur, I., Bux, F., Guldhe, A., Tumba, K., Singh, B., Ramjugernath, D., Moodley, K.G., **2014**. Assessment of Potential of *Croton Gratissimus* Oil for Macro-scale Production of Biodiesel based on Thermophysical Properties. Energy and Fuel 12, 7576-7581.

Bas, D., Boyaci, I.H., **2007**. Modeling and optimisation I: Usability of response surface methodology. Journal of Food Engineering 78, 836-845.

Betiku, E., Omilakin, O.R., Ajala, S.O., Okeleye, A.A., Taiwo, A.E., Solomon, B.O., **2014**. Mathematical modelling and process parameters optimization studies by artificial neural network and response surface methodology: A case of non-edible neem (*Azadirachta indica*) seed oil biodiesel synthesis. Energy 72, 266-273.

Blanchard, R., Richardson, D.M., O'Farrell, P.J., von Maltitz, G.P., **2011**. Biofuels and biodiversity in South Africa. South African Journal of Science 107 (5/6), Art. #186, 8 pages. doi:10.4102/sajs.v107i5/6.186.

Blanco, M., Adenauer, M., Shrestha, S., Becker, A., **2013**. Methodology to assess EU biofuel policies: the CAPRI approach. Research Centre, Institute for Prospective Technological Studies. European Commission.

BP, **2014**. BP Statistical Review of World Energy 2014. London, UK. BP p.l.c.

BP, **2016**. BP Statistical Review of World Energy 2016. London, UK. BP p.l.c.

Brent Crude Oil Prices – 10 Year Daily Chart, **2017**. Available from: http://www.macrotrends.net/2480/brent-crude-oil-prices-10-year-daily-chart. [accessed 18.07.17].

Chen, F.R., Coudurier, G., Joly, J.F., Vedrine, J.C., **1993**. Superacid and Catalytic Properties of Sulfated Zirconia. Journal of Catalysis 143, 616-626.

Chouhan, A.P.S., Sarma, A.K., **2011**. Modern heterogeneous catalysts for biodiesel production: A comprehensive review. Renewable and Sustainable Energy Reviews 15, 4378-4399.

Coates, P.M., **2002**. Keith Coates Palgrave Trees of Southern Africa. Struik Publishers, Cape Town.

Crabbe, E., Nolasco-Hipolito, C., Kobayashi, G., Sonomoto, K., Ishizaki, A., **2001**. Biodiesel production from crude palm oil and evaluation of butanol extraction and fuel properties. Process Biochemistry 37, 65-71.

Department of Minerals and Energy, **2006**. An Investigation into the Feasibility of Establishing a Biofuels Industry in the Republic of South Africa. Renewable Energy Directorate of the Government of the Republic of South Africa.

Department of Minerals and Energy, **2007**. Biofuels Industrial Strategy of the Republic of South Africa. Renewable Energy Directorate of the Government of the Republic of South Africa.

Dermirbas, A., **2008**. Comparison of transesterification methods for production of biodiesel from vegetable oils and fats. Energy Conversion and Management 49, 125-130.

Doehlert, D.H., **1970**. Uniform Shell Designs. Journal of the Royal Statistical Society. Series C (Applied Statistics) 19 (3), 231-239.

Dwivedi, A., Sharma, M.P., **2015**. Application of Box-Behnken design in optimization of biodiesel yield from Pongamia oil and its stability analysis. Fuel 145, 256-262.

Eikani, M.H., Golmohammad, F., Homani, S.S., **2012**. Extraction of pomegranate (*Punica granatum L.*) seed oil using superheated hexane. Food and Bioproducts Processing 90, 32-36.

Endalew, A.K., Kiros, Y., Zanzi, R., **2011**. Inorganic heterogeneous catalysts for biodiesel production from vegetable oils. Biomass and Bioenergy 35, 3787-3809.

Ferreira, S.L.C., Bruns, R.E., da Silva, E.G.P., dos Santos, W.N.L., Quintella, C.M., David, J.M., de Andrade, J.B., Breitkreitz, M.C., Jardim, I.C.S.F., Neto, B.B., **2007**a. Statistical design and response surface techniques for the optimization of chromatographic systems. Journal of Chromatography A 1158, 2-14.

Ferreira, S.L.C., Bruns, R.E., Ferreira, H.S., Matos, G.D., David, J.M., Brandao, G.C., da Silva, E.G.P., Portugal, L.A., dos Reis, P.S., Souza, A.S., dos Santos, W.N.L., **2007**b. Box-Behnken design: An alternative for optimization of analytical methods. Analytica Chimica Acta 597, 179-186.

Graboski, M.S., McCormick, R.L., **1998**. Combustion of Fat and Vegetable Oil Derived Fuels in Diesel Engines. Progress Energy Combustion Science 24, 125-164.

Hameed, B.H., Lai, L.F., Chin, L.H., **2009**. Production of biodiesel from palm oil (*Elaeis guineensis*) using heterogeneous catalyst: An optimized process. Fuel Processing Technology 90, 606-610.

Hattori, H., **2004**. Solid base catalysts: Generation, characterization, and catalytic behaviour of basic sites. Journal of the Japan Petroleum Institute 47 (2), 67-81.

Helwani, Z., Othman, M.R., Aziz, N., Kim, J., Fernando, W.J.N., **2009**. Solid heterogeneous catalysts for transesterification of triglycerides with methanol: A review. Applied Catalysis A: General 363, 1-10.

Hill, J., Nelson, E., Tilman, D., Polasky, S., Tiffany, D., **2006**. Environmental, economic, and energetic costs and benefits of biodiesel and ethanol biofuels. Proceedings of the National Academy of Sciences of the United States of America 103 (30), 11206-11210.

Jeong, G., Yang, H., Park, D., **2009.** Optimization of Transesterification of Animal Fat Esters using Response Surface Methodology. Bioresource Technology 100, 25-30.

Kafuku, G., Mbarawa, M., **2010**. Biodiesel production from *Croton megalocarpus* oil and its process optimization. Fuel 89, 2556-2560.

Kostic, M.D., Jokovic, N.M., Stamenkovic, O.S., Rajkovic, K.M., Milic, P.S., Veljkovic, V.B., **2013**. Optimization of hempseed oil extraction by *n*-hexane. Industrial Crops and Products 48, 133-143.

Kumar, M., Sharma, M.P., **2015**. Assessment of potential of oils for biodiesel production. Renewable and Sustainable Energy Reviews 44, 814-823.

Lee, H.V., Yunus, R., Juan, J.C., Taufiq-Yap, Y.H., **2011**. Process optimisation design for Jatropha-based biodiesel production using response surface methodology. Fuel Processing Technology 92, 2420-2428.

Leung, D.Y.C., Wu, X., Leung, M.K.H., **2010**. A review on biodiesel production using catalysed transesterification. Applied Energy 87, 1083-1095.

Li, H., Pordesimo, L., Weiss, J., **2004**. High intensity ultrasound-assisted extraction of oil from soybeans. Food Research International 37, 731-738.

Liauw, M.Y., Natan, F.A., Widiyanti, P., Ikasari, D., Indraswati, N., Soetaredjo, F.E., **2008**. Extraction of Neem oil (*Azadirachta indica A. Juss*) using n-hexane and ethanol: Studies of oil quality, kinetic and thermodynamic. ARPN Journal of Engineering and Applied Sciences 3 (3), 49-54.

Lopez, D.E., Goodwin Jr, J.G., Bruce, D.A., Furuta, S., **2008**. Esterification and transesterification using modified-zirconia catalyst. Applied Catalysis A: General 339, 76-83.

Lotero, E., Goodwin, J.G., Bruce, D.A., Suwannakarn, K., Liu, Y., Lopez, D.E., **2006**. The catalysis of biodiesel synthesis. Catalysis 19, 41-83.

Madras, G., Kolluru, C., Kumar, R., **2004**. Synthesis of biodiesel in supercritical fluids. Fuel 83, 2029-2033.

Mani, S., Jaya, S., Vadivambal, R., **2007**. Optimization of solvent extraction of Moringa (*Moringa oleifera*) seed kernel oil using response surface methodology. Food and Bioproducts Processing 85 (C4), 328-335.

Mendonca, D.R., Andrade, H.M.C., Guimaraes, P.R.B., Vianna, R.F., Meneghetti, S.M.P., Pontes, L.A.M., Teixeira, L.S.G., **2011**. Application of full factorial design and Doehlert matrix for the optimisation of beef tallow methanolysis via homogeneous catalysts. Fuel Processing Technology 92, 342-348.

Miranda, C.D., Ramirez, A.E., Jurado, S.G., Vera, C.R., **2015**. Superficial effects and catalytic activity of ZrO_2–SO_4^{2-} as a function of the crystal structure. Journal of Molecular Catalysis A: Chemical 398, 325-335.

Montgomery, D.C., Runger, G.C., **2003**. Applied Statistics and Probability for Engineers, Third Edition. John Wiley and Sons, United States of America.

Mulholland, D.A., Langat, M.K., Crouch, N.R., Coley, H.M., Mutambi, E.M., Nuzillard, J.M., **2010**. Cembranolides from the stem bark of the southern African medicinal plant, *Croton gratissimus* (Euphorbiaceae). Phytochemistry 71, 1381-1386.

Muthu, H., SathyaSelvabala, V., Varathachary, T.K., Selvaraj, D.K., Nandagopal, J., Subramanian, S., **2010**. Synthesis of biodiesel from Neem oil using sulphated zirconia via transesterification. Brazilian Journal of Chemical Engineering 27 (4), 601-608.

Ndhlala, A.R., Aderogba, M.A., Ncube, B., Van Staden, J., **2013**. Anti-Oxidative and Cholinesterase inhibitory effects of leaf extracts and their isolated compounds from two closely related *Croton* species. Molecules 18, 1916-1932.

Park, J., Kim, B., Chang, Y.K., Lee, J.W., **2017**. Wet *in situ* transesterification of microalgae using ethyl acetate as a co-solvent and reactant. Bioresource Technology 230, 8-14.

Pradhan, A., Mbohwa, C., **2014**. Development of biofuels in South Africa: Challenges and opportunities. Renewable and Sustainable Energy Reviews 39, 1089-1100.

Rattanaphra, D., Harvey, A.P., Thanapimmetha, A., Srinophakun, P., **2012**. Simultaneous tranesterification and esterification for biodiesel production with and without a sulphated zirconia catalyst. Fuel 97, 467-475.

Reddy, B.M., Sreekanth, P.M., Lakshmanan, P., **2005**. Sulfated zirconia as an efficient catalyst for organic synthesis and transformation reactions. Journal of Molecular Catalysis A: Chemical 237, 93-100.

Roy, P.K., Datta, S., Nandi, S., Al Basir, F., **2014**. Effect of mass transfer kinetics for maximum production of biodiesel from *Jatropha curcas* oil: A mathematical approach. Fuel 134, 39-44.

Samios, D., Pedrotti, F., Nicolau, A., Reiznautt, Q.B., Martini, D.D., Dalcin, F.M., **2009**. A transesterification double step process – TDSP for biodiesel preparation from fatty acid triglycerides. Fuel Processing Technology 90, 599-605.

Sanchez-Arreola, E., Martin-Torres, G., Lozada-Ramirez, J., Hernandez, L.R., Bandala-Gonzalez, E.R., Bach, H., **2015**. Biodiesel production and de-oiled seed cake nutritional values of a Mexican edible *Jatropha curcas*. Renewable Energy 76, 143-147.

Sani, Y.M., Wan Daud, W.M.A., Abdul Aziz, A.R., **2014**. Activity of solid catalysts for biodiesel production: A critical review. Applied Catalysis A: General 470, 140-161.

Santacesaria, E., Vicente, G.M., Di Serio, M., Tesser, R., **2012**. Main technologies in biodiesel production: State of the art and future challenges. Catalysis Today 195, 2-13.

Sarin, R., Sharma, M., Sinharay, S., Malhotra, R.K., **2007**. Jatropha-Palm biodiesel blends: An optimum mix for Asia. Fuel 86, 1365-1371.

Semwal, S., Arora, A.K., Badoni, R.P., Tuli, D.K., **2011**. Biodiesel production using heterogeneous catalysts. Bioresource Technology 102, 2151-2161.

Shuit, S.H., Lee, K.T., Kamaruddin, A.H., Yusup, S., **2010**, Reactive extraction and in situ esterification of *Jatropha curcas L*. seeds for the production of biodiesel. Fuel 89, 527-530.

Singh, R.K., Padhi, S.K., **2009**. Characterization of Jatropha oil for the preparation of biodiesel. Natural Product Radiance 8 (2), 127-132.

Srinivasan, R., Keogh, R.A., Milburn, D.R., Davis, B.H., **1995**. Sulfated zirconia catalysts: Characterization by TGA/DTA/Mass spectrometry. Journal of Catalysis 153, 123-130.

Talha, N.S., Sulaiman, S., **2016**. Overview of catalysts in biodiesel production. ARPN Journal of Engineering and Applied Sciences 11 (1), 439-448.

Tan, I.A.W., Ahmad, A.L., Hameed, B.H., **2008**. Optimization of preparation conditions for activated carbons from coconut husk using response surface methodology. Chemical Engineering Journal 137 (3), 462-470.

Tiwari, A.K., Kumar, A., Raheman, H., **2007**. Biodiesel production from Jatropha oil (*Jatropha curcas*) with high free fatty acids: An optimized process. Biomass and Bioenergy 31, 569-575.

U.S. Energy Information Administration, **2013**. International Energy Outlook 2013 with Projections to 2040. Washington DC, United States of America.

U.S. Energy Information Administration, **2016**. International Energy Outlook 2016 with Projections to 2040. Washington DC, United States of America.

van Eijck, J., Batidzirai, B., Faaij, A., **2014**. Current and future economic performance of first and second generation biofuels in developing countries. Applied Energy 135, 115-141.

Van Vuuren, S.F., Viljoen, A.M., **2008**. *In vitro* evidence of phyto-synergy for plant part combinations of *Croton Gratissimus* (Euphorbiaceae) used in African traditional healing. Journal of Ethnopharmacology 119, 700-704.

Vera, C.R., Pieck, C.L., Shimizu, K., Parera, J.M., **2002**. Tetragonal structure, anionic vacancies and catalytic activity of SO_4^{2-}–ZrO_2 catalysts for *n*-butane isomerization. Applied Catalysis A: General 230, 137-151.

Vicente, G., Coteron, A., Martinez, M., Aracil, J., **1998**. Application of the factorial design of experiments and response surface methodology to optimise biodiesel production. Industrial Crops and Products 8, 29-35.

Vicente, G., Martinez, M., Aracil, J., **2007**. Optimisation of integrated biodiesel production. Part 1. A study of the biodiesel purity and yield. Bioresource Technology 98, 1724-1733.

Wu, J., Alam, M.A., Pan, Y., Huang, D., Wang, Z., Wang, T., **2017**. Enhanced extraction of lipids from microalgae with eco-friendly mixture of methanol and ethyl acetate for biodiesel production. Journal of the Taiwan Institute of Chemical Engineers 71, 323-329.

Yuan, X., Liu, J., Zeng, G., Shi, J., Tong, J., Huang, G., **2008**. Optimization of conversion of waste rapeseed oil with high FFA to biodiesel using response surface methodology. Renewable Energy 33, 1678-1684.

Zabeti, M., Wan Daud, W.M.A., Aroua, M.K., **2009**. Activity of solid catalysts for biodiesel production: A review. Fuel Processing Technology 90, 770-777.

Zanuttini, M.S., Pisarello, M.L., Querini, C.A., **2014**. *Butia Yatay* coconut oil: Process development for biodiesel production and kinetics of esterification with ethanol. Energy Conversion and Management 85, 407-416.

Zhang, L., Wu, H.-T., Yang, F.-X., Zhang, J.-H., **2015**. Evaluation of Soxhlet extractor for one-step biodiesel production from *Zanthoxylum bungeanum* seeds. Fuel Processing Technology 131, 452-457.

Appendix

A: Model Development

Table A1: Fatty Acid composition for *Croton gratissimus* oil

Fatty Acid				Triglyceride		
Structure	**Formula**	**Common Name**	**Molar Mass**	**Mass Composition X_i**	**Molar Mass M_i**	
C16:0	$C_{16}H_{32}O_2$	Palmitic	256	35.8	(3 x 256) + 38	806
C16:1	$C_{16}H_{30}O_2$	Palmitoleic Acid	254	0.3	(3 x 254) + 38	800
C18:0	$C_{18}H_{36}O_2$	Stearic Acid	284	31.2	(3 x 284) + 38	890
C18:1	$C_{18}H_{34}O_2$	Oleic Acid	282	8.7	(3 x 282) + 38	884
C18:2	$C_{18}H_{32}O_2$	Linoleic Acid	280	10.5	(3 x 280) + 38	878
C18:3	$C_{18}H_{30}O_2$	Linolenic Acid	278	5.9	(3 x 278) + 38	872
C20:0	$C_{20}H_{40}O_2$	Arachidic Acid	312	2.2	(3 x 312) + 38	974
Other			271	5.4	(3 x 271) + 38	851

- **Average Molar Mass of Triglycerides in *Croton gratissimus* oil, $\overline{M}$:**

$$\overline{M} = \frac{1}{\sum \frac{x_i}{M_i}} = 854.57 \text{ g/mol}$$

where: x_i is the mass fraction of a fatty acid, and
M_i is the molar mass of a fatty acid.

- **Assumptions:**

Molar mass of MeOH = 32 g/mol

Molar mass of $ZrOCl_2 \cdot 8H_2O$ = 323.13 g/mol

Molar mass of H_2SO_4 = 98.09 g/mol

Molar mass of KOH = 56.10 g/mol

Molar mass of HCl = 36.46 g/mol

Density of MeOH = 0.790 g/ml

Density of H_2SO_4 = 1.8355 g/ml

- **SO_4^{2-}/ZrO_2 Catalyst Preparation**

Amount of precursor needed to prepare 0.60 M solution in 100 ml volumetric flask:

Mass of $ZrOCl_2 \cdot 8H_2O$

$$= 0.6\,\text{mol/litre} \times 0.10\,\text{litre} \times 323.13\,\text{g/mol} = \boxed{19.3878\ \text{g}\ ZrOCl_2 \cdot 8H_2O}$$

Amount of H_2SO_4 needed to prepare 0.50 M solution in a 500 ml volumetric flask:

Volume of H_2SO_4

$$= \frac{0.50\,\text{mol/litre} \times 0.50\,\text{litre}}{1.8355\,\text{g/ml}} \times 98.09\,\text{g/mol} = \boxed{13.36\ \text{ml}\ H_2SO_4}$$

- **Acid Value and Saponification Value of Oil:**

Amount of KOH needed to prepare 0.50 M solution in a 250 ml volumetric flask:

Mass of KOH = $0.5\,\text{mol/litre} \times 0.250\,\text{litre} \times 56.10\,\text{g/mol} = 7.0125$ g KOH

Acid Value (AV) = $\frac{56.10 \times 0.50 \times 2.00}{2.58} = \boxed{21.74\ \text{mg KOH/g}}$

Average AV = $\frac{21.74 + 21.17}{2} = \boxed{21.455\ \text{mg KOH/g}}$

Amount of HCl needed to prepare 0.50 M solution in a 250 ml volumetric flask:

Mass of HCl = $0.5\,\text{mol/litre} \times 0.250\,\text{litre} \times 36.46\,\text{g/mol} = 4.5575$ g HCl

Saponification Value (SV) = $\frac{56.10 \times 0.50 \times (22.10 - 7.90)}{2.10} = \boxed{189.67\ \text{g KOH/g}}$

Average SV = $\frac{189.67 + 190.63}{2} = \boxed{190.15\ \text{mg KOH/g}}$

- **The Esterification Process:**

Experimental Run 1:

Catalyst concentration = 10 mass %; Methanol-to-oil ratio = 32.5

Basis: 10.10 g of oil

Mass of catalyst = $\frac{10\,\text{g ZrO2SO4} \times 10.1\,\text{g Oil}}{\text{g Oil} \times 100} =$ 1.01 g SO_4^{2-}/ZrO_2

Moles of Oil = $\frac{10.10\,\text{g Oil}}{854.57\,\text{g/mol}} = 0.01182\,\text{moles Oil}$

Moles of MeOH = $\frac{32.5\,\text{moles MeOH}}{\text{moles Oil}} \times 0.01182\,\text{moles Oil} = 0.38415\,\text{moles MeOH}$

Volume of MeOH required = $\frac{0.38415\,\text{moles MeOH}}{0.790\,\text{g/ml}} \times 32\,\text{g/mol} =$ 15.56 ml MeOH

From equation 2:

$$\text{Acid Value (AV)} = \frac{56.1 \times \text{N} \times \text{V}}{\text{m}}$$

Acid Value (AV) after esterification = $\frac{56.10 \times 0.50 \times 0.25}{2.50} =$ 2.805 mg KOH/g

---

The OPTIMA1 Model:

Process Optimisation for Optimum Acid Value:

Catalyst concentration, $X_1 = 10.96$ mass %

Methanol-to-oil ration, $X_2 = 27.60$

Reaction Temperature, $X_3 = 64\ ^0\text{C}$

From equation 6:

$$Y_A = 17.362 - 0.456X_1 - 0.152X_2 - 0.239X_3 - 2.958\times10^{-4}X_1X_2 - 2.854\times10^{-3}X_1X_3 + 9.917\times10^{-4}X_2X_3 + 0.020X_1^2 + 1.254\times10^{-3}X_2^2 + 1.670\times10^{-3}X_3^2$$

Acid Value of *Croton gratissimus* oil is:

$$Y_A = 17.36176 - 0.45554(10.96) - 0.15161(27.60) - 0.23943(64) - 2.95843\times10^{-4} \times(10.96\times27.60) - 2.85439\times10^{-3}(10.96\times64) + 9.91667\times10^{-4}(27.60\times64) + 0.019788(10.96)^2 + 1.25430\times10^{-3}(27.60)^2 + 1.66985\times10^{-3}(64)^2$$

Acid Value, Y_A = 2.693 mg KOH/g

- **The Transesterification Process:**

Experimental Run 1:

Catalyst concentration = 1.70 mass %; Methanol-to-oil ratio = 6

Basis: 8.50 g of oil

Mass of catalyst = $\frac{1.70\,\text{g KOH}\times8.50\,\text{g Oil}}{\text{g Oil}\times100}$ = 0.1445 g KOH

Moles of Oil = $\frac{8.50\,\text{g Oil}}{854.57\,\text{g/mol}} = 0.00995\,\text{moles Oil}$

Moles of MeOH = $\frac{6.00\,\text{moles MeOH}}{\text{moles Oil}}\times0.00995\,\text{moles Oil} = 0.0597\,\text{moles MeOH}$

Volume of MeOH required = $\frac{0.0597\,\text{moles MeOH}}{0.790\,\text{g/ml}}\times32\,\text{g/mol}$ = 2.42 ml MeOH

FAME characterisation:

Mass of *Croton gratissimus* oil fed into the reactor = 8.50 g

Mass of biodiesel collected after transesterification = 6.90 g

$$\% \text{ FAME Yield} = \frac{6.90\,\text{g FAME}}{8.50\,\text{g Oil}} \times 100$$

$$= \boxed{81.18\% \text{ FAME Yield}}$$

Internal FAME standard: Methyl heptadecanoate

Concentration of internal standard, C_{IS} = 33 mg/ml

Volume of internal standard, V_{IS} = 100 µl = 0.10 ml

Peak Area of internal standard, A_{IS} = 98147 x 10^3

Mass of FAME sample = 107.50 mg

From equation 5:

$$\text{Percentage FAME Purity } (\%\,P) = \frac{\left(\sum A_{FS}\right) - A_{IS}}{A_{IS}} \times \frac{C_{IS} \times V_{IS}}{m_{FS}} \times 100 \qquad (5)$$

% FAME Purity is:

$$\% \text{ FAME Purity} = \frac{3012250946 - 98146656}{98146656} \times \frac{33 \times 0.10}{107.5} \times 100 = \boxed{91.15\% \text{ FAME Purity}}$$

The OPTIMA2 Models:

Process Optimisation for Optimum FAME Yield:

Catalyst concentration, $X_1 = 1.22$ mass %

Methanol-to-oil ration, $X_2 = 7.30$

Reaction Temperature, $X_3 = 68\ ^0C$

From equation 7:

$$Y_Y = -53.369 + 3.983X_1 + 21.410X_2 + 0.598X_3 + 3.019X_1X_2 + 0.152X_1X_3 - 0.042X_2X_3 - 10.563X_1^2 - 1.296X_2^2 + 4.748\times10^{-4}X_3^2$$

% FAME Yield is:

$$Y_Y = -53.369 + 3.983(1.22) + 21.410(7.30) + 0.598(68) + 3.019(1.22\times7.30) + 0.152(1.22\times68) - 0.042(7.30\times68) - 10.563(1.22)^2 - 1.296(7.30)^2 + 4.748\times10^{-4}(68)^2$$

FAME Yield, Y_Y = 84.51%

Process Optimisation for Optimum FAME Purity:

Catalyst concentration, $X_1 = 1.20$ mass %

Methanol-to-oil ration, $X_2 = 7.80$

Reaction Temperature, $X_3 = 66\ ^0$C

From equation 8:

$$Y_P = -70.150 + 17.102X_1 + 19.212X_2 + 1.676X_3 + 1.102X_1X_2 + 0.687X_1X_3 - 9.444\times10^{-3}X_2X_3 - 22.719X_1^2 - 1.276X_2^2 - 0.016X_3^2$$

% FAME Purity:

$$Y_P = -70.150 + 17.102(1.20) + 19.212(7.80) + 1.676(66) + 1.102(1.20\times7.80) + 0.687(1.20\times66) - 9.444\times10^{-3}(7.80\times66) - 22.719(1.20)^2 - 1.276(7.80)^2 - 0.016(66)^2$$

FAME Purity, Y_P = 90.66%

The OPTIMA3 (Combined) Model:

Catalyst concentration, $X_1 = 1.439$ mass %

Methanol-to-oil ration, $X_2 = 7.472$

Reaction Temperature, $X_3 = 63.50\ ^0\text{C}$

Process Optimisation for Optimum FAME Yield:

$$\begin{aligned} Y_Y = &-53.36858 + 3.98306(1.439) + 21.41007(7.472) + 0.59802(63.5) + 3.01875 \\ &\times (1.439 \times 7.472) + 0.15208(1.439 \times 63.5) - 0.041825(7.472 \times 63.5) \\ &- 10.56327(1.439)^2 - 1.29594(7.472)^2 + 4.74771 \times 10^{-4}(63.5)^2 \end{aligned}$$

FAME Yield, Y_Y = 84.51%

Process Optimisation for Optimum FAME Purity:

$$\begin{aligned} Y_P = &-70.15014 + 17.10182(1.439) + 19.21155(7.472) + 1.67582(63.5) + 1.10208 \\ &\times (1.439 \times 7.472) + 0.68720(1.439 \times 63.5) - 9.44444 \times 10^{-3}(7.472 \times 63.5) \\ &- 22.71914(1.439)^2 - 1.27604(7.472)^2 - 0.016278(63.5)^2 \end{aligned}$$

FAME Purity, Y_P = 90.66%

B: Biodiesel Production: World vs Africa

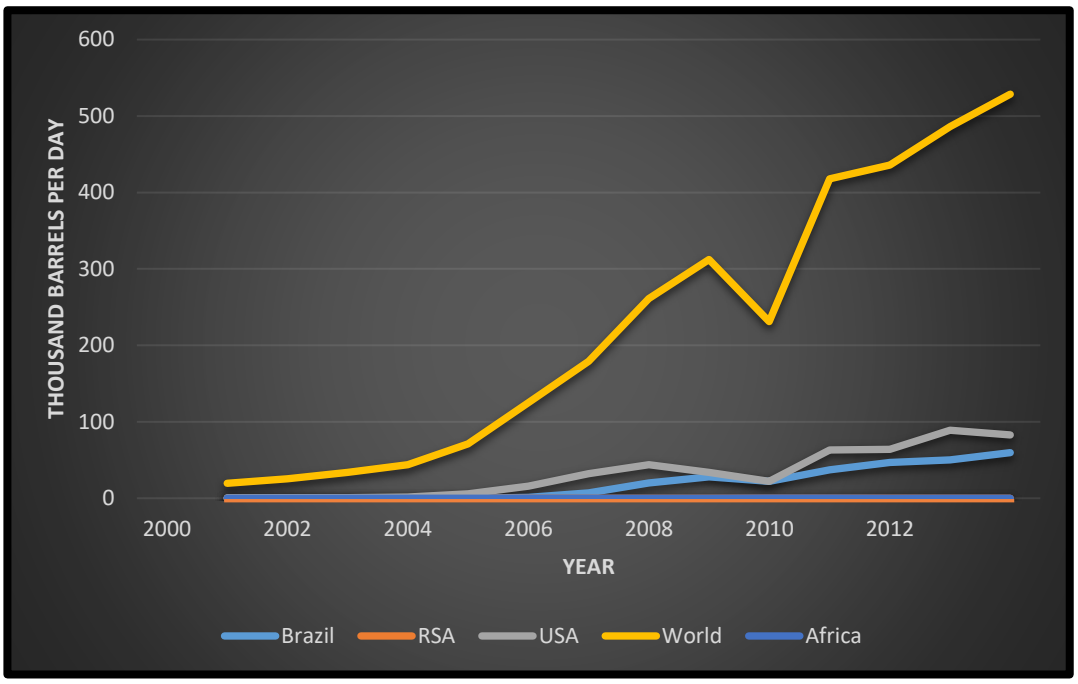

Fig. B1: Comparison of the Biodiesel Production Rate between the African Continent and High Biodiesel Producers in the World

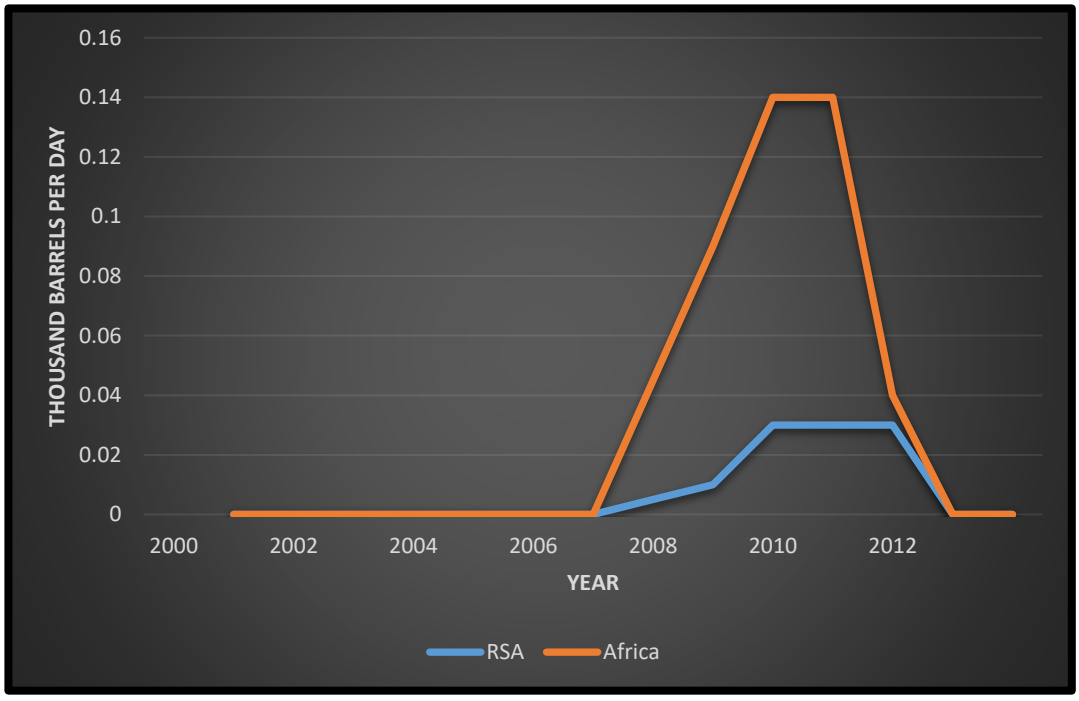

Fig. B2: Comparison of the Biodiesel Production Rate between the Republic of South Africa and the Rest of Africa

C: SEM Micrographs for the SO_4^{2-}/ZrO_2 catalyst

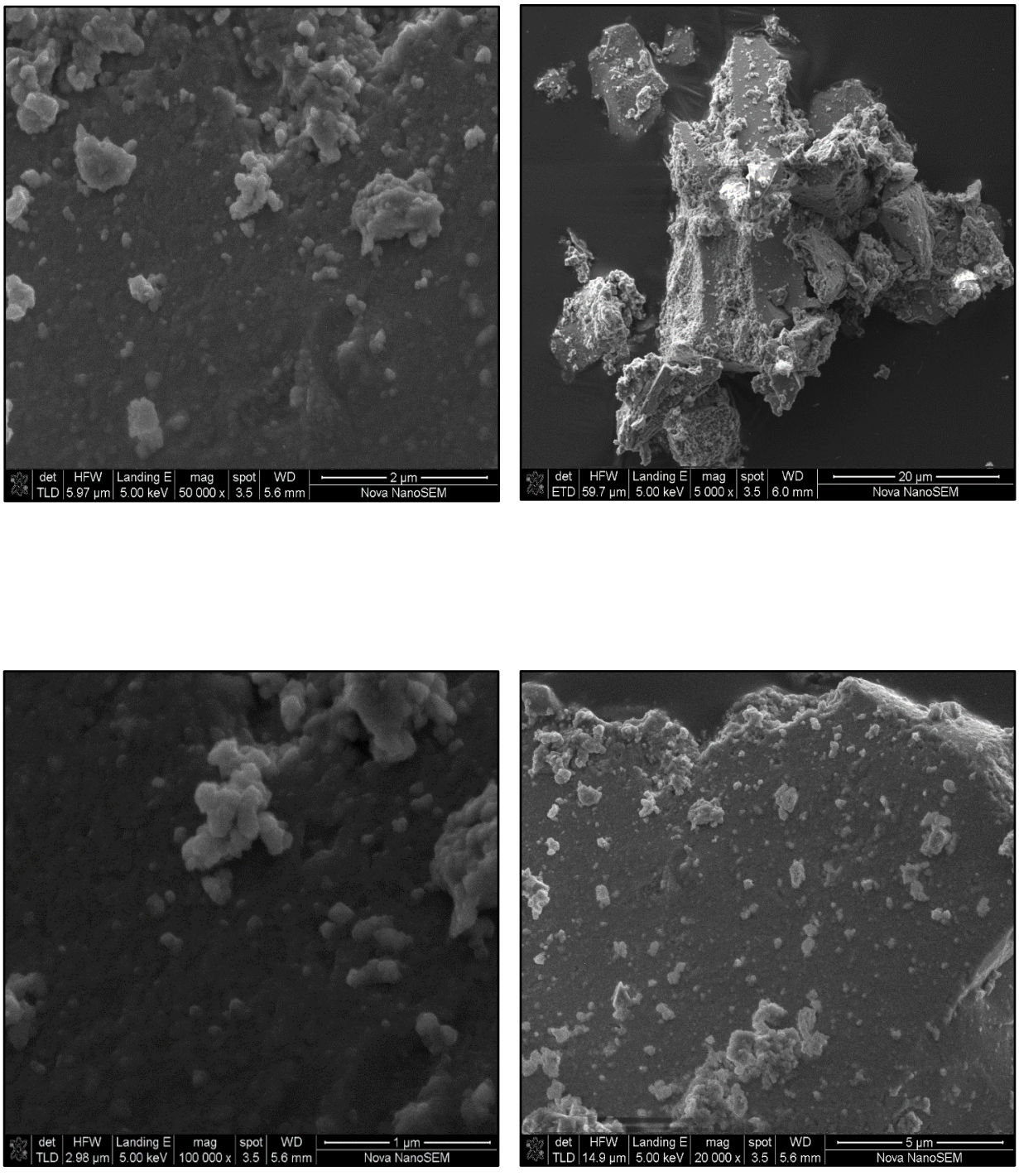

Fig. C1: SEM micrographs of the sulphate-doped monoclinic Zirconia, SO_4^{2-}/ZrO_2 catalyst

D: TEM Micrographs for the SO_4^{2-}/ZrO_2 catalyst

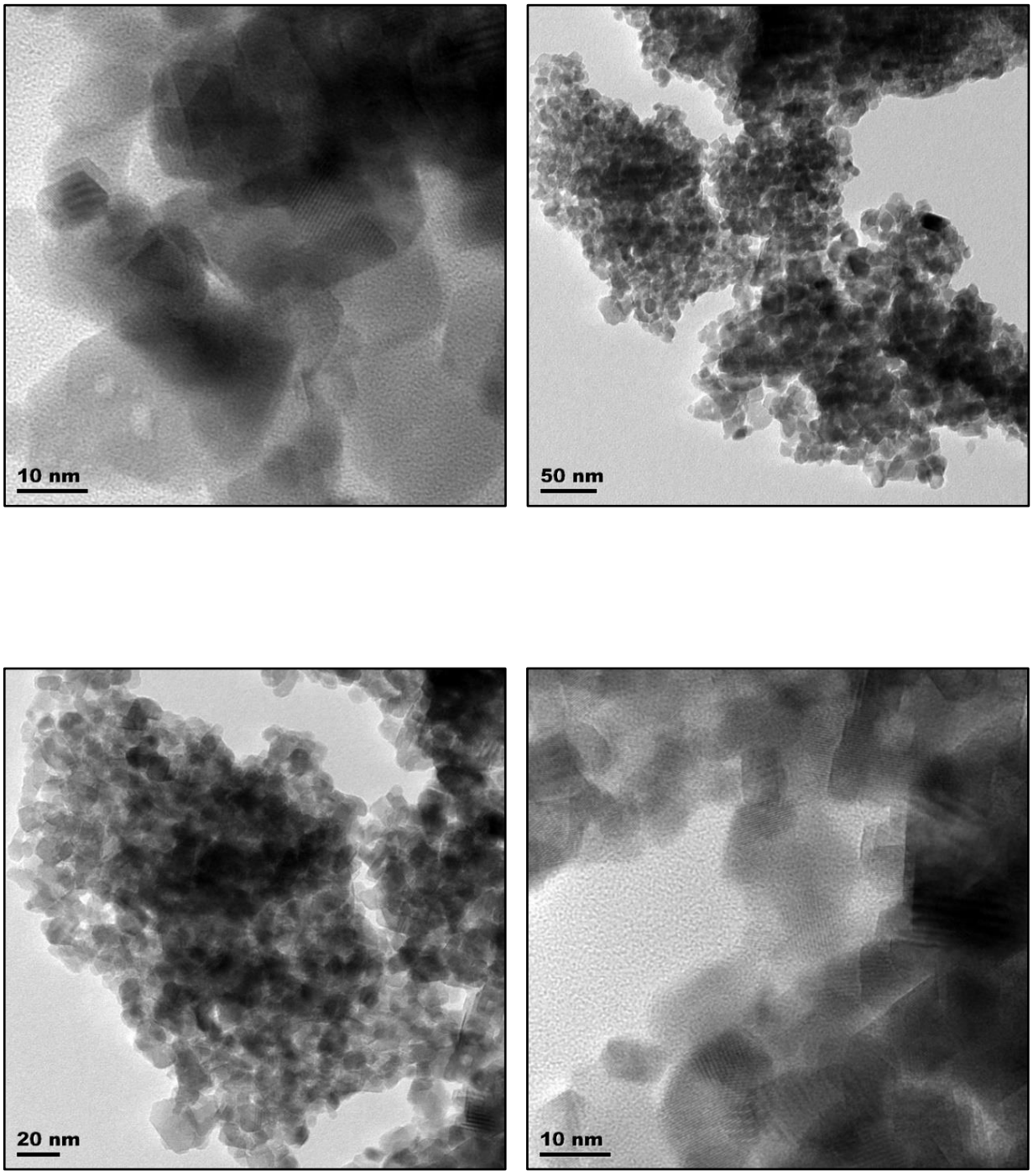

Fig. D1: TEM micrographs of the sulphate-doped monoclinic Zirconia, SO_4^{2-}/ZrO_2 catalyst

E: SEM- EDS Report on SO_4^{2-}/ZrO_2 catalyst

Project: Charles
Owner: supervisor
Site: Site of Interest 1

Sample: Zr Catalyst
Type: Default
ID:

Processing option : All elements analysed (Normalised)

All results in weight%

Spectrum	In stats.	O	S	Zr	Total
Spectrum 1	Yes	39.85	0.83	59.32	100
Spectrum 2	Yes	34.84	0	65.16	100
Spectrum 3	Yes	34.96	1.18	63.85	100
Spectrum 4	Yes	40.44	0.74	58.82	100
Spectrum 5	Yes	38.24	0	61.76	100
Mean		37.67	0.55	61.78	100
Std. deviation		2.65	0.53	2.76	
Max.		40.44	1.18	65.16	
Min.		34.84	0	58.82	

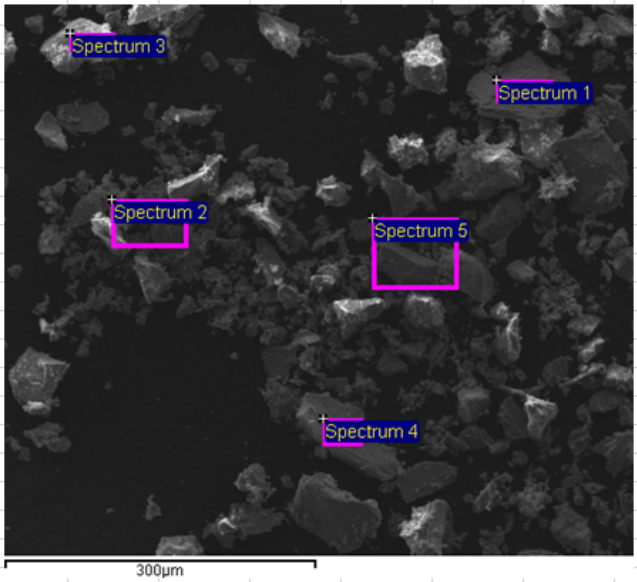

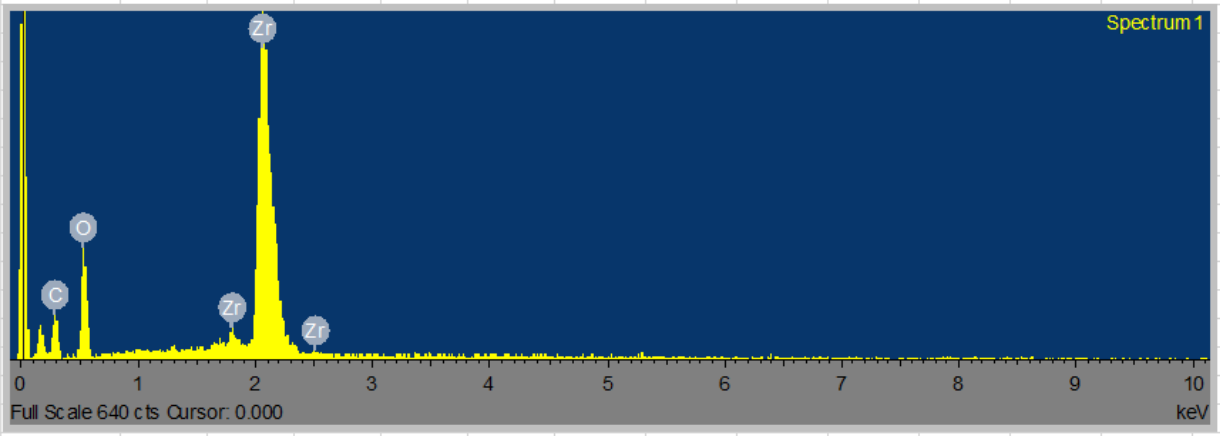

F: XRD Report on SO_4^{2-}/ZrO_2 catalyst

National Research Foundation | Laboratory for Accelerator Based Sciences

iThemba LABS

P O Box 722
Somerset West
7129
South Africa

Tel : +27 21 843 1145
Fax : +27 21 843 3543
Email : lusanda@tlabs.ac.za
Internet : http://www.tlabs.ac.za

31 Oct 2017

Mr Charles Jiyane
Chem. Dept.
Mangosuthu University of Technology
P.O. Box 12363
Jacobs 4026
Durban

Measurements were carried out with a D8 ADVANVE diffractometer from BRUKER axs using an X-ray tube with copper Kα-radiation operated at 40 kV and 40 mA. The measurement parameter were:

Measurement range: [15° – 90°]
Step size: 0.034° in 2θ
Measurement time: 0.5 sec/step

A position sensitive detector, Lynx-Eye, enables fast data acquisition of quality and helps to reduce measurements costs.

XRD results:

The analysis of the specimen was done using Zr, S and O as elements of consideration used for the search in the database. Besides the main ZrO2 phase, the presence of Baddeleyite, ZrO2, (PDF ref: 00-037-1484) was found (see Baddeleite.pdf graph).

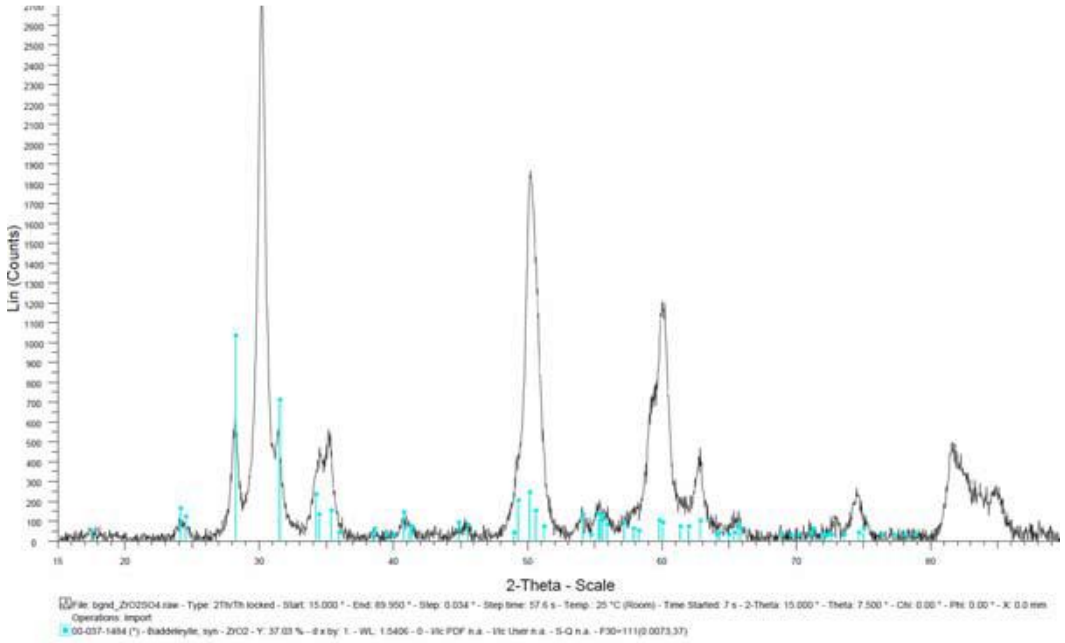

The main phase was found to be ZrO but the matching reference pattern was not unambiguous as both orthorhombic and tetragonal reference patterns do not satisfactorily match the measured peaks (see attached graphs for these two lattices).

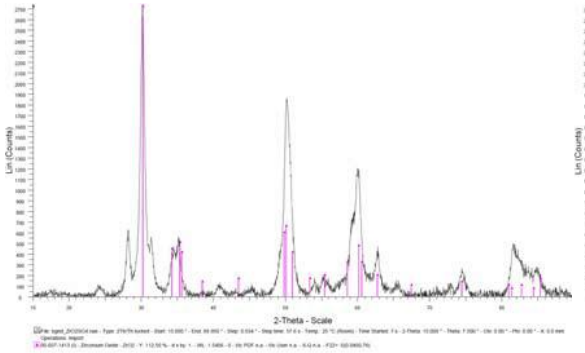

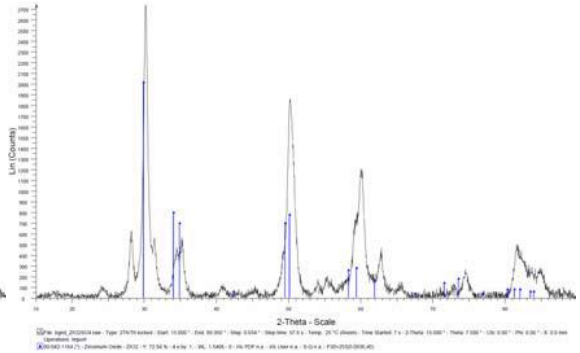

By compressing the unit cell of the tetragonal reference pattern by 1.04% one gets however a relative good match for the tetragonal lattice (PDF ref: 00-042-1164), showing the red lines (corrected unit cell) as compared to the blue lines (original lattice constants).

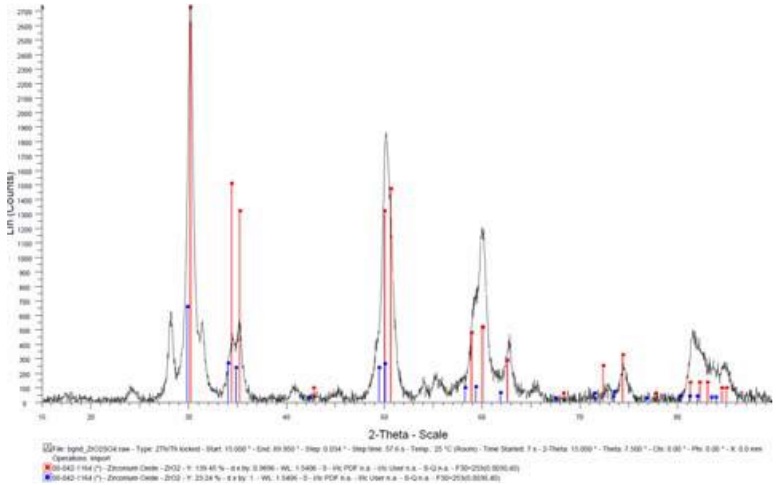

This offers a good match comparable to the deleted tetragonal reference pattern (00-14-0534) which was not considered in this analysis.

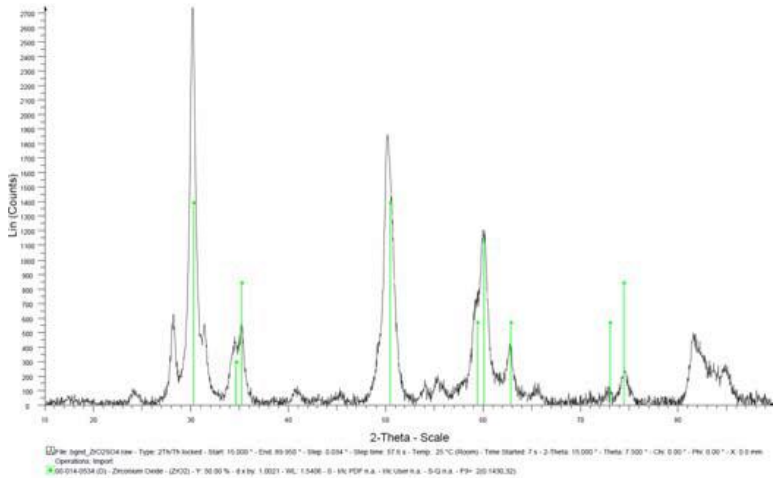

This contraction of the unit cell could be related to substitutional sulfur atoms which have a smaller radius size as Zirconium atoms. This is supported by the fact that no sulphur related phase could be identified.

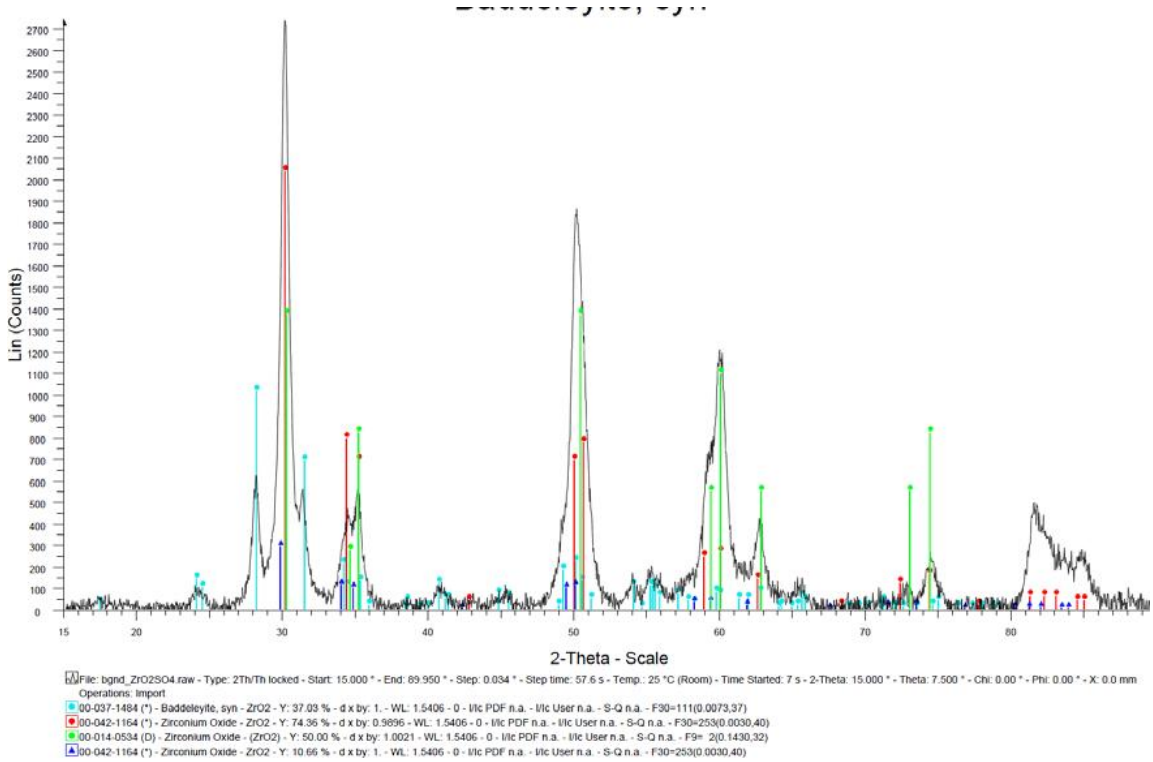

Attached files show the non matching state of various ZrOSO4 reference patterns found in the database.

For any further question regarding these samples or new prospective measurements, do not hesitate to contact us.

Dr. R. Bucher
iThemba LABS
Materials Research Department
Old Faure Road, Faure 7131
South Africa
e-mail: xrd@tlabs.ac.za
Tel: 021-843 11 54
Fax: 021 843 3543

Mr. Z.M. Khumalo
iThemba LABS
Materials Research Department
Old Faure Road, Faure 7131
South Africa
e-mails: xrd@tlabs.ac.za
Tel: 021-843 1154/1271
Fax: 021 843 354

G: Published Work

Jiyane, P.C., Tumba, K., Musonge, P., **2018**. Optimisation of *Croton gratissimus* Oil Extraction by *n*-Hexane and Ethyl Acetate Using Response Surface Methodology. Journal of Oleo Science 67 (4), 369-377.

Journal of Oleo Science
Copyright ©2018 by Japan Oil Chemists' Society
J-STAGE Advance Publication date : April, 2018
doi : 10.5650/jos.ess17197
J. Oleo Sci. 67, (4) 369-377 (2018)

Optimisation of *Croton gratissimus* Oil Extraction by *n*-Hexane and Ethyl Acetate Using Response Surface Methodology

Phiwe Charles Jiyane[1, 2], Kaniki Tumba[1]* and Paul Musonge[2]

[1] *Department of Chemical Engineering, Mangosuthu University of Technology, Umlazi, Durban, SOUTH AFRICA*
[2] *Durban University of Technology, Department of Chemical Engineering, P.O. Box 1334, Durban 4000, SOUTH AFRICA*

Abstract: The extraction of oil from *Croton gratissimus* seeds was studied using the three-factor five-level full-factorial central composite rotatable design (CCRD) of the response surface methodology (RSM). The effect of the three factors selected, *viz*., extraction time, extraction temperature and solvent-to-feed ratio on the extraction oil yield was investigated when *n*-hexane and ethyl acetate were used as extraction solvents. The coefficients of determination (R^2) of the models developed were 0.98 for *n*-hexane extraction and 0.97 for ethyl acetate extraction. These results demonstrated that the models developed adequately represented the processes they described. From the optimized model, maximum extraction yield obtained from *n*-hexane and ethyl acetate extraction were 23.88% and 23.25%, respectively. In both cases the extraction temperature and solvent-to-feed ratio were 35℃ and 5 mL/g, respectively. In *n*-hexane extraction the maximum conditions were reached only after 6 min whereas in ethyl acetate extraction it took 20 min to get the maximum extraction oil yield. Oil extraction of *Croton gratissimus* seeds, in this work, favoured the use of *n*-hexane as an extraction solvent as it offered higher oil yields at low temperatures and reduced residence times.

Key words: *Croton gratissimus*, oil extraction, Central Composite Rotatable Design (CCRD), Response Surface Methodology (RSM), optimisation

1 Introduction

Croton gratissimus is a terrestrial plant of a semi-deciduous tree species belonging to the family of *Euphorbiaceae*. It is commonly found in rocky or stony terrains throughout much of the warmer and drier regions, from north-eastwards regions of South Africa to the horn of Africa[1)] . Almost the entire plant（from roots to leaves）is used in traditional medicine to treat a wide variety of ailments. Recently it has been reported that oil extracted from *Croton gratissimus* seeds could be a promising feedstock in the large-scale production of biodiesel[2)] . However, information that would help to effectively design and optimise industrial scale processes for *Croton gratissimus* oil extraction is not available in the literature. This motivated the present study, aimed at generating experimental oil extraction data in view of further valorisation of this African crop.

Generally, large-scale seed oil extraction is achieved either by mechanically pressing the seeds against a solid surface or by using chemical solvents（in hot water extraction, Soxhlet extraction and ultrasonic techniques）. Alternatives to these well-established industrial processes include supercritical fluid extraction（SFE）, ultrasonic-assisted extraction（UAE）and enzymatic oil extraction which are currently investigated by many researchers over the world[3)] . The most common and efficient solid-liquid extraction method used in producing oil for biodiesel production is the solvent extraction method; where a solute fraction（oil）is transferred from a solid material（seed）to a liquid solvent[4)] .

Sánchez-Arreola *et al.*[5)] performed a Soxhlet extraction of *Jatropha curcas* using *n*-hexane, ethyl acetate and ethyl ether as extraction solvents. Of the three solvents used, the best yield was obtained with ethyl acetate extraction（54.3 %）. Extractions using *n*-hexane and ethyl ether gave oil yields of 47.7% and 45.9%, respectively[5)] . In their study on biodiesel production from *Croton grassimus* oil, Bahadur *et al.*[2)] reported only one extraction data point, *i.e.* 23.5% oil yield when *n*-hexane was used as solvent. In the present

* Correspondence to: Kaniki Tumba, Department of Chemical Engineering, Mangosuthu University of Technology, Umlazi, Durban, SOUTH AFRICA
E-mail: tumba@mut.ac.za
Accepted November 7, 2017 (received for review September 1, 2017)
Journal of Oleo Science ISSN 1345-8957 print / ISSN 1347-3352 online http://www.jstage.jst.go.jp/browse/jos/
http://mc.manusriptcentral.com/jjocs

study however, systematic yield measurements were undertaken at various conditions, with two different solvents, *viz*. *n*-hexane and ethyl acetate.

In addition to experimental data, modelling studies are an important step towards industrial implementation of a process. The two major approaches towards modelling oil extraction from seeds, grains and fruits include theoretical and empirical models. The most commonly used theoretical correlations are the single stage washing and diffusion model, the two stage washing and diffusion model, the first order rate equation, the second order rate equation and the simplified model based on Ficks's equation[6] . These are kinetic models as they relate yield to contact time. In relation to thermodynamic modeling, enthalpy and entropy changes are generally determined from experimental data through the van't Hoff equation[6] . Popular empirical models for oil extraction are those based on response surface methodology and artificial neural network[7] .

In this article, the effects of extraction time, extraction temperature and solvent-to-feed ratio on the oil extraction yield (measured in terms of mass of oil produced per mass of seeds used) of the two solvents, *n*-hexane (non-polar solvent) and ethyl acetate (polar solvent) , in the extraction of oil from *Croton gratissimus* seeds are reported. Furthermore, response surface methodology coupled with the central composite design of experiments is used to model and optimise the extraction process in both cases. It is worth noting that *n*-hexane is currently the oil extraction solvent of choice in industry[4] . However the rising concern over its environmentally-unfriendly nature justifies the quest for alternative solvents among the so-called generally recognised as safe solvents. One such solvent is ethyl acetate[5] whose extraction ability is compared with that of *n*-hexane in this study. The effect of particle size on the extraction oil yield has been extensively studied by a number of researchers who showed that a decrease in the particle size results in an increase in the extraction rate leading to high extraction oil yields[8] . It is for this reason that no attempts were made in this study to investigate the effect of particle size.

2 Materials and Methods

2.1 Materials

Croton gratissimus grains were obtained from selected trees in the city of Lubumbashi, Upper Katanga province, South-Eastern region of the Democratic Republic of the Congo (DRC) . Grains were allowed to dry in open air under direct sunlight for 2 days. Thereafter they were de-shelled with a hammer to remove the 3-lobed fruit capsules and expose the seeds. A high speed kitchen blender was used to crush the seeds to the desired particle size. Classification of ground seeds was done using a set of stainless steel laboratory sieves. Seeds collected for extraction were the ones that passed through a 1000 μm (18 mesh) sieve tray but still got retained by a 500 μm (35 mesh) sieve tray. The average moisture content of the seeds was found to be 3.42 ±0.5% on dry basis. Hence collected seeds were oven dried at 105℃ for 5 hours and a half to remove moisture before extraction.

Solvents selected for oil extraction were *n*-hexane (with a boiling point range of 68℃–69℃ and a purity of 99.9 mole%) and ethyl acetate (with a boiling point range of 76.5℃–77.5℃ and a purity of 99.9 mole%) , both purchased from Merck Laboratories in South Africa.

2.2 Experimental set up and extraction procedure

2.2.1 Experimental set up

A 100 mL jacketed beaker fitted with a reflux condenser was used for the extraction of oil. Agitation was achieved through the use of magnetic stirrer equipped with a speed controller. A rectangular hot water bath with an immersion temperature regulator-circulator was used to offer consistent heating at predetermined temperatures. Solvents were recovered from the extracted oil by heating the mixture in a round-bottomed flask fitted with a reflux condenser and immersed in a thermostated water bath.

2.2.2 Extraction procedure

A known mass of dried seeds (10 g) was placed in a 100 mL jacketed beaker fitted with a reflux condenser. For every gram of dried seeds fed to the beaker, a range of known volumes of extraction solvent was added (1.65 mL to 5.85mL) . A variable speed magnetic stirrer set at 600RPM (revolutions per minute) was used for agitation. Different operating temperatures were explored and the minimum and maximum being 26.5℃ and 68.5℃, respectively. Extraction times per batch ranged between 1.75 and 24.75 minutes. Uncertainties in measuring experimental parameters were estimated as ±0.5℃, 0.05 mL and 0.005 g for temperature, volume and mass, respectively. After the set time had elapsed and extraction completed, the miscella was filtered using a laboratory filtration equipment set up, *i.e.*, a Buchner flask fitted with a dropping funnel and connected onto a vacuum supply line. To avoid solvent loss during vacuum filtration, another condenser was fitted to the dropping funnel. A mixture of oil and solvent was collected in the flask and the residue discarded. The mixture was then fed to a flash distillation equipment set up to separate the solvents from oil. The extraction yield was calculated as the ratio of the mass of the extracted oil to that of the *Croton gratissimus* seeds used in the experiment.

3 Experimental Design

The response surface methodology (RSM) , used in this study, is a collection of mathematical and statistical techniques that are useful for modelling and analysis in applications where a response of interest is influenced by several variables and the objective is to optimize this

response[9] . The techniques selected were the central composite design (CCD) and the analysis of variance (ANOVA) . The CCD was applied with three design factors, *viz.*, extraction time (ET) , extraction temperature (TT) and solvent-to-feed ratio (SF) , selected to optimise the oil extraction yield (Y) . The coded and un-coded levels of independent variables used in *n*-hexane and ethyl acetate oil extraction are given in **Table 1**.

A 2^3 full-factorial rotatable CCD for three independent variables at five levels was employed and the total number of experiments was 20; evaluated from 2^k+2k+n_c, where k is the number of independent variables. Six axial points are represented by $2k$ and n_c represents replications taken at the centre points to predict a good estimation of errors. Experiments were performed in a randomized order to minimise the effects of the uncontrolled factors. The DesignExpert® version 10 software was used to design the experiments and for regression and graphical analyses of the data obtained. The values of the yield were taken as the responses of the designed experiments. Statistical analysis of the model was performed to evaluate the analysis of variance (ANOVA) [10] .

The selection of levels (uncoded variables) for each factor was based on the literature related to the uses of *n*-hexane and ethyl acetate as solvents in liquid extraction operations[11] . The lower levels of temperature were limited by mass transfer constraints. At low temperatures, the viscosity of the extract (oil) is at its highest and its diffusivity greatly reduced leading to low extraction rates[12] . The upper levels of the temperature were limited by boiling temperatures of the selected solvents. Higher temperatures are beneficial to the solubility of *Croton gratissimus* oil in the extracting solvent, and could accelerate the extraction process. However, increasing temperature will bring about not only the increase in costs in view of industrialisation but also lipids oxidation[13] .

The extraction yield (Y) response was used to develop an empirical model that correlated the response to the oil extraction variables using the second-order polynomial equation[9] :

$$Y = \beta_0 + \sum_{i=1}^{k} \beta_i X_i + \sum_{i=1}^{k} \beta_{ii} X_{i2} + \sum \sum_{i<j} \beta_{ij} X_i X_j + \varepsilon \quad (1)$$

where Y is the predicted response, β_0 is the constant coefficient, β_i is the linear coefficient, β_{ij} is the interaction coefficient, β_{ii} is the quadratic coefficient, X_i and X_j are the uncoded values of the independent variables, ET, TT and SF, and ε is the random error[14] .

3 Results and Discussion

The RSM, utilising the CCD and ANOVA, was applied in the optimization of selected independent variables to obtain maximum oil extraction yields. The effects of extraction time, extraction temperature and solvent-to-feed ratio on the oil yield were determined for *n*-hexane and ethyl acetate and the results are summarised in **Table 2**. From the experimental runs, the highest oil yield of 23.92% was obtained when *n*-hexane was used as a solvent in the extraction of oil from *Croton gratissimus* seeds.

3.1 *n*-Hexane Extraction

When *n*-hexane was used as an extraction solvent in different combinations of independent variables, the average yield was found to be 18.92% from a range of between 5.24 % and 23.92%, as shown in **Table 2**. Results obtained in this work in the temperature range from 47.5℃ to 60℃ are close to the only oil yield data point reported by Bahadur *et al.*[5] when they carried out an *n*-hexane oil extraction on *croton gratissimus* seeds for 6 hours in a round-bottomed flask fitted with a mechanical stirrer at a temperature of 50℃ and a solvent-to-feed ratio of 2.5 mL/g. They found an extraction oil yield of 23.5% from *Croton gratissimus* seeds of an average particle size of 1500±50 μm. It is worth mentioning that the present study is more comprehensive than that of Bahadur *et al.*[5] who had a rather different aim from systematically investigating the extraction process. The present study involves the use of two solvents, *i.e* ethyl acetate and *n*-hexane. Attempts were made to model and optimise the process whereas Bahadur *et al.*[5] merely reported a single oil extraction experiment using *n*-hexane only.

3.1.1 Modelling and Optimisation

The experimental data obtained in the *n*-hexane oil ex-

Table 1 Independent variables and levels used for the CCD in *Croton gratissimus* oil extraction.

Variables	Symbols	Levels				
		−α	−1	0	+1	+α
Extraction time (*min*)	ET	1.25	5	12.5	20	24.75
Extraction temperature (℃)	TT	26.5	35	47.5	60	68.5
Solvent-to-feed ratio (*mL/g*)	SF	1.65	2.5	3.75	5	5.85

Table 2 Central composite rotatable design（CCRD）arrangement and responses.

Experimental run	Coded independent variable levels			Type of factor	% Extraction Yield	
	Extraction time (*min*)	Extraction temperature (℃)	Solvent-to-feed ratio (*mL/g*)		*n*-Hexane (Y_H)	Ethyl acetate (Y_A)
1	−1	−1	−1	Factorial	15.03	13.66
2	1	−1	−1	Factorial	13.51	12.67
3	−1	1	−1	Factorial	13.67	14.66
4	1	1	−1	Factorial	14.24	14.03
5	−1	−1	1	Factorial	23.92	23.01
6	1	−1	1	Factorial	22.46	22.98
7	−1	1	1	Factorial	22.88	22.09
8	1	1	1	Factorial	22.13	21.02
9	−1.682	0	0	Axial	18.79	18.28
10	1.682	0	0	Axial	20.54	21.41
11	0	−1.682	0	Axial	21.07	18.93
12	0	1.682	0	Axial	21.42	20.39
13	0	0	−1.682	Axial	5.24	5.28
14	0	0	1.682	Axial	22.83	20.36
15	0	0	0	Centre	20.17	20.46
16	0	0	0	Centre	19.66	20.32
17	0	0	0	Centre	20.41	20.89
18	0	0	0	Centre	20.35	20.32
19	0	0	0	Centre	20.23	18.69
20	0	0	0	Centre	19.92	20.44

Table 3a *n*-Hexane extraction: -Analysis of variance（ANOVA）for the quadratic model.

Source of variation	Sum of squares	Degrees of freedom	Mean square	*F*-value	*p*-value Prob > *F*
Model	375.76	9	41.75	62.75	< 0.0001
Residual	6.65	10	0.67		
Lack of fit	6.25	5	1.25	15.50	0.00459
Pure error	0.40	5	0.081		
Total	382.41	19			

CV = 4.31%　R^2 = 0.98　Pred. R^2 = 0.88　Adj. R2 = 0.97　Adeq. Precision = 30.526

traction was analysed by the ANOVA and the following quadratic regression model that best describes this extraction process was obtained:

$$Y_H = -5.633 - 0.087X_1 - 0.314X_2 + 14.316X_3 + 0.004X_1X_2 - 0.017X_1X_3 - 0.006X_2X_3 - 0.001X_1^2 + 0.003X_2^2 - 1.339X_3^2 \quad (2)$$

where Y_H is the percentage oil extracted using *n*-hexane, X_1, X_2 and X_3 are the uncoded values of the independent variables, viz., extraction time (ET), extraction temperature (TT) and solvent-to-feed ratio (SF), respectively.

The analysis of variance (ANOVA) for the experimental results of the CCD is shown in **Table 3a**. From the developed quadratic model, the Fisher's *F*-test gave an *F* value for the model of 62.75 with a very low probability value ($p < 0.0001$). This implied that the model was significant and that a value that large had only a 0.01% chance to be due to noise. The goodness of fit of the model was evaluated by the determination coefficient (R^2), adjusted determination

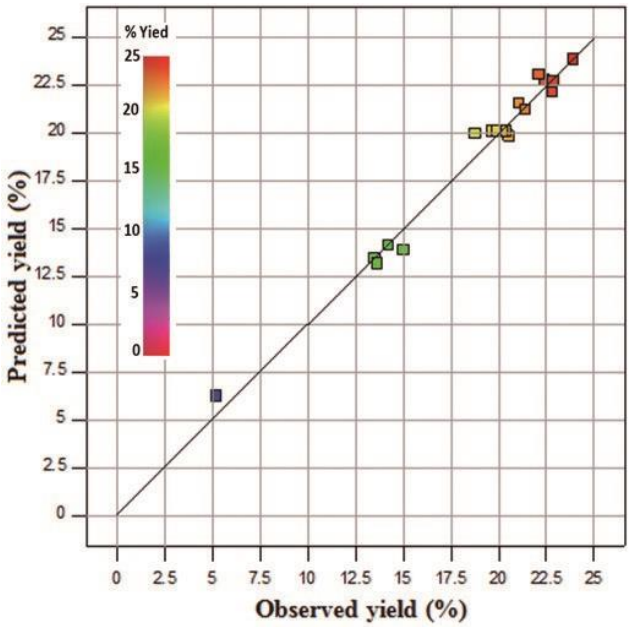

Fig. 1 Plot of experimental results versus predicted results of percentage oil yield for *n*-hexane extraction.

coefficient (Adj. R^2) and the coefficient of variance (C.V). The coefficient of determination (R^2) of the model was 0.9826, indicating that the model adequately represented the real relationship between the parameters chosen (**Fig. 1**). This meant that only 0.17% of the total variations was not explained by the developed model[15]. The coefficient of variation (C.V.) of 4.31% indicated that the model was reproducible. The predicted R^2 of 0.8775 was in reasonable agreement with the adjusted R^2 of 0.9669, *i.e.*, the difference was less than 0.2. The Adequate Precision, a measure of the signal-to-noise ratio that should ideally be greater than 4, was also evaluated and found to be high enough at 30.526. This meant that the developed model had a high degree of precision and could thus be used to navigate the design space.

The regression equation (equation 2) showed a negative correlation with extraction time (X_1) and extraction temperature (X_2) but was positively correlated with the solvent-to-feed ratio (X_3). This implied that an increase in either the extraction time or the extraction temperature resulted in a decreased extraction oil yield whereas an increase in solvent-to-oil ratio increased the extraction oil yield. This trend of oil yield change as a function of solvent-to-feed ratio was consistent with mass transfer principles. In mass transfer the concentration gradient between the solid and the bulk of the liquid is the main driving force; and this driving force is greater when higher solvent-to-feed ratios are used[13]. A larger magnitude of the coefficient for solvent-to-feed ratio ($p < 0.01$) when compared to the magnitudes of the coefficients of the other two independent variables ($p > 0.05$) further proved that solvent-to-feed ratio had a greater significance in *n*-hexane oil extraction process.

3.1.2 Effect of independent variables on percentage extraction oil yield using *n*-hexane

Figure 2 shows the response surface plots of extraction oil yield, for various combinations of extraction time, solvent-to-feed ratio and extraction temperature, when *n*-hexane was used as an extraction solvent. **Figure 2a** reveals that oil extraction yield is a very weak function of extraction temperature and time. As evidence, an almost flat plot was observed showing a 1.08% reduction in the extraction oil yield when the extraction temperatures and the extraction times were increased from 35℃ to 60℃ and from 5 min to 20 min, respectively. In both these cases the solvent-to-feed ratio was kept constant at 5 mL/g. On the other hand, the solvent-to-feed ratio had a significant effect on the percentage oil yield. The percentage oil yield showed a markedly sharp increase, from 6.79% to 23.78%, when the solvent-to-feed ratio was increased from 1.65 mL/ g to 5 mL/g and the extraction temperature kept constant at 35℃ (**Fig. 2b**). **Figure 2c** showed an increase in the percentage oil yield from 6.69% to 23.77% over the full range of solvent-to-feed ratio values (1.65 mL/g – 5 mL/g) when the extraction time was kept constant at 6 min.

From the developed model (equation 2), it was found that an optimum extraction oil yield of 23.88% could be obtained under the following operating conditions: extraction time, 6 min; extraction temperature, 35℃ and solvent-to-feed ratio, 5 mL/g.

3.2 Ethyl Acetate Extraction

When ethyl acetate was used as an extraction solvent in different combinations of independent variables, the extraction oil yield obtained ranged between 5.28% and 23.01% with an average of 18.50% (**Table 2**).

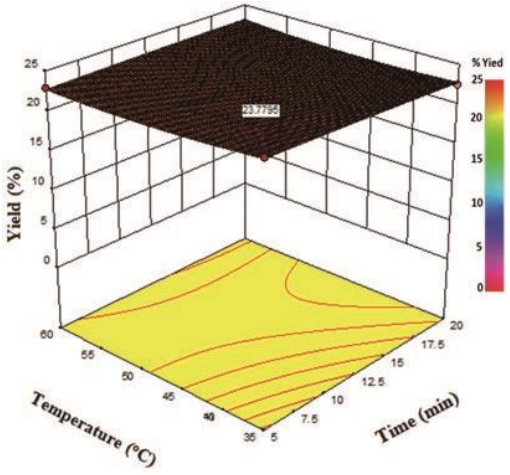

Fig. 2a Effect of time and temperature on yield at a solvent-to-feed ratio of 5:1 (mg/L) for *n*-hexane extraction.

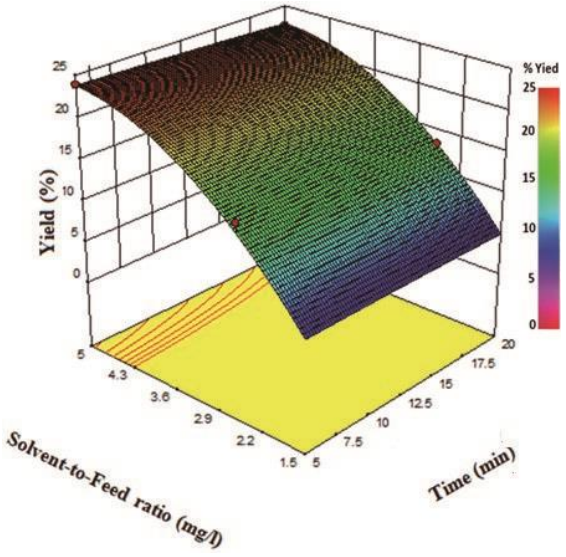

Fig. 2b Effect of time and solvent-to-feed ratio on yield at 35℃ for *n*-hexane extraction.

3.2.1 Modelling and Optimisation

The experimental data obtained in the ethyl acetate oil extraction was analysed by the ANOVA and the following quadratic regression model that best describes this extraction process was obtained:

$$Y_E = -23.513 + 0.011X_1 + 0.195X_2 + 17.138X_3 - 0.001X_1X_2 + 0.007X_1X_3 - 0.042X_2X_3 + 0.002X_1^2 - 0.0002X_2^2 - 1.567X_2^3 \quad (3)$$

where Y_E is the percentage oil extracted using ethyl acetate, X_1, X_2 and X_3 are uncoded values of the independent variables, *viz.*, extraction time (ET), extraction temperature (TT) and solvent-to-feed ratio (SF), respectively.

Equation 3 showed all linear coefficient terms as positive meaning that they all had a positive effect on the percentage oil yield. An increase in the extraction time, extraction temperature or the solvent-to-feed ratio resulted in an increase in the percentage oil extraction yield. But larger magnitudes of the coefficient of solvent-to-feed ratio ($p < 0.01$) when compared to the magnitudes of the coefficients of the other two independent variables ($p > 0.05$) indicated that the solvent-to-feed ratio was the most significant independent variable in controlling the ethyl acetate oil extraction process.

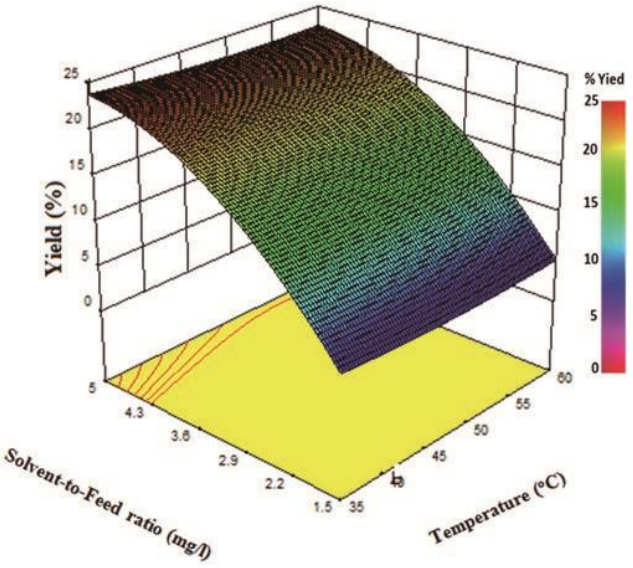

Fig. 2c Effect of temperature and solvent-to-feed ratio at 6 min for *n*-hexane extraction.

The developed quadratic model was evaluated through the analysis of variance (ANOVA) and the results are shown in **Table 3b**. The ANOVA of the regression model (Equation 3) showed that the quadratic model was highly significant. This was evident from the Fisher's *F*-test which gave an *F* value for the model of 34.60 with a very low probability value ($p<0.0001$). The goodness of fit of the model was evaluated by the determination coef-ficient (R^2), adjusted determination coefficient (Adj. R^2) and the coefficient of variance (C.V.). The value of the coefficient of determination (R^2) was found to be 0.9689, indicating that only 0.31% of the total variations was not explained by the developed regression model (**Fig. 3**). The predicted R^2 of 0.8282 was in reasonable agreement with the adjusted R^2 of 0.9409.

The Lack of fit *F*-value of 2.87 implied that the Lack of Fit was not significant and that there was a 13.57% chance that a Lack of Fit that large could occur due to noise. The Adequate Precision was also evaluated and found to be high enough at 22.696. This meant that the developed model had a high degree of precision. The coefficient of variation (C.V.) of 5.74% indicated that the model was reproducible.

3.2.2 Effect of independent variables on percentage extraction oil yield using ethyl acetate

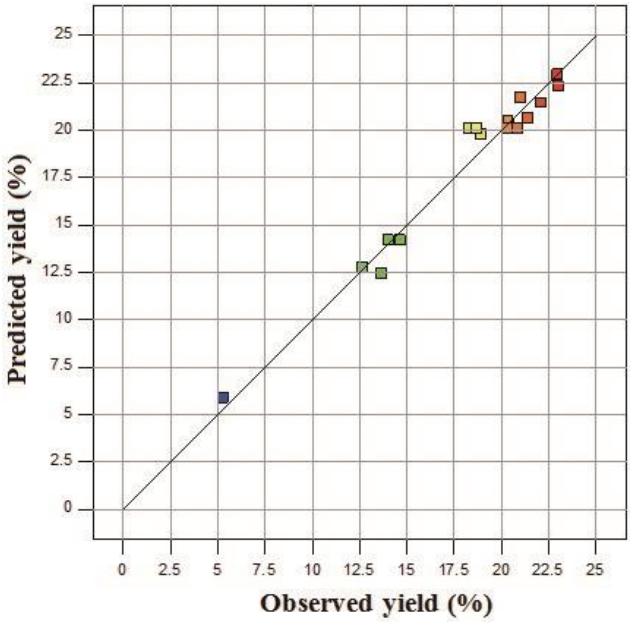

Fig. 3 Plot of experimental results versus predicted results of percentage oil yield for ethyl acetate extraction.

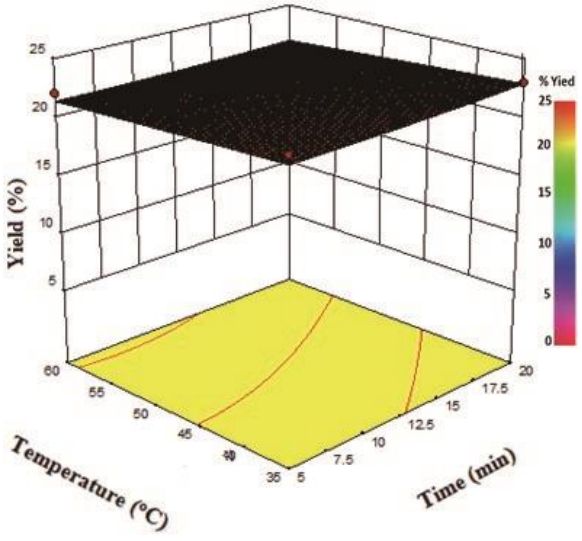

Fig. 4a Effect of temperature and time at a solvent-to-feed ratio of 5:1 (mg/L) for ethyl acetate extraction.

Table 3b Ethyl Acetate extraction:- Analysis of variance (ANOVA) for the quadratic model.

Source of variation	Sum of squares	Degrees of freedom	Mean square	*F*-value	*p*-value Prob > *F*
Model	351.00	9	39.00	34.60	< 0.0001
Residual	11.27	10	1.12		
Lack of fit	8.36	5	1.67	2.87	0.13565
Pure error	2.91	5	0.58		
Total	362.27	19			

CV = 5.74% R^2 = 0.97 Pred. R^2 = 0.83 Adj. R^2 = 0.94 Adeq. Precision = 22.696

The effects of extraction temperature, extraction time and solvent-to-feed ratio on the percentage extraction oil yield when ethyl acetate was used as an extraction solvent are shown in the surface plots in **Fig. 4**. The profile of the surface plot in **Fig. 4a**, where the solvent-to-feed ratio was kept constant at 5 mL/g, was almost flat, indicating a slight increase (1.44**%**) in the extraction oil yield when the extraction temperatures and the extraction times were varied within their low and high factor levels. The *p* values of these two factors were far greater than 0.05 (0.6056 and 0.6328, respectively), indicating that their effects on the extraction oil yield were insignificant within the range of factor levels chosen. **Figure 4b** shows the extraction yield as a function of solvent-to-feed ratio and extraction time when the extraction temperature is at 35℃. An increase in the extraction oil yield was observed, from 4.63 **%** to 22.92**%**, when the solvent-to-feed ratio was increased from 1.65 mL/g to 5 mL/g. The same could not be said for the extraction time that showed a mere 0.61**%** increase in the extraction oil yield when the extraction time was varied

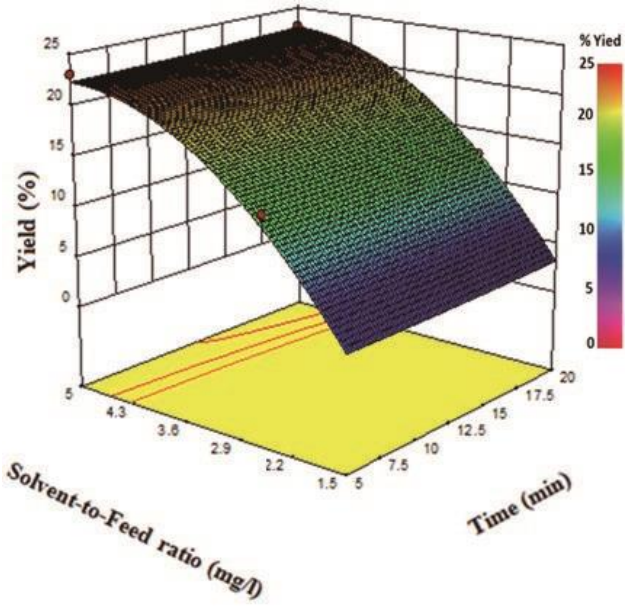

Fig. 4b Effect of time and solvent-to-feed ratio at 35℃ for ethyl acetate extraction.

between 5 min and 20 min. Figure 4c showed an equally similar increase in the percentage oil yield from 4.66**%** to 22.90**%** over the full range of solvent-to-feed ratio values (1.65 mL/g – 5 mL/g) when the extraction time was kept constant at 20 min.

From the developed model, it was found that an optimum extraction oil yield of 23.25**%** could be obtained under the following operating conditions: extraction time, 20 min; extraction temperature, 35℃ and solvent-to-feed ratio, 5 mL/g.

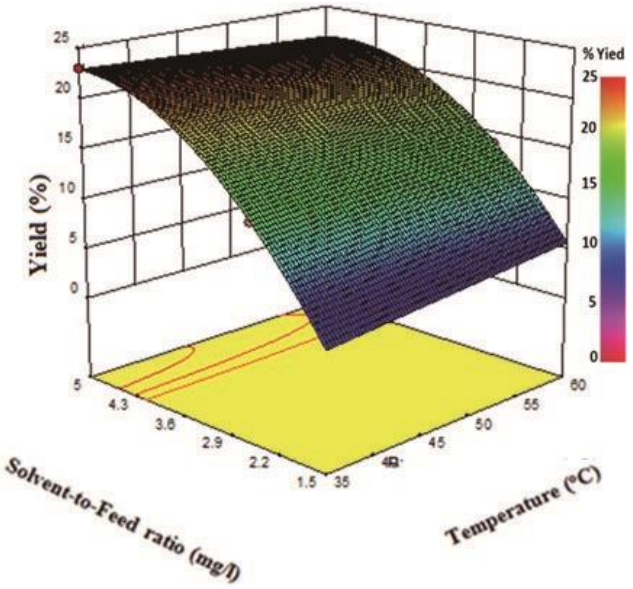

Fig. 4c Effect of temperature and solvent-to-feed ratio at 20 min for ethyl acetate extraction.

4 Conclusions

The RSM models developed for both *n*-hexane and ethyl acetate extraction processes revealed that comparable oil extraction yields could be obtained at low temperatures and shorter residence times when *Croton gratissimus* seed particles used are less than 1000 μm. Optimum conditions for both solvents were obtained when the extraction temperature and solvent-to-feed ratio were 35℃ and 5 mL/g, respectively. For *n*-hexane extraction, a better extraction oil yield of 23.88**%** was found in this work at an extraction time of only 6 min compared to 23.25**%** yield obtained for ethyl acetate extraction after 20 min. *n*-Hexane was therefore a better extraction solvent for *Croton gratissimus* seeds as its low residence times and low extraction temperatures, the critical energy saving parameters, could offer economic benefits to many process industries. The finding of this study can be used to accurately design *Croton gratissimus* oil extraction processes. Furthermore, they can be helpful when undertaking in-depth analysis on the suitability of ethyl acetate as green replacement for *n*-hexane. This analysis, as part of future work to be done, should focus on other solvent selection criteria such as recoverability, density, viscosity, interfacial tension and cost, in order to establish whether ethyl acetate is a better compromise than *n*-hexane between environmental benefits and process economics.

References

1) Mulholland, D.A.; Langat, M.K.; Crouch, N.R.; Coley, H.M.; Mutambi, E.M.; Nuzillard, J.-M. Cembranolides from the stem bark of the Southern African medicinal plant, *Croton gratissimus* (Euphorbiaceae). *Phytochem.* **71**, 1381-1386 (2010).

2) Bahadur, I.; Bux, F.; Guldhe, A.; Tumba, K.; Singh, B.; Ramjugernath, D.; Moodley, K.G. Assessment of potential of *Croton gratissimus* oil for macroscale production of biodiesel based on thermophysical properties. *Energy Fuels.* **28**, 7576-7581 (2014).

3) Atabani, A.; Silitonga, A.; Ong, H.; Mahlia, T.; Masjuki, H.; Badruddin, I.A.; Fayaz, H. Non-edible vegetable oils: A critical evaluation of oil extraction, fatty acid compositions, biodiesel production, characteristics, engine performance and emissions production. *Renew. Sustainable Energy Rev.* **18**, 211-245 (2013).

4) Amin, S.K.; Hawash, S.; El Diwani, G.; El Rafei, S. Kinetics and thermodynamics of oil extraction from *Jatropha curcas* in aqueous acidic hexane solutions. *J. Am. Sci.* **6**, 293-300 (2010).

5) Sánchez-Arreola, E.; Martin-Torres, G.; Lozada-Ramírez, J.D.; Hernández, L.R.; Bandala-González, E.R.; Bach, H. Biodiesel production and de-oiled seed cake nutritional values of a Mexican edible Jatropha curcas. *Renew. Energy* **76**, 143-147 (2015).

6) Kostić, M.D.; Joković, N.M.; Stamenković, O.S.; Rajković, K.M.; Milić, P.S.; Veljković, V.B. The kinetics and thermodynamics of hempseed oil extraction by *n*hexane. *Ind. Crop. Prod.* **52**, 679-686 (2014).

7) Akintunde, A.M.; Ajala, S.O.; Betiku, E. Optimization of *Bauhinia monandra* seed oil extraction via artificial neural network and response surface methodology: A potential biofuel candidate. *Ind. Crop. Prod.* **67**, 387-394 (2015).

8) Mani, S.; Jaya, S.; Vadivambal, R. Optimization of solvent extraction of Moringa (*Moringa oleifera*) seed kernel oil using response surface methodology. *Food Bioprod. Process.* **85**, 328-335 (2007).

9) Montgomery, D.C.; Runger, G.C. *Applied statistics and probability for engineers*, John Wiley & Sons 2010).

10) Yuan, X.; Liu, J.; Zeng, G.; Shi, J.; Tong, J.; Huang, G. Optimization of conversion of waste rapeseed oil with high FFA to biodiesel using response surface methodology. *Renew. Energy* **33**, 1678-1684 (2008).

11) Kostić, M.D.; Joković, N.M.; Stamenković, O.S.; Rajković, K.M.; Milić, P.S.; Veljković, V.B. Optimization of hempseed oil extraction by *n*-hexane. *Ind. Crop. Prod.* **48**, 133-143 (2013).

12) Treybal, R.E. *Mass transfer operations*. McGraw-Hill, New York (1980).

13) Zhang, Q.-A.; Zhang, Z.-Q.; Yue, X.-F.; Fan, X.-H.; Li, T.; Chen, S.-F. Response surface optimization of ultrasound-assisted oil extraction from autoclaved almond powder. *Food Chem.* **116**, 513-518 (2009).

14) Tan, I.; Ahmad, A.; Hameed, B. Optimization of preparation conditions for activated carbons from coconut husk using response surface methodology. *Chem. Eng. J.* **137**, 462-470 (2008).

15) Maran, J.P.; Priya, B. Modeling of ultrasound assisted intensification of biodiesel production from neem (*Azadirachta indica*) oil using response surface methodology and artificial neural network. *Fuel* **143**, 262-267 (2015